

From the
Comprehensive Pneumology Center (CPC)
of the Ludwigs-Maximilians-Universität München
Board of directors: Prof. Dr. Oliver Eickelberg

FK506-binding protein 11, a novel antibody
folding catalyst in plasma cells

Dissertation
for the attainment of the Doctor of Medicine
at the Faculty of Medicine
at the Ludwigs-Maximilians-Universität München

by
Stefan Preisendörfer
from Aschaffenburg

2020

**With permission from the Medical Faculty
of the Ludwigs-Maximilians-Universität München**

Supervisor: PD Dr. Claudia Staab-Weijnitz

Coreporter: PD Dr. Reinhard Obst
PD Dr. Amanda Tufmann
Prof. Dr. Dr. Michael von Bergwelt-Baildon

Dean: Prof. Dr. med. Thomas Gudermann

Date of oral defense: 21.10.2021

Affidavit

I, Stefan Preisendörfer, hereby declare that the submitted thesis entitled

“FK506-binding protein 11, a novel antibody folding catalyst in plasma cells”

is my own work. I have only used the sources indicated and have not made unauthorized use of services of a third party. Where the work of others has been quoted or reproduced, the source is always given.

I further declare that the submitted thesis or parts thereof have not been presented as part of an examination degree to any other university.

Munich, October 23, 2021

Place, date

Stefan Preisendörfer

Signature of doctoral candidate

Confirmation of congruency between printed and electronic version of the doctoral thesis

I, Stefan Preisendörfer, hereby declare that the electronic version of the submitted thesis, entitled

“FK506-binding protein 11, a novel antibody folding catalyst in plasma cells”

is congruent with the printed version both in content and format.

Munich, October 23, 2021

Place, date

Stefan Preisendörfer

Signature of doctoral candidate

Für Johanna

Table of contents

Abbreviations	1
Summary	10
Zusammenfassung	12
1 Introduction	2
1.1 <i>The innate and adaptive immune system: An overview</i>	2
1.2 <i>B cells in the adaptive immune system</i>	3
1.2.1 B cell development	3
1.2.2 Activation of B cells	3
1.2.3 Differentiation of activated B cells into antibody secreting cells (ASCs)	4
1.2.4 Role of the unfolded protein response (UPR) in plasma cell differentiation	5
1.3 <i>Antibodies as the final effectors of the humoral part of the adaptive immune system</i>	7
1.3.1 Structure of antibodies.....	7
1.3.2 An overview of antibody folding.....	8
1.3.3 Peptidyl-prolyl <i>cis-trans</i> isomerization in antibody folding	11
1.3.4 Antibodies in autoimmune diseases: Autoantibodies	11
1.4 <i>FK506 binding proteins (FKBPs)</i>	12
1.4.1 Overview	12
1.4.2 Classification and structure of FKBP.....	13
1.4.3 FKBP11	15
1.5 <i>Idiopathic pulmonary fibrosis (IPF)</i>	16
1.5.1 Overview of IPF	16
1.5.2 Autoimmune features in lung fibrosis and IPF	18
2 Objectives	20
3 Materials	22

3.1	<i>Instruments</i>	22
3.2	<i>Technical equipment</i>	24
3.3	<i>Chemicals and reagents</i>	25
3.4	<i>Cell culture</i>	27
3.4.1	Cell lines	27
3.4.2	Cell culture media.....	28
3.5	<i>Small interfering RNA (siRNA)</i>	28
3.6	<i>Kits</i>	29
3.7	<i>Cytokines, enzymes and inhibitors</i>	29
3.8	<i>Antibodies</i>	30
3.8.1	Antibodies for Western Blot	30
3.8.2	Antibodies for immunofluorescence stainings.....	31
3.8.3	Antibodies for ELISA.....	32
3.8.4	Antibodies for flow cytometry.....	32
3.9	<i>Primers for qRT-PCR</i>	33
3.10	<i>Software</i>	34
4	Methodology	35
4.1	<i>Human materials</i>	35
4.1.1	Patient samples	35
4.1.2	Gene expression data	35
4.2	<i>Cell culture experiments</i>	35
4.2.1	Cell culture conditions	35
4.2.2	Isolation of peripheral blood mononuclear cells (PBMCs)	36
4.2.3	Plasma cell differentiation of PBMCs	36
4.2.4	Generation of cytopins	36

4.2.5	MTT cytotoxicity assay	37
4.2.6	Trypan Blue exclusion assay	37
4.2.7	Tunicamycin treatment of A549 and RAJI cells.....	37
4.2.8	SiRNA-mediated transfection of A549 cells	38
4.2.9	SiRNA-mediated transfection of the hybridoma cell line H3	39
4.3	<i>Unfolding and refolding of immunoglobulin G</i>	39
4.4	<i>Immunological methods</i>	41
4.4.1	Enzyme-linked immunosorbent assay (ELISA)	41
4.4.2	Flow cytometry.....	42
4.4.3	Immunohistochemistry	43
4.4.4	Protein analysis.....	44
4.5	<i>Molecular biological methods</i>	47
4.5.1	RNA expression analysis.....	47
4.5.2	SiRNA-mediated transfections	48
4.6	<i>Statistical analysis</i>	48
5	Results	50
5.1	<i>FKBP11 is highly increased in IPF lung tissues</i>	50
5.2	<i>FKBP11 is identified in CD27+/CD38+/CD138+/CD3-/CD20-/CD45- plasma cells in IPF lungs</i>	52
5.2.1	FKBP11 is identified in CD27+/CD38+/CD138+/CD3-/CD20-/CD45- plasma cells in IPF lungs.	52
5.2.2	IPF lungs show an elevated number of plasma cells as compared to donor lungs.....	55
5.2.3	FKBP11 is expressed by CD38- secretory cells	56
5.3	<i>In vitro plasma cell differentiation leads to an upregulation of FKBP11.</i>	57
5.3.1	IL2/R848 treatment induces plasma cell differentiation.....	58
5.3.2	Plasma cell differentiation induces FKBP11	60

5.4	<i>FKBP11 is upregulated upon ER stress in an XBP1-dependent manner</i>	60
5.4.1	FKBP11 is upregulated upon ER stress	61
5.4.2	FKBP11 localizes to the ER	62
5.4.3	XBP1 mediates upregulation of FKBP11 in ER stress	62
5.4.4	FKBP11 protects from ER stress induced cell death	64
5.5	<i>FKBP11 is a capable antibody folding catalyst</i>	65
5.5.1	FKBP11 is highly expressed in antibody producing hybridoma cell lines	65
5.5.2	Silencing of FKBP11 results in depressed antibody production.....	67
5.5.3	FKBP11 is capable of antibody folding <i>in vitro</i>	68
5.6	<i>Antibody yields are elevated in IPF</i>	71
6	Discussion	73
6.1	<i>Overview</i>	73
6.2	<i>FKBP11 is a plasma cell specific protein and increased in IPF</i>	73
6.3	<i>Plasma cell differentiation and the unfolded protein response upregulate FKBP11</i>	75
6.4	<i>FKBP11 acts as a competent antibody folding catalyst</i>	76
6.5	<i>Conclusions and outlook</i>	79
7	References	82
8	List of tables	92
9	List of figures	94
10	Acknowledgements	96
11	Publications	98
11.1	<i>Original works</i>	98
11.2	<i>Poster presentations</i>	98
12	Curriculum vitae	99

Abbreviations

A

ACTB	Actin-beta
AD	Alzheimer's Disease
AEC	Alveolar epithelial cell
ALAT	Latin American Thoracic Society
APC (cell)	Antigen presenting cell
APC (FACS stain)	Allophycocyanin
APRIL	A proliferation-inducing ligand
APS	Ammonium peroxodisulfide
ASC	Antibody secreting cell
ATF6 α	Activating transcription factor 6 α
ATS	American Thoracic Society

B

BACH2	Transcription regulator protein BACH2
BAFF	B cell activating factor
BCA	Bicinchoninic acid assay
BCL-6	B cell lymphoma 6
BCR	B cell receptor
BiP	Binding immunoglobulin protein
BLIMP-1	B lymphocyte-induced maturation protein 1
BLM	Bleomycin
BLyS	Plasma B lymphocyte stimulating factor
BSA	Bovine serum albumin

C

°C	Celsius
CBD	Calmodulin binding domain
cDNA	Complementary deoxyribonucleic acid
CD	Cluster of differentiation
CH	Constant domain of the heavy chain
CHO	Chinese hamster ovary
CHOP	C/EBP homologous protein
CL	Constant domain of the light chain
CLP	Common lymphoid progenitor cell
CO ₂	Carbon dioxide
Con A	Concanavalin A
C _p	Heat capacity
CPC-M	Comprehensive Pneumology Center Munich
CsA	Cyclosporin A
CTD-ILD	Interstitial lung diseases associated with connective tissue disease
Ctrl	Control
Cy7	Cyanine 7
CypB	Cyclophilin B
D	
DAPI	4',6-diamino-2-phenylindole
ΔC _p	Change in heat capacity
DMEM	Dulbecco's Modified Eagle Medium
DMSO	Dimethyl sulfoxide
dNTP	Desoxyribonucleotides
DNA	Desoxyribonucleic acid
DNase	Deoxyribonuclease

DPBS	Dulbecco's phosphate-buffered saline
DTT	Dithiothreitol
E	
ECM	Extracellular matrix
ECL	Enhanced chemiluminescence
EDTA	Ethylenediaminetetraacetic acid
ELISA	Enzyme-linked Immunosorbent Assay
EMT	Epithelial to mesenchymal transition
ER	Endoplasmatic reticulum
ERAD	Endoplasmic-reticulum-associated protein degradation
Erp57	Endoplasmic reticulum resident protein 57
ERS	European Respiratory Society
F	
F	Farad
F12	Ham's F-12 nutrient mixture
Fab	Fragment antigen binding
FACS	Fluorescence-activated cell sorting
FBS	Fetal bovine serum
FC	Fragment crystallizable
FDA	Food and Drug Administration
FGF	Fibroblast growth factor
FKBP	FK506-binding protein
FO B cell	Follicular B cell

G

<i>g</i>	Gravity
GAPDH	Glyceraldehyde 3-phosphate dehydrogenase
GdnHCl	Guanidine hydrochloride
GRP-78	78 kDa glucose-regulated protein

H

h	Hour
H1, 2, 3	Hybridoma cell line 1, 2, 3
H ₂ O	Dihydrogenoxide (water)
HC	Heavy chain
HLA	Human leukocyte antigen
HRCT	High-resolution computer tomography
HRP-linked	Horseradish peroxidase-linked
HSC	Hematopoetic stem cell
Hsp	Heat shock protein

I

Ig	Immunoglobulin
IgA	Immunoglobulin A
IgD	Immunoglobulin D
IgE	Immunoglobulin E
IgG	Immunoglobulin G
IgM	Immunoglobulin M
IL-2	Interleukin-2

ILD	Interstitial lung disease
IPF	Idiopathic pulmonary fibrosis
IRE1 α	Inositol-requiring enzyme 1 α
IRF4	Interferon regulatory factor 4
J	
JRS	Japanese Respiratory Society
K	
kDa	Kilodalton
L	
LC	Light chain
LSM	Laser-scanning microscope
M	
M	Molar unit
mA	Milliampere
mAB	Monoclonal antibody
mM	Millimolar unit
μ	Micro
μ F	Microfarad
μ l	Microliter
μ M	Micromolar unit
MEM	Minimal essential medium
MgCl ₂	Magnesium chloride

MHC	Major histocompatibility complex
min	Minutes
mg	Milligrams
mL	Milliliter
mm	Millimeters
MMP	Matrix metalloproteinase
MPP	Multi-potent progenitor cell
mRNA	Messenger ribonucleic acid
MTT	Methylthiazolyldiphenyl-tetrazolium bromide
MZB1	Marginal zone B and B1 cell-specific protein
MZ B cell	Marginal zone B cell
N	
NaCl	Sodium chloride
Na ₂ HPO ₄	Disodium hydrogen phosphate
NaOH	Sodium hydroxide
NF-AT	Nuclear-factor of activated T cells
ng	Nanogram
nM	Nanomolar unit
nm	Nanometer
P	
p	Passage
PAMP	Pathogen-associated molecular pattern
PAX5	Paired box protein 5
PBS	Phosphate buffered saline

PBMC	Peripheral blood mononuclear cell
PCR	Polymerase chain reaction
PD	Parkinson's Disease
PDI	Protein disulfide-isomerase
PDIA3	Protein disulfide-isomerase A3
PE	Phycoerythrin
PERK	PKR-like ER kinase
PFA	Paraformaldehyde
pH	Power of hydrogen
PhosSTOP	Phosphatase-inhibitor
pNPP	Para-nitrophenyl phosphate
PPIase	Peptidyl-prolyl <i>cis-trans</i> isomerase
PRDM1	PR domain zinc finger protein 1
PRR	Pattern recognition receptor
p-value	Calculated probability
PVDF	Polyvinylidene difluoride
 Q	
qRT-PCR	Quantitative real-time polymerase chain reaction
 R	
R848	Resiquimod
RA	Rheumatoid Arthritis
RIPA	Radioimmunoprecipitation assay
RNA	Ribonucleic acid
RNase	Ribonuclease

RPM	Rounds per minute
RPMI 1690	Roswell Park Memorial Institute 1690
S	
SD	Standard deviation
SDS	Sodium dodecyl sulfate
SDS-PAGE	Sodium dodecyl sulfate – polyacrylamide gel electrophoresis
SEM	Standard error of the mean
siRNA	Small interfering ribonucleic acid
SLE	Systemic lupus erythematosus
SLO	Secondary lymphoid organ
SSC	Side scattered
sXBP1	Spliced X-box binding protein 1
T	
T1, T2, T3	Transitional state 1, transitional state 2, transitional state 3
TBS	2-Amino-2-(hydroxymethyl)propane-1,3-diol buffered saline
TCR	T cell receptor
TD	T cell-dependent
TEMED	Tetramethylethylenediamine
TGF β	Transforming growth factor beta
TI	T cell independent
TLR	Toll-like receptor
TM	Transmembrane region

TMB	3,3',5,5'-Tetramethylbenzidine
TPR domain	Tetratricopeptide repeat domain
TRIS	2-Amino-2-(hydroxymethyl)propane-1,3-diol
U	
UGMLC	Universities of Giessen and Marburg Lung Center
UIP	Usual interstitial pneumonia
UPR	Unfolded protein response
V	
V	Volt
V(D)J recombination	Variable, joining and diversity gene segment recombination
VH	Variable domain of the heavy chain
VL	Variable domain of the light chain
W	
WB	Western Blot
X	
XBP1	X-box binding protein 1

Summary

Antibodies are glycoproteins produced by terminally differentiated B cells known as plasma cells. They are the central effectors of adaptive immunity, as they specifically bind invading pathogens leading to their neutralization. Besides their substantial function in the immune system, they are used as monoclonal antibodies for the treatment of many diseases, including cancer and autoimmune disorders, and are therefore produced recombinantly in large numbers. In the form of autoantibodies, on the other hand, antibodies may represent disease causing and promoting molecules.

All processes mediated by antibodies rely on a functional, three-dimensional structure, which in turn is attained in the endoplasmatic reticulum (ER) and aided by several ER-resident chaperones and folding catalysts. Therefore, a profound knowledge of antibody folding is substantial not only to gain a deeper understanding of the immune system, but also to improve recombinant antibody folding and to develop novel strategies to deal with autoimmune diseases. Still, antibody folding is insufficiently characterized so far. Here, expression, localization, regulation and function of FKBP11, a potential novel antibody folding peptidyl-prolyl *cis-trans* isomerase (PPIase), was analyzed.

Idiopathic pulmonary fibrosis (IPF) is an interstitial lung disease (ILD) with increasing incidence worldwide and a poor prognosis with median survival rates of 3-5 years upon diagnosis. It is a fibrotic disease defined by an excessive deposition of extracellular matrix (ECM) resulting in an irreversible, ultimately fatal disruption of the lung architecture. Treatment with the Food and Drug Administration (FDA) approved antifibrotic compounds pirfenidone and nintedanib can slow down disease progression, but does not stop it, highlighting the need for a better understanding of this disease along with novel treatment strategies. Importantly, there is emerging evidence of autoimmune features present in IPF, including lymphocytic aggregates within IPF lung tissue and elevated levels of autoantibodies in the serum of IPF patients. A better understanding of these features could provide novel therapeutic targets in the treatment of IPF.

Consistent with preceding proteomics data, protein levels of FKBP11 were highly increased in lung tissue of IPF patients. In IPF lungs, immunofluorescence revealed that FKBP11 was specifically expressed by CD27+/CD38+/CD138+/CD3-/CD20-/CD45- plasma cells, the number of which was drastically elevated in IPF lungs. Accordingly, *in vitro* B cell to plasma cell differentiation induced by a mixture of Interleukin-2 (IL-2) and

R848 (resiquimod) was accompanied by an upregulation of FKBP11. More specifically, FKBP11 was upregulated as a part of the unfolded protein response (UPR) in an XBP1-dependent manner, with XBP1 being an important driver of the plasma cell differentiation process. This was assessed by artificial induction of ER stress using tunicamycin upon two different cell lines. Interestingly, prior knockdown of FKBP11 made the cells more susceptible to ER stress induced cell death. Finally, the function of FBKBP11 was determined using an *in vitro* antibody folding assay, showing that addition of human recombinant FKBP11 increased both the speed of antibody folding as well as total yields of correctly folded antibodies. This effect was inhibited by prior incubation of FKBP11 with tacrolimus (FK506). In agreement with a function in antibody folding, knockdown of FKBP11 in an antibody secreting hybridoma cell line reduced antibody levels in the cell culture supernatant.

Overall, FKBP11 was identified as a novel, plasma cell specific antibody folding catalyst in IPF. This provides new insights into plasma cell biology and the process of antibody folding, supporting a role of autoimmunity in IPF and allowing for the conception of innovative, targeted therapies not only in IPF, but also in autoimmune disorders. Moreover, these insights may help to overcome present limitations in the production of therapeutic, monoclonal antibodies.

Zusammenfassung

Antikörper sind Glykoproteine, die von ausdifferenzierten B-Zellen, den Plasmazellen, produziert werden. Sie sind zentraler Bestandteil des adaptiven Immunsystems, indem sie eingedrungene Erreger binden und somit zu deren Beseitigung führen. Außerdem werden sie als monoklonale Antikörper zur Behandlung vieler Krankheiten, wie etwa Krebs und Autoimmunerkrankungen, genutzt und daher in großen Mengen rekombinant hergestellt. Andererseits können Antikörper auch in Form von Autoantikörpern zur Entstehung von Krankheiten führen und diese aufrecht erhalten.

All diese Prozesse, die durch die Bindung von Antikörpern ausgelöst werden, erfordern eine funktionierende, dreidimensionale Struktur des Antikörpers, die unter Zuhilfenahme von Chaperonen und Faltungskatalysatoren im endoplasmatischen Retikulum (ER) entsteht. Daher ist ein tiefgreifendes Verständnis von Antikörperfaltung nicht nur wesentlich, um neue Erkenntnisse zum Immunsystem zu gewinnen, sondern kann auch die rekombinante Herstellung monoklonaler Antikörper verbessern sowie dazu beitragen, neue Strategien zur Behandlung von Autoimmunerkrankungen zu gewinnen. Bislang ist der Vorgang der Antikörperfaltung jedoch unzureichend dargestellt worden. In dieser Arbeit wurde die Expression, Lokalisation, Regulation sowie Funktion von FKBP11, einer Peptidyl-Prolyl-cis/trans-Isomerase (PPIase), im Hinblick auf eine mögliche Funktion als antikörperfaltendes Enzym analysiert.

Die idiopathische Lungenfibrose (IPF) gehört zu den interstitiellen Lungenerkrankungen (ILDs) und hat eine schlechte Prognose mit einer mittleren Überlebenszeit von 3-5 Jahren bei Diagnosestellung. Die Inzidenz der IPF ist weltweit steigend. Die Krankheit ist gekennzeichnet durch eine zunehmende Vernarbung (Fibrosierung) des Lungengewebes, die durch eine enorme Ablagerung von extrazellulärer Matrix (ECM) gekennzeichnet ist. Dies führt zu einer zunehmenden Zerstörung der Lungenarchitektur, die am Ende zum Tod der Patienten führt. Die derzeit von der Arzneimittelzulassungsbehörde der USA (Food and Drug Administration, FDA) zugelassenen, anti-fibrotischen Medikamente, namentlich Pirfenidon und Nintedanib, verlangsamen lediglich das Voranschreiten der Erkrankung, verhindern es jedoch nicht. Dies verdeutlicht, dass ein besseres Verständnis der IPF notwendig ist, um neue Behandlungsansätze zu identifizieren. Weiterhin wird zunehmend ersichtlich, dass Eigenschaften von Autoimmunerkrankungen in der IPF zu finden sind, wie etwa lymphozytäre Infiltrate in den Lungen der Patienten sowie zirkulierende Autoantikörper im Serum der Patienten. Eine bessere Charakterisierung

dieser autoimmunen Eigenschaften in der IPF könnte dazu führen, neue Behandlungsansätze zu verwirklichen.

Übereinstimmend mit einer vorhergehenden Proteomikstudie der IPF zeigten Lungengewebeproben von IPF-Patienten höhere Proteinnengen von FKBP11. In der Immunfluoreszenz war ersichtlich, dass *FKBP11* in IPF Lungen ausschließlich von Plasmazellen (CD27+/CD38+/CD138+/CD3-/CD20-/CD45-) exprimiert wird. Entsprechend war die Zahl der Plasmazellen in IPF-Lungen deutlich erhöht. Damit übereinstimmend führte eine *in vitro* Plasmazelldifferenzierung mithilfe von Interleukin-2 (IL-2) und R848 (Resiquimod) zu einer Hochregulierung von FKBP11. Eine künstliche Herbeiführung von ER-Stress mittels Tunicamycin in zwei unabhängigen Zelllinien führte zur Hochregulierung der ungefalteten Protein-Antwort (UPR) und zeigte auf, dass FKBP11 als Teil der UPR in der Plasmazelldifferenzierung hochreguliert wird. Genauer noch bestätigte der vorhergehende Knockdown von XBP1, einem wichtigen Transkriptionsfaktor der Plasmazelldifferenzierung, dass die Hochregulierung von FKBP11 über XBP1 vermittelt wird. Weiterhin zeigte sich bei Herbeiführung von ER-Stress nach vorhergehendem Knockdown von FKBP11 eine erhöhte Empfindlichkeit der Zellen gegenüber ER-Stress-induziertem Zelltod. Letztlich konnte durch ein *in vitro* Antikörperfaltungssystem demonstriert werden, dass rekombinantes, humanes FKBP11 die Fähigkeit besitzt, Antikörper *in vitro* zu falten, da es sowohl den Faltungsprozess selbst beschleunigte, als auch den Ertrag an korrekt gefalteten Antikörpern steigerte. Diese Effekte konnten durch vorhergehende Inkubation von FKBP11 mit Tacrolimus (FK506) verhindert werden. Damit übereinstimmend führte ein Knockdown von FKBP11 in einer antikörperproduzierenden Hybridomzelllinie zu geringeren Antikörperkonzentrationen im Zellkulturüberstand.

Abschließend lässt sich sagen, dass mit FKBP11 ein neuartiges Protein identifiziert wurde, das in der Lage ist, Antikörper in Plasmazellen zu falten. Dies gewährt neuartige Einblicke in die Biologie der Plasmazelle sowie den Prozess der Antikörperfaltung, und unterstützt weiterhin die Rolle von Autoimmunität in der IPF. Dies ermöglicht die Entwicklung neuartiger Therapieansätze, sowohl in der Behandlung der IPF, als auch in der Behandlung von Autoimmunerkrankungen. Darüber hinaus können diese Erkenntnisse dazu beitragen, die Herstellung rekombinanter, monoklonaler Antikörper zu verbessern.

1 Introduction

1.1 The innate and adaptive immune system: An overview

The human organism is permanently exposed to a wide variety of pathogens, including bacteria, viruses, and parasitic worms. To be protected from these, the human organism evolved a host defense system known as the immune system, which consists of two major immune strategies: the innate immune system and the adaptive immune system. Both subsystems possess humoral and cell-mediated mechanisms to face pathogens (Marrack and Kappler 1994).

If a pathogen breaks through the body's surface barriers (e.g. skin, mucous membranes), the innate immune system provides a first line, however, non-specific reaction. This reaction is triggered by highly conserved pattern recognition receptors (PRRs), such as toll-like receptors (TLRs), which bind highly conserved components expressed on the surface of the invading pathogens, for instance, pathogen-associated molecular patterns (PAMPs). Cells participating in the innate immune system include phagocytes (neutrophils, macrophages, dendritic cells), innate lymphoid cells, mast cells, eosinophils, basophils and natural killer cells. The humoral component of innate immunity is achieved by the complement system, a biochemical cascade attacking the surface of invading cells (Chaplin 2010).

In case that a pathogen evades the innate immune system, a second layer of protection is provided via the adaptive immune system. In contrast to the innate immune system, the adaptive immune system is highly specific towards distinct antigens and requires activation by the innate immune system. This second line reaction is carried out by B cells and T cells, carrying a wide variety of distinct receptors (B cell receptors: BCR, T cell receptors: TCR), corresponding to a wide variety of distinct antigens. In order for a B cell or T cell to identify a receptor specific antigen, it needs to be presented by the major histocompatibility complex (MHC). The presentation of the antigen in the MHC is realized by antigen presenting cells (APCs). After activation, B cells mediate the humoral component of the adaptive immune system via secretion of soluble antibodies. T cells, on the other hand, act as the cellular component (Hoebe, Janssen et al. 2004, Chaplin 2010).

1.2 B cells in the adaptive immune system

1.2.1 B cell development

As outlined above, B cells represent the humoral branch of the adaptive immune system by secretion of soluble antibodies (also known as immunoglobulins, Igs). Once fully matured and activated, they are referred to as plasma cells and secrete antibodies with a single defined antigen specificity, which is accomplished by a complicated developmental process originating in the bone marrow from hematopoietic stem cells (HSCs). The high diversity of antibodies matching almost any potential antigen is attained during B cell development by joining separate gene segments randomly together before their transcription is initiated, a process known as V(D)J recombination, with the letters standing for variable (V), joining (J) and diversity (D) gene segments (Rolink, ten Boekel et al. 1999).

Starting with early B cell development in the bone marrow, HSCs differentiate into multipotent progenitor cells (MPPs), followed by common lymphoid progenitor cells (CLPs). After completion of further developmental stages (pro-B cell, pre-B cell) in the bone marrow, each defined by distinct gene expression patterns and gene loci rearrangements, they become immature B cells. Of note, during early B cell development in the bone marrow, B cells start to undergo both positive and negative selection. As a consequence, the BCR is able to bind foreign antigens (positive selection), while not binding self-antigens (negative selection) (LeBien and Tedder 2008).

After completing early B cell development in the bone marrow, the immature B cells transmigrate as transitional B cells (at this point in transitional state 1, T1) to the spleen, where they transit further transitional states, T2 and T3, finally differentiating into follicular (FO) or marginal zone (MZ) B cells. These steps within the spleen are considered as transitional B cell development. Once differentiated, they are referred to as mature (or naïve) B cells. Similar to early B cell development, both positive and negative selection processes occur during transitional B cell development. (Chung, Silverman et al. 2003).

1.2.2 Activation of B cells

B cell activation occurs in secondary lymphoid organs (SLOs), such as lymph nodes and spleen, finally resulting in differentiation into terminally differentiated B cells known as

antibody secreting cells (ASCs). There, naïve B cells get into contact with antigens delivered by circulating lymph and can be either activated in dependence of T cells, usually by T cell-dependent (TD) antigens, or without the help of T cells, usually by T cell-independent (TI) antigens. TD antigens include foreign proteins, TI antigens include foreign polysaccharides and unmethylated DNA (Cyster and Allen 2019).

1.2.3 Differentiation of activated B cells into antibody secreting cells (ASCs)

B cell activation finally results in the formation of antibody secreting cells (ASCs). ASCs include two subsets, namely plasmablasts (or immature plasma cells) and plasma cells. The latter are postmitotic and develop from plasmablasts. To be able to secrete vast amounts of antibodies (up to 10.000 antibodies per cell per second (Lanzavecchia 2018)), B cells need to undergo crucial changes during differentiation to ASCs with respect to cellular structure, metabolism and protein expression profile. ASCs expand their endoplasmatic reticulum (ER) along with upregulation of ER-resident chaperones and folding catalysts, as well as their Golgi apparatus. (Nguyen, Joyner et al. 2019). Therefore, the gene expression profile changes fundamentally, which is accomplished by silencing of transcription factors and repressors defining B cell identity and upregulation of factors driving ASC differentiation. Factors defining B cell identity include paired box protein 5 (PAX5), transcription regulator protein BACH2, and B cell lymphoma 6 (BCL-6). The most important drivers of ASC differentiation are interferon regulatory factor 4 (IRF4), PR domain zinc finger protein 1 (PRDM1, also known as BLIMP-1) and X-box binding protein 1 (XBP1) (Nutt, Hodgkin et al. 2015). Along with the change in the gene expression profile, cell surface molecules change, which can be used as targets for immunophenotyping of cells. Table 1 summarizes important characteristics in gene expression of naïve B cells, plasmablasts and plasma cells.

Table 1: Overview of characteristics of naïve B cells and ASCs (plasmablasts and plasma cells). Table adapted from (Tellier and Nutt 2018).

	Naïve B cells	Plasmablasts	Plasma cells
Lifespan	++	+	++++
Proliferation	-	++	-
CD27, CD38, CD138	-	+	+++
CD19, CD20, CD45	+++	++	+/-
PRDM1	-	+	++

1.2.4 Role of the unfolded protein response (UPR) in plasma cell differentiation

Whenever protein folding is impaired in the ER, misfolded and unfolded proteins accumulate in the ER. This can be a consequence of an impaired ER resident folding machinery, an overload of proteins to be folded or a disrupted ER environment. The accumulation of misfolded proteins usually leads to the induction of ER stress, ultimately resulting in upregulation of the unfolded protein response (UPR), a highly conserved collection of intracellular signaling pathways. In the context of the UPR, translation of new protein is transiently paused, degradation of misfolded protein is supported and the secretory apparatus in the ER is expanded to recover maintenance of protein folding in the ER (Liu and Kaufman 2003).

ER stress is detected by three transmembrane ER stress sensors: inositol-requiring enzyme 1 α (IRE1 α), PKR-like ER kinase (PERK) and activating transcription factor 6 α (ATF6 α). Under homeostatic conditions, these ER stress sensors remain inactive as a consequence of interaction with binding immunoglobulin protein (BiP, also known as GRP78). Once misfolded proteins accumulate, BiP dissociates from the ER stress sensors due to its higher affinity for misfolded proteins, resulting in release of the ER stress sensors. Subsequently, the ER stress sensors promote the UPR by several parallel pathways. Of these, the most conserved pathway is mediated by IRE1 α , which, after autophosphorylation and forming dimers upon its release from BiP, exhibits RNase activity. With its RNase activity, the IRE1 α dimer performs non-conventional splicing of a single mRNA encoding XBP1, resulting in a translational frameshift, finally creating a potent transcription factor known as XBP1s (spliced XBP1). XBP1s then induces a large

variety of ER-resident molecular chaperones and protein-folding enzymes, promoting the UPR. If the response is not sufficient, the UPR switches to a pro-apoptotic mode, known as terminal UPR, leading to apoptosis via upregulation of C/EBP homologous protein (CHOP); (Hetz and Papa 2018).

In plasma cells, the ER and Golgi apparatus are strongly hypertrophied as compared to naïve B cells in order to fold enormous amounts of antibodies. This is accompanied by an upregulation of the ER-resident protein folding machinery necessary for sufficient folding of antibodies, consisting of molecular chaperones, peptidyl-prolyl *cis-trans* isomerases (PPIases), disulfide isomerases and glycosyl transferases. These changes occur during the process of B cell to plasma cell differentiation and are induced in the context of the UPR (Tellier and Nutt 2018). Notably, in B cell to plasma cell differentiation, the UPR is induced even *before* onset of Ig synthesis, indicating the UPR to be a physiological process of plasma cell differentiation rather than a stress induced response as in other cells (Grootjans, Kaser et al. 2016). Moreover, it has been implied that the pro-apoptotic pathway leading to upregulation of CHOP is selectively downregulated in order to be capable of dealing with enormous amounts of proteins (Ma, Shimizu et al. 2010).

For upregulation of the UPR in plasma cell differentiation, the XBP1s pathway of the UPR was particularly shown to play a crucial role (Iwakoshi, Lee et al. 2003, Shaffer, Shapiro-Shelef et al. 2004). Of note, loss of XBP1 in B cells leads to an absence of plasma cells (Todd, McHeyzer-Williams et al. 2009). After activation of a naïve B cell, BCL-6, an important factor of B cell maintenance, is phosphorylated leading to its degradation. This results in de-repression of PRDM1, one of the main drivers for ASC differentiation. PRDM1 acts as a transcriptional repressor, and restrains, among other genes, the expression of PAX5, another key regulator of the B cell program. As a result, XBP1, which is usually repressed by PAX5, is activated, leading to induction of the UPR along with the ER-resident protein folding machinery (Grootjans, Kaser et al. 2016). This pathway is visualized in Figure 1.

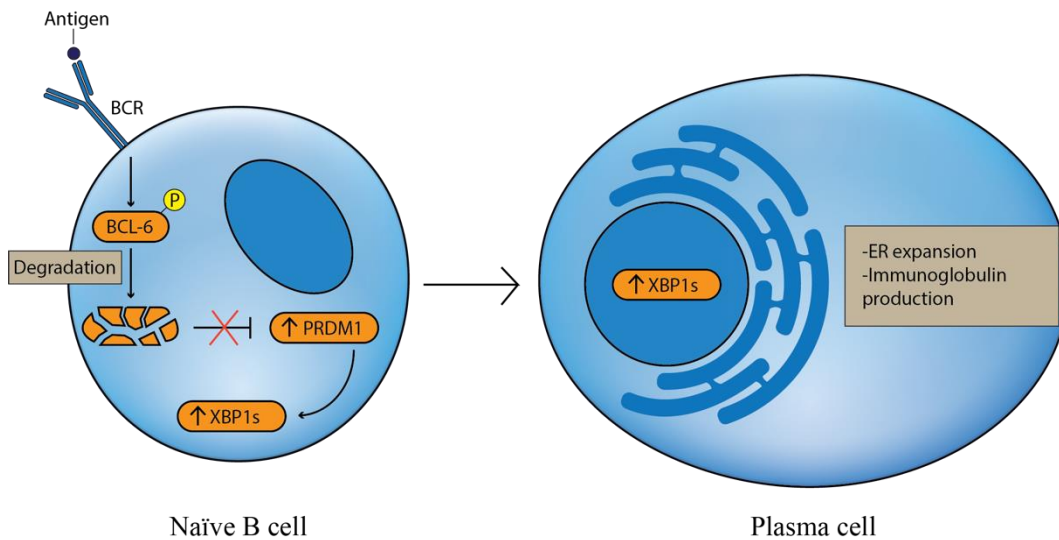


Figure 1: Induction of the UPR as part of plasma cell differentiation.

Activation of a naïve B cell by binding of an antigen to its B cell receptor (BCR) initiates the process of B cell to plasma cell differentiation. As a consequence, BCL-6 is phosphorylated, leading to its degradation, which then results in disinhibition of PRDM1 (BLIMP1). PRDM1 promotes splicing of XBP1, inducing the UPR and plasma cell differentiation. ER = endoplasmatic reticulum. Figure modified from (Grootjans, Kaser et al. 2016).

1.3 Antibodies as the final effectors of the humoral part of the adaptive immune system

1.3.1 Structure of antibodies

Antibodies (also known as immunoglobulins, Igs) represent the final effector molecules of the humoral part of the adaptive immune system. Once secreted, antibodies bind a unique site of a specific antigen, a so-called epitope, leading to its neutralization (Forthal 2014).

IgG, the most basic antibody isoform, is a Y-shaped, multidomain glycoprotein, consisting of two identical heavy chains (HCs), which are linked to each other via disulfide bonds, and two identical light chains (LCs), being attached to the HCs via disulfide bonds. The HC comprises four domains (three constant and one variable domain: CH1-3 and VH), the LC is half the size comprising two domains (constant and variable domain: CL and VL). IgG can be proteolytically cleaved into two Fab fragments (“fragment antigen binding”) and one Fc fragment (“fragment crystallizable”), being usually connected to each other by a hinge region. The amino-terminal ends of each Fab fragment, called paratopes, form variable domains, which bind specific, corresponding

epitopes of the antigen, while the remains of the Fab fragments as well as the Fc fragment make up the constant domains. The Fc fragment couples antigen binding to antibody effector functions (Figure 2) (Schroeder and Cavacini 2010).

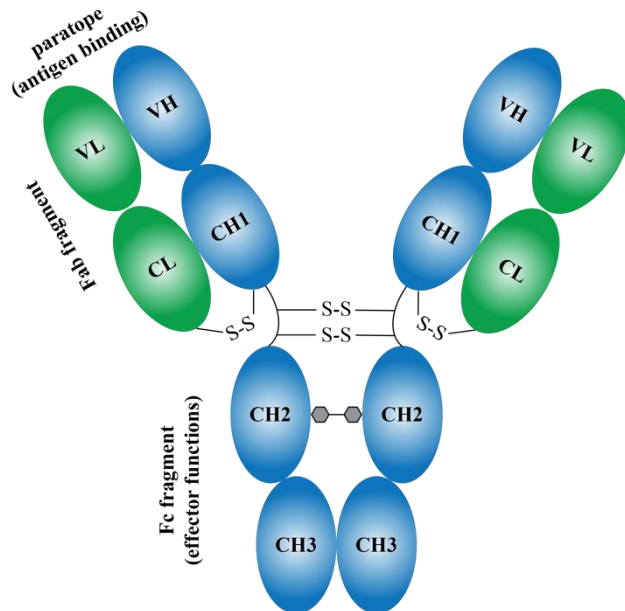


Figure 2: Structure of an IgG molecule (antibody).

An IgG molecule is composed of two heavy (blue: VH, CH1, CH2, CH3) and two light chains (green: VL and CL), which are linked by disulfide bonds (S-S). The CH2 domains are further interconnected by oligosaccharides (grey hexagons). Figure adapted from (Feige, Hendershot et al. 2010).

Depending on the type of heavy chain (α , δ , ϵ , γ and μ), different Ig isotypes can be distinguished: IgA, IgD, IgE, IgG and IgM (corresponding to the Greek letters). Every isotype has a different function. The types of light chains (κ and λ), on the other hand, are irrespective of the Ig subtype. While the antibody isotypes IgD, IgE and IgG are found in the monomeric form only, IgA and IgM exist as both monomeric and polymeric antibodies (Schroeder and Cavacini 2010).

1.3.2 An overview of antibody folding

Binding of specific antigens, finally mediating the effector function of the humoral part of the adaptive immune system, strictly relies on a functional, three-dimensional structure of the antibody (Tello, Spinelli et al. 1990). Therefore, correct folding of antibodies within the ER is essential, and checkpoints for correct protein structure must be controlled accurately. The folding process in the ER relies on several chaperones and folding

catalysts, including heat shock proteins (Hsp), peptidyl-prolyl *cis-trans* isomerases (PPIases), glycan-binding proteins and oxidoreductases, all of them being part of the ER-resident protein folding machinery (Feige, Hendershot et al. 2010, Feige and Buchner 2014). Most of them are upregulated during differentiation of naïve B cells to ASCs via the UPR, with XBP1 being a central transcription factor orchestrating the UPR in this differentiation process (Janssens, Pulendran et al. 2014). If folding is non-sufficient, and antibodies become terminally misfolded, they are marked for degradation by ER-associated protein degradation (ERAD) by the proteasome (Qi, Tsai et al. 2017).

HCs and LCs are co-translationally translocated into the ER, and before translation is finished, the folding process starts. All antibody domains except CH1 fold autonomously, reaching on-pathway intermediates within the folding process. The molecular chaperone BiP interoperates with most domains temporarily before their folding is finished. After CH3 is folded, dimerization of the HCs is induced, which will then be stabilized by formation of a disulfide bond in the hinge region. CH1 resides unfolded, being stabilized in its unfolded state by BiP, which also prevents secretion of single HCs. BiP is then dislocated by CL, with interaction of CL with CH1 inducing folding of CH1. Only after CH1 is folded correctly, disulfide bonds linking HCs and LCs to each other are formed, making the antibody ready for its secretion. By this mechanism, only correctly folded antibodies will leave the ER (Feige, Hendershot et al. 2010). A summary of the folding process in the ER is shown in Figure 3.

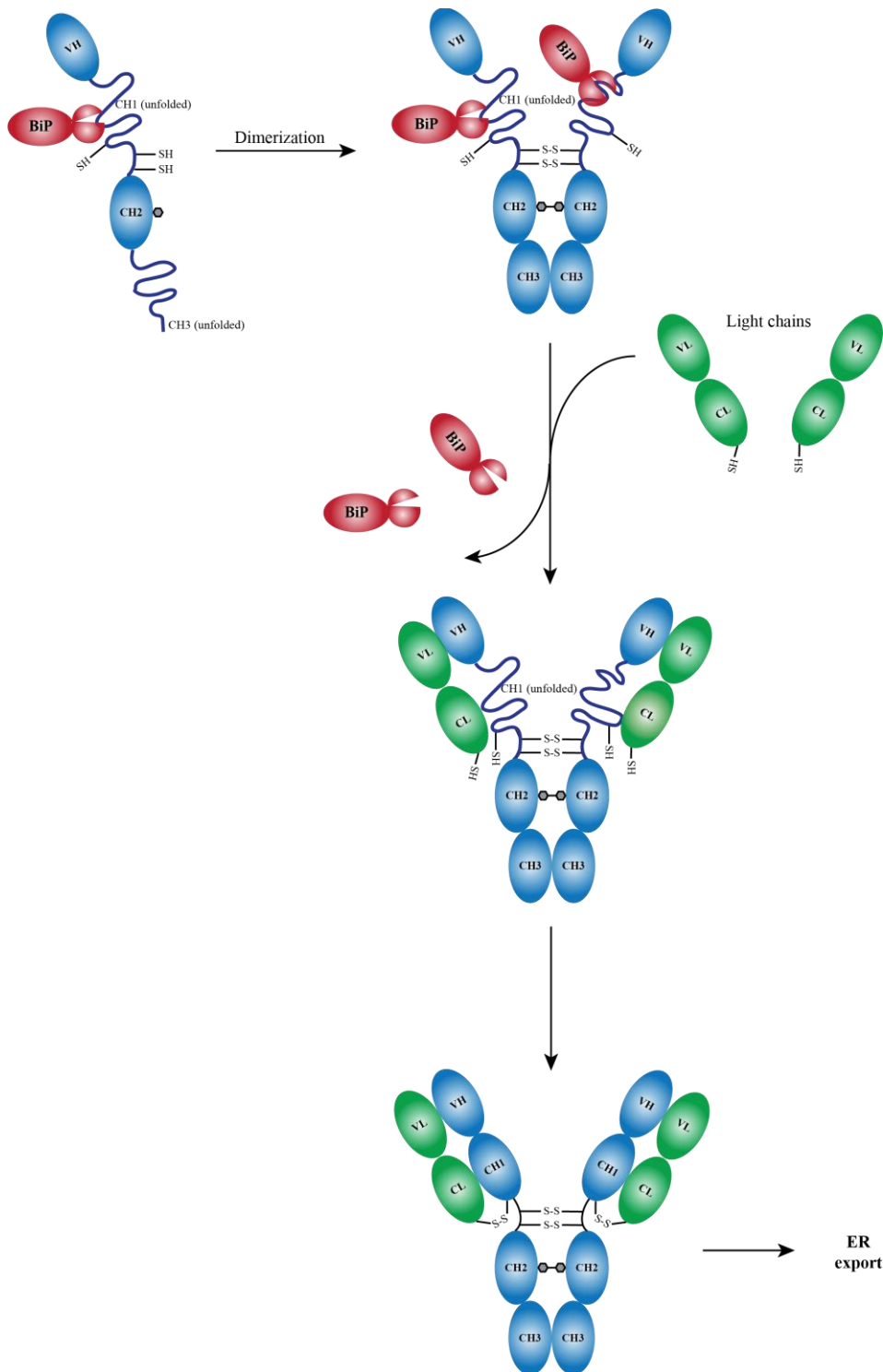


Figure 3: An overview on antibody folding in the ER.

The molecular chaperone BiP temporarily interacts with most antibody domains. After CH3 is folded correctly, dimerization of the heavy chains is initiated. Importantly, CH1 is kept in an unfolded state by association with BiP, until the light chains displace BiP. This promotes folding of CH1, after which the disulfide bonds between heavy and light chains are formed, making the antibody molecule ready for secretion from the ER. Most of the individual folding steps are supported by chaperones, protein disulfide isomerases (PDIs) and peptidyl-prolyl *cis-trans* isomerases. Figure modified from (Feige, Hendershot et al. 2010).

1.3.3 Peptidyl-prolyl *cis-trans* isomerization in antibody folding

In protein folding, peptidyl-prolyl *cis-trans* isomerizations are crucial, as they often represent rate limiting steps. Importantly, prolines constitute 5-10% of an antibody's primary sequence. Accordingly, peptidyl-prolyl *cis-trans* isomerizations are an essential part of the antibody folding process (Feige and Buchner 2014). Peptidyl-prolyl *cis-trans* isomerizations are catalyzed by PPIases, which are grouped into two main families: FK506-binding proteins (FKBPs) and cyclophilins (Göthel and Marahiel 1999). More details on PPIases can be found in 1.4.1. Within antibody folding, only two PPIases being capable of antibody folding *in vitro* have been identified so far, namely Cyclophilin B (CypB) (Meunier, Usherwood et al. 2002, Feige, Groscurth et al. 2009, Jansen, Määttänen et al. 2012, Lee, Choi et al. 2012) and FKBP1A (also termed FKBP12) (Lilie, Lang et al. 1993).

1.3.4 Antibodies in autoimmune diseases: Autoantibodies

As outlined above, B cells undergo both positive and negative selection during B cell development. However, if negative selection (also known as central tolerance) is non-sufficient, B cells can secrete antibodies that react to self-molecules (autoantigens), leading to their destruction and ultimately promoting autoimmune diseases (Grimaldi, Hicks et al. 2005).

Organ-specific autoimmune diseases, such as type 1 diabetes mellitus, primary biliary cirrhosis or thyroiditis, are characterized by the presence of autoantibodies highly specific for target organs (e.g. thyroglobulin in thyroiditis), leading to destruction of specific organs. In systemic autoimmune diseases, such as systemic lupus erythematosus (SLE) or rheumatoid arthritis (RA), on the other hand, autoantibodies bind free molecules (e.g. phospholipids), resulting in formation of pathogenic antigen-antibody (immune) complexes. These complexes cause a non-specific inflammation of different organ systems (Davidson and Diamond 2001).

Given the crucial role of B cells and autoantibodies in autoimmune diseases, a variety of treatment strategies has evolved specifically targeting B cells and autoantibodies (Hofmann, Clauder et al. 2018). One noteworthy example is rituximab, a monoclonal antibody directed against CD20, a pan B-cell surface protein. Binding of rituximab to CD20 triggers apoptosis, leading to specific depletion of the B cell lineage. This has been shown beneficial in many autoimmune diseases, including RA. (Gottenberg, Guillevin et

al. 2005). Moreover, there are monoclonal antibodies against CD19 (Mei, Schmidt et al. 2012) and CD22 (Steinfeld and Youinou 2006), directly targeting distinct B cell subtypes. Other strategies include the proteasome inhibitor Bortezomib, leading to depletion of antibody secreting plasma cells (Alexander, Sarfert et al. 2015), and suppressants of B cell and plasma survival factors, such as B cell activating factor (BAFF) and A proliferation-inducing ligand (APRIL) (Samy, Wax et al. 2017). Another promising approach is extracellular cleavage of autoantibodies, as this has been shown effective in a murine model of RA (Nandakumar, Johansson et al. 2007).

The process of antibody production within the ER, however, has barely been addressed as a target within autoimmune diseases so far. There is considerable treatment potential for development of novel treatment strategies directly targeting the process of autoantibody folding, which in turn requires further elucidation of the specific antibody folding machinery.

1.4 FK506 binding proteins (FKBPs)

1.4.1 Overview

Immunophilins are highly conserved proteins and distributed across all tissues and organelles of the cell. Depending on which immunosuppressant drug they preferentially bind to, immunophilins can be subdivided into two subfamilies: Cyclophilins, binding to cyclosporin A (CsA), and FKBP, binding to tacrolimus (also known as FK506 or fujimycin) or rapamycin (also known as sirolimus) (Amaravadhi and Ho Sup 2016).

Both FKBP and cyclophilins show intrinsic PPIase activity. Usually, peptide bonds, covalently linking consecutive amino acids, are energetically highly in favor of the *trans* state, meaning that the angle between the connected amino acids is $\omega=180^\circ$, and the $C\alpha$ atoms of the connected amino acids are on opposite sides of the peptide bond. Peptide bonds with a preceding proline residue, however, are energetically only slightly more favorable of the *trans* state over the *cis* state ($\omega=0^\circ$), due to the cyclic side chain of proline, making isomerization from *cis* to *trans* state an intrinsically slow reaction with a high activation energy (~80 kJ/mol). As a consequence, peptidyl-prolyl *cis-trans* isomerizations often represent rate limiting steps in protein folding (Göthel and Marahiel 1999). The chemical reaction is shown in Figure 4.

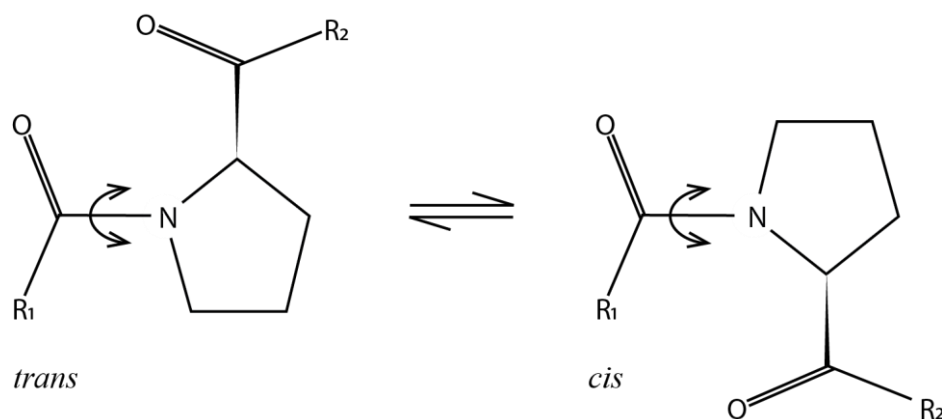


Figure 4: Peptidyl-prolyl *cis-trans* isomerization reaction.

Figure adapted from (Göthel and Marahiel 1999).

Along with their intrinsic PPIase activity, FKBP5s have been shown to carry out numerous functions, including protein folding, chaperone activity, receptor signaling, protein trafficking and transcription (Kang, Hong et al. 2008). Moreover, FKBP5s have been linked to various pathologies, including neurodegenerative disorders such as Alzheimer's Disease (AD) and Parkinson's Disease (PD) (FKBP1A, FKBP4, FKBP5), malignancies (FKBP4, FKBP5, FKBP8) and acquired and inherited, cardiac disease (FKBP1A) (Tong and Jiang 2015, Bonner and Boulianne 2017). This implies that a deeper understanding of FKBP5s may provide novel insights on various pathologies, along with novel treatment strategies.

1.4.2 Classification and structure of FKBP5s

So far, fifteen human FKBP5s have been identified. Each FKBP5s contains at least one FK506-binding domain (FKBD), which usually shows PPIase activity. Moreover, FKBP5s can contain further functional domains, such as calmodulin binding domains (CBDs), transmembrane motifs or tetratricopeptide repeat (TPR) domains, leading to versatile functions of each FKBP5s. Depending on their functional domains, FKBP5s can be categorized into four subgroups: The cytoplasmic, nuclear, TPR domain and secretory-pathway FKBP5s (Rulten, Kinloch et al. 2006). Figure 5 gives an overview of the domain structure of exemplary FKBP5s proteins.

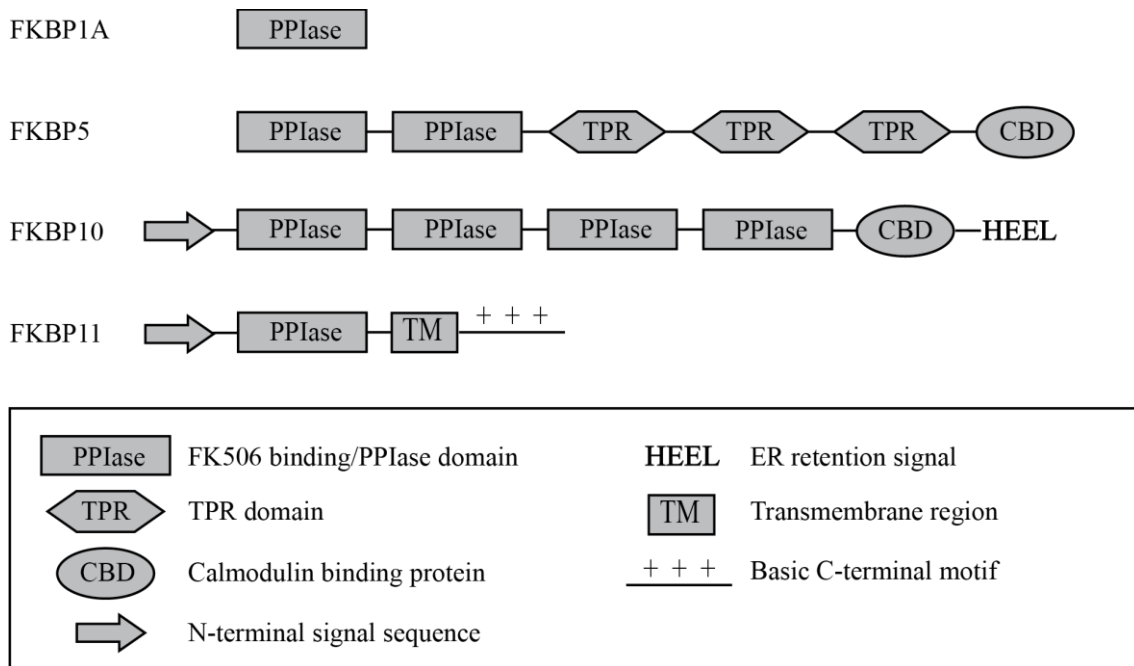


Figure 5: Domain structure of exemplary FKBP proteins.

Figure adapted from (Rulten, Kinloch et al. 2006).

In the literature, FKBP proteins are either referred to according to their gene name, or according to their protein name, which is based on molecular weight. In the present study, gene names will be used as recommended by the Universal Protein resource (UniProt: <http://www.uniprot.org/>, Table 2).

Table 2: Overview on the nomenclature of FKBP proteins.

Molecular weight is indicated in kDa (kilodaltons). Table adapted from (Rulten, Kinloch et al. 2006).

Gene name	Protein name	Molecular weight	Subgroup
<i>FKBP1A</i>	FKBP12	12 kDa	Cytoplasmatic
<i>FKBP1B</i>	FKBP12.6	12.6 kDa	Cytoplasmatic
<i>FKBP3</i>	FKBP25	19 kDa	Nuclear
<i>FKBP15</i>	FKBP133	133 kDa	Nuclear
<i>FKBP4</i>	FKBP52	52 kDa	TPR-domain
<i>FKBP5</i>	FKBP51	51 kDa	TPR-domain
<i>FKBP6</i>	FKBP36	36 kDa	TPR-domain
<i>FKBP8</i>	FKBP38	38 kDa	TPR-domain

Table 2: Overview on the nomenclature of FKBP proteins. (continued)

Gene name	Protein name	Molecular weight	Subgroup
<i>FKBP37.3</i>	FKBP37	37 kDa	TPR-domain
<i>FKBP7</i>	FKBP23	23 kDa	Secretory domain
<i>FKBP9</i>	FKBP60	60 kDa	Secretory domain
<i>FKBP10</i>	FKBP65	65 kDa	Secretory domain
<i>FKBP11</i>	FKBP19	19 kDa	Secretory domain
<i>FKBP14</i>	FKBP22	22 kDa	Secretory domain

The prototype and most abundant FKBP member is FKBP1A, which has been characterized extensively. It is expressed ubiquitously and contains only a single FKBD domain (Figure 5) with high PPIase activity which can therapeutically be inhibited by tacrolimus. By binding of tacrolimus to FKBP1A, a binary complex is formed, which inhibits calcineurin. As a consequence, the nuclear-factor of activated T cells (NF-AT), a transcription factor necessary for upregulation of IL-2 in T cells, is no longer dephosphorylated, resulting in diminished activation and proliferation of T cells (Kang, Hong et al. 2008).

1.4.3 FKBP11

FKBP11 is an ER-resident PPIase and is strongly expressed in secretory tissues, including stomach, pancreas, pituitary glands and lymph nodes. It belongs to the subgroup of secretory pathway FBKPs, and is composed of an N-terminal signal sequence (in keeping with ER residency), a PPIase domain as well as a TM (Figure 5). It possesses a lysine-rich C-terminal tail, which is often found in ER-membrane proteins. Due to its N-terminal signal sequence, anti-FKBP11 antibodies detect a doublet of 19-22 kDa corresponding to a mixture of FKBP11 either containing the N-terminal signal sequence or FKBP11 with a cleaved signal sequence. FBKP11 was shown to bind tacrolimus weakly in vitro, and is supposed to be involved in protein folding of secreted proteins and to act as a molecular chaperone (Rulten, Kinloch et al. 2006, Ishikawa, Mizuno et al. 2017). A distinct function or substrate, however, have not been characterized so far.

Interestingly, FKBP11 is suggested to play a role in B cell biology and (auto-)immunity: The transcriptome of B cells sorted from patients being in the non-active phase of SLE, a severe autoimmune disease, has been shown to express elevated levels of *FKBP11*. Of note, *FKBP11* was elevated along with other genes associated with UPR (Garaud, Schickel et al. 2011). Furthermore, FKBP11^{high} lentiviral mice have been reported to display elevated serum IgG levels, as well as a higher T cell-independent B cell response. Also, the same mice produced increased levels of autoantibodies, including anti-double stranded DNA, anti-thyroglobulin and anti-actin antibodies. In the same publication, FKBP11^{high} lentiviral mice favored plasma cell differentiation, suggesting a role in B cell to plasma cell differentiation (Ruer-Laventie, Simoni et al. 2015). However, these effects have not been shown in a human model so far.

Regulation of FKBP11 is thought to be associated with ER stress and the UPR (Wang, Cui et al. 2018). Various ER stress associated disorders display elevated levels of FKBP11, including SLE (Ruer-Laventie, Simoni et al. 2015), type 2 diabetes mellitus (Lu, Yang et al. 2008) and hepatitis (Lin, Yen et al. 2013). More recently, FKBP11 has been identified as a transcriptional target of XBP1, an important transcription factor within the UPR, in cardiomyocytes, and overexpression of XBP1 along with consequent upregulation of FKBP11 has led to cardiac growth, protecting from heart failure (Wang, Deng et al. 2019).

1.5 Idiopathic pulmonary fibrosis (IPF)

1.5.1 Overview of IPF

Idiopathic pulmonary fibrosis (IPF) is a fatal lung disease with median survival rates ranging from 3-5 years and increasing incidence worldwide. It is the most common type of interstitial lung diseases (ILDs), a large group of parenchymal lung diseases consisting of more than 200 diseases affecting the lung interstitium. In most patients, IPF presents with dyspnea and unproductive coughing. Further findings include myalgia and fine respiratory crackles upon auscultation. Ultimately, patients die due to asphyxiation caused by a severely disrupted gas exchange (King, Pardo et al. 2011, Nalysnyk, Cid-Ruzafa et al. 2012).

The histopathological hallmark of IPF is termed usual interstitial pneumonia (UIP), which is characterized by a heterogeneous pattern consisting of fibroblasts and myofibroblasts,

making up fibroblastic foci, and enormous amounts of deposited collagen and extracellular matrix (ECM). This results in a highly disorganized lung architecture, with honeycomb cyst formation corresponding to large spaces surrounded by fibrotic areas. So far, the mechanisms initiating these changes are not described precisely. Current concepts suggest that environmental threats, such as cigarette smoke, dust and infections, cause recurrent microinjuries to an inherently dysfunctional epithelium, resulting in leakage of the alveolar capillary barrier. Reparation processes then lead to activation of an abnormal remodeling, and finally to accumulation of fibrotic foci with excessive deposition of ECM. The most important profibrotic mediators in this process include transforming growth factor β 1 (TGF β 1), vascular endothelial growth factor (VEGF), platelet-derived growth factor (PDGF) and fibroblast growth factor (FGF) (Fernandez and Eickelberg 2012, Sgalla, Iovene et al. 2018, Butler and Keane 2019). Figure 6 gives a summary on important features in the pathogenesis of IPF.

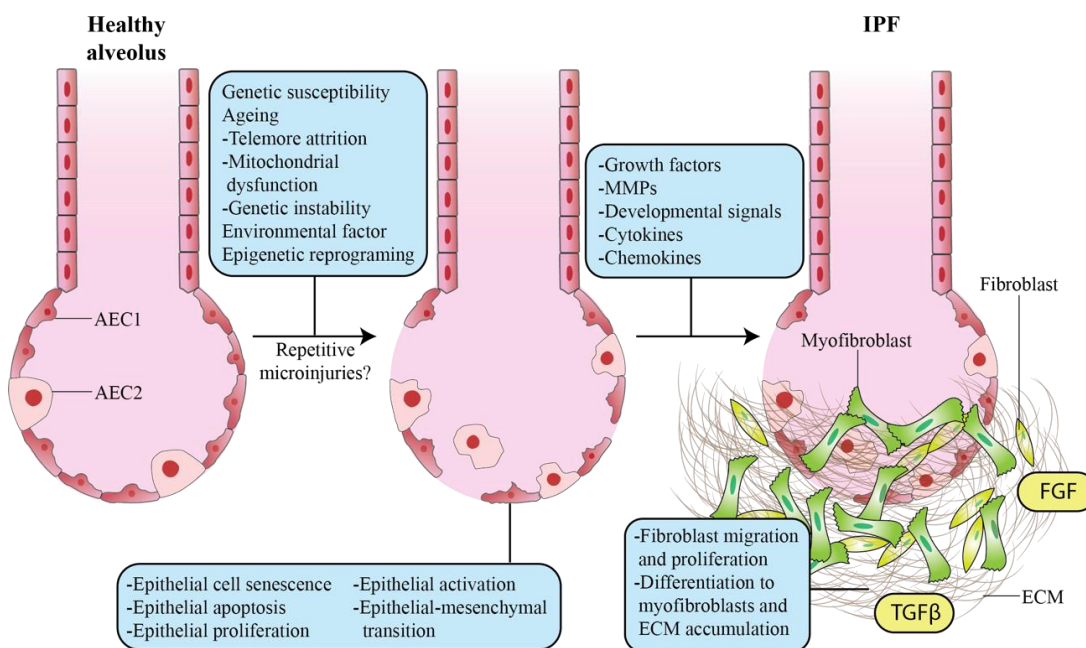


Figure 6: IPF pathogenesis.

IPF is believed to be a result of repetitive microinjuries to a susceptible alveolar epithelium, resulting in fibroblasts differentiating into myofibroblasts with subsequent accumulation of extracellular matrix (ECM). This process is promoted by several growth factors, such as fibroblast growth factor (FGF) and transforming growth factor β (TGF β), cytokines and chemokines. AEC = alveolar epithelial cell, MMP = matrix metalloproteinase. Figure adapted from (Butler and Keane 2019).

The treatment approach towards IPF changed fundamentally within the last two decades. A nonspecific, immunosuppressive approach consisting of prednisolone and azathioprine

once being the standard therapy of IPF has been shown to go along with increased risk of death and hospitalization, and was therefore abandoned (Raghu, Anstrom et al. 2012). Only in the last few years, two novel antifibrotic medications, pirfenidone and nintedanib, were admitted for IPF therapy, and are both listed with “Conditional recommendation for use” in the “Official ATS/ERS/JRS/ALAT Clinical Practice Guideline” (Raghu, Rochwerg et al. 2015). Both compounds were shown to slow down the decline in lung function, however, they do not cease disease progression (Spagnolo, Tzouveleakis et al. 2018).

1.5.2 Autoimmune features in lung fibrosis and IPF

Numerous systemic autoimmune diseases, including SLE, RA and systemic sclerosis, can affect the lung and lead to lung fibrosis (Mayberry, Primack et al. 2000). Underlying autoimmune processes involve inappropriate activation of autoreactive T cells as well as autoreactive B cells (Chizzolini 2008). Of note, experimental setups in the mouse model have shown that autoantibodies in particular can cause and deteriorate lung fibrosis (Komura, Yanaba et al. 2008, Shum, Alimohammadi et al. 2013, Vittal, Mickler et al. 2013, Mehta, Goulet et al. 2016), while B cell depletion is protective towards development of lung fibrosis (Yoshizaki, Iwata et al. 2008, François, Gombault et al. 2015, Matsushita, Kobayashi et al. 2018).

In IPF, there is increasing evidence arguing for autoimmune features present in this disease. A recent proteomic study revealed elevated numbers of MZB1-positive plasma cells in lung tissues from IPF patients, as well as elevated IgG levels in the same tissues (Schiller, Mayr et al. 2017). In serum of IPF patients, an increased ratio of circulating plasmablasts has been detected, along with elevated Plasma B lymphocyte stimulating factor (BlyS), a soluble factor promoting B cell growth and differentiation. Interestingly, concentrations of BlyS have been associated with disease activity. Serum analysis of IPF patients has also shown increased concentrations of both non-organ specific as well as organ specific antibodies (Xue, Kass et al. 2013). Moreover, distinct HLA class II alleles are overrepresented in patients with IPF (Xue, Gochuico et al. 2011, Fingerlin, Zhang et al. 2016).

These autoimmune features demonstrate high potential for novel specific, targeted therapies in IPF. Plasma exchange therapy, for instance, with subsequent elimination of autoantibodies, has led to an improved gas exchange in patients with acute exacerbations

of IPF (Donahoe, Valentine et al. 2015). In interstitial lung diseases associated with connective tissue disease (CTD-ILD), several studies have shown an improvement of functional lung parameters upon rituximab treatment (Bellan, Patrucco et al. 2020). Rituximab could also be a therapeutic option in IPF in particular and is currently being evaluated in a Phase II clinical trial (ClinicalTrials.gov; Identifier NCT01969409).

2 Objectives

Soluble antibodies constitute the final effector molecules of adaptive immunity. Their effector functions are mediated by specific binding of antigen structures, which is strictly dependent on a functional three-dimensional structure attained in the endoplasmic reticulum (ER) with the aid of the ER-resident protein folding machinery (Feige, Hendershot et al. 2010, Feige and Buchner 2014). Peptidyl-prolyl *cis-trans* isomerases (PPIases) represent an essential part of this machinery and catalyze important, rate limiting reactions in the process of antibody folding. Still, only two PPIases have been identified in this context, namely Cyclophilin B (CypB) (Meunier, Usherwood et al. 2002, Feige, Groscurth et al. 2009, Jansen, Määttänen et al. 2012, Lee, Choi et al. 2012) and FKBP1A (Lilie, Lang et al. 1993).

Immunophilins represent a family of highly conserved PPIases. They can be classified into two main subfamilies, according to which immunosuppressive drug they preferentially bind to: Cyclophilins, binding to cyclosporin A (CsA), and FK506-binding proteins (FKBPs), binding to tacrolimus (also known as FK506) or rapamycin (Amaravathi and Ho Sup 2016). Interestingly, FKBPs have not only been recognized as important factors within physiological processes such as protein folding or receptor signaling, but have also been linked to various diseases including cancer, cardiac diseases and neurodegenerative disorders (Bonner and Boulianne 2017).

In idiopathic pulmonary fibrosis (IPF), a fibrotic lung disease involving autoimmune features, FKBP10 has been shown to be highly elevated and to promote disease progression (Staab-Weijnitz, Fernandez et al. 2015, Knüppel, Heinzelmann et al. 2018). Other FKBPs, however, have not been investigated in the context of IPF. Therefore, the former working group of Prof. Eickelberg has previously analyzed the expression of FKBP proteins in IPF using RNA microarray data from 99 IPF patients and 43 normal controls, identifying differential expression of four additional FKBPs, namely FKBP11, FKBP1A, FKBP5, and FKBP6 in IPF (Figure 10). Only FKBP11 and FKBP5 have had altered expression by more than 2-fold, which for FKBP5 could not be confirmed on protein level. Based on these findings, FKBP11 was chosen for further characterization. In particular, the following questions were addressed in this thesis:

1. Are FKBP11 protein levels upregulated in another, independent IPF cohort?
2. Which cell types express FKBP11 in IPF lung tissue and other human tissues?

-
3. How is FKBP11 regulated in the context of B cell to plasma cell differentiation?
 4. Which function does FKBP11 execute in plasma cells and how does it contribute to antibody folding?

3 Materials

3.1 Instruments

Table 3: Instruments

Device name	Company
-80°C freezer U570 HEF	New Brunswick; Hamburg, Germany
-20°C freezer MediLine Lgex 410	Liebherr; Biberach, Germany
2100 Antigen Retriever	Aptum Biologics; Southampton, U.K.
Analytical scale XS20S Dual Range	Mettler Toledo; Gießen, Germany
Autoclave DX-45	Systec; Wettenberg, Germany
Autoclave VX-120	Systec; Wettenberg, Germany
Axiomager M2	Zeiss; Jena, Germany
BD LSR II Flow Cytometer	Becton Dickinson; Heidelberg, Germany
Cell culture work bench Herasafe KS180	Thermo Fisher Scientific; Darmstadt, Germany
Centrifuge MiniSpin plus	Eppendorf; Hamburg, Germany
Centrifuge Rotina 420R	Hettich; Tuttlingen, Germany
Centrifuge with cooling, Micro200R	Hettich; Tuttlingen, Germany
CO ₂ cell incubator BBD6620	Thermo Fisher Scientific; Darmstadt, Germany
Confocal microscope LSM 710	Zeiss; Jena, Germany
Corning® LSETM Mini Microcentrifuge, 120V	Corning; Wiesbaden, Germany
Coulter Q-Prep working station	Beckman Coulter, München, Germany
Cytospin™ 4 Cytocentrifuge	Thermo Fisher Scientific; Darmstadt, Germany
Dry ice container Forma 8600 Series, 8701	Thermo Fisher Scientific; Darmstadt, Germany
Electronic pipet filler	Eppendorf; Hamburg, Germany
Fridge MediLine LKv 3912	Liebherr; Biberach, Germany

Table 3: Instruments (continued)

Device name	Company
Gel image system ChemiDoc XRS+	Biorad; Hercules, USA
Gene Pulser Mxcell™ Electroporation System	Biorad; München, Germany
Ice machine ZBE 110-35	Ziegra; Hannover, Germany
Light Cycler LC480II	Roche Diagnostic; Mannheim, Germany
Liquid nitrogen cell tank BioSafe 420SC	Cryotherm; Kirchen/Sieg, Germany
Magnetic stirrer KMO 2 basic	IKA; Staufen, Germany
Mastercycler Nexus	Eppendorf; Hamburg, Germany
Microm HMS 740 Robot-Stainer	Thermo Fisher Scientific; Darmstadt, Germany
Mikro-Dismembrator	Sartorius, Göttingen, Germany
Multipette stream	Eppendorf; Hamburg, Germany
Nalgene® Freezing Container	Omnilab; Munich, Germany
NanoDrop 1000	PeqLab; Erlangen, Germany
Neubauer Chamber	Celeromics; Grenoble, France
pH meter InoLab pH 720	WTW; Weilheim, Germany
Plate reader Sunrise	Tecan; Crailsheim, Germany
VWR® Tube Rotator and Rotisseries	VWR International; Darmstadt, Germany
Roll mixer	VWR International; Darmstadt, Germany
Power Supply Power Pac HC	Biorad; Hercules, USA
Scale XS400 2S	Mettler Toledo; Gießen, Germany
Shaker Duomax 1030	Heidolph; Schwabach, Germany
Thermomixer compact	Eppendorf; Hamburg, Germany
Ultra-pure water supply MilliQ Advantage A10	Merck Millipore; Darmstadt, Germany

Table 3: Instruments (continued)

Device name	Company
Vortex Mixer	IKA; Staufen, Germany
Vacuum pump NO22AN.18 with switch 2410	KNF; Freiburg, Germany
Water bath Aqua Line AL 12	Lauda; Lauda-Königshofen, Germany

3.2 Technical equipment

Table 4: Technical equipment

Product name	Company
24-well microplates	Ibidi; Planegg/Martinsried, Germany
96-well imaging plates	Corning, Thermo Fisher Scientific; Schwerte, Germany
96-well microplates	Berthold Technologies; Bad Wildbad, Germany
Cell culture dishes	Corning, Thermo Fisher Scientific; Schwerte, Germany
Cell culture multi-well plates	TPP Techno Plastic Producers; Trasadingen, Switzerland
Cell scrapers	Corning, Thermo Fisher Scientific; Schwerte, Germany
Combitips advanced®	Eppendorf; Hamburg, Germany
Cryovials 1.5 ml	Greiner Bio-One; Frickenhausen, Germany
EDTA-coated vacutainer tubes	Sarstedt; Nümbrecht, Germany
FACS tubes	BD Bioscience; Heidelberg, Germany
Falcon tubes	BD Bioscience; Heidelberg, Germany
Filter tips	Biozym Scientific; Hessisch Oldendorf, Germany
Gene Pulser®/MicroPulser™ Electroporation cuvettes	Biorad; München, Germany
High binding ELISA plates	COSTAR; New York, USA
Measuring pipettes, sterile, single use	VWR International; Darmstadt, Germany

Table 4: Technical equipment (continued)

Product name	Company
Microscope slides	Thermo Fisher Scientific; Darmstadt, Germany
Nylon filters, pore size 70 µm	BD Bioscience; Heidelberg, Germany
PCR plates, 96-well plate	Kisker Biotech; Steinfurt, Germany
Pipettes Research Plus	Eppendorf; Hamburg, Germany
Pipetting tips	Eppendorf; Hamburg, Germany
PVDF membranes	Merck Millipore; Darmstadt, Germany
Reaction tubes	Eppendorf; Hamburg, Germany
Reagent reservoirs	Corning; New York, USA
Sealing foils for PCR plates	Kisker Biotech; Steinfurt, Germany
Shandon™ Single Cytofunnel™ with White Filter Cards	Thermo Fisher Scientific; Darmstadt, Germany
Whatman blotting paper, 3 mm	GE Healthcare; Freiburg, Germany

3.3 Chemicals and reagents

Table 5: Chemicals and reagents

Chemical name	Company
3,3',5,5'-Tetramethylbenzidine (TMB) substrate	Sigma-Aldrich; St. Louis, USA
8M Guanidine-HCl (GdnHCl) Solution	ThermoFisher Scientific; Rockford, USA
87% Glycerol	AppliChem; Darmstadt, Germany
Ammonium peroxodisulfate (APS)	AppliChem; Darmstadt, Germany
Antibody diluent	Zytomed Systems; Berlin, Germany
Bovine serum albumin (BSA)	Sigma-Aldrich; Taufkirchen, Germany
Bromophenol blue sodium salt	Sigma-Aldrich; Taufkirchen, Germany

Table 5: Chemicals and reagents (continued)

Chemical name	Company
Citrate Buffer, pH 6.0, 10×, Antigen Retriever	Sigma-Aldrich; Taufkirchen, Germany
Complete® Mini without EDTA (Protease-inhibitor)	Roche Diagnostics; Mannheim, Germany
DAPI (4', 6-diamino-2-phenylindole)	Sigma-Aldrich; Taufkirchen, Germany
Demineralized water	Thermo Fisher Scientific; Darmstadt, Germany
Desoxyribonucleotides mix (dNTPs)	Fermentas, Thermo Fisher Scientific; Schwerte, Germany
Dimethyl sulfoxide (DMSO)	Carl Roth; Karlsruhe, Germany
Dithiothreitol (DTT)	AppliChem; Darmstadt, Germany
ECL Plus Western Blotting Substrate	Pierce, Thermo Fisher Scientific; Schwerte, Germany
Ethanol	AppliChem; Darmstadt, Germany
Fetal bovine serum (FBS) GOLD, heat inactivated	PAA, GE Healthcare; Freiburg, Germany
Fluorescence mounting medium	Dako; Hamburg, Germany
Isopropanol	AppliChem; Darmstadt, Germany
Light Cycler 480 SybrGreen 1 Master Mix	Roche Diagnostics; Mannheim, Germany
Lipofectamine RNAiMAX	Invitrogen, Life Technologies; Carlsbad, USA
Lymphoprep™	Axis-Shield; Oslo, Norway
Methanol	AppliChem; Darmstadt, Germany
Methylthiazolyldiphenyl-tetrazolium bromide (MTT)	Sigma-Aldrich; St. Louis, USA
Non-essential Amino Acid Solution	Sigma-Aldrich; St. Louis, USA
Non-fat dried milk powder	AppliChem; Darmstadt, Germany
Paraformaldehyde (PFA)	AppliChem; Darmstadt, Germany
Penicillin-Streptomycin (100 U/ml)	Gibco, Life Technologies; Carlsbad, USA
PhosSTOP (Phosphatase-inhibitor)	Roche Diagnostics; Mannheim, Germany

Table 5: Chemicals and reagents (continued)

Chemical name	Company
Protein marker V	Peqlab; Erlangen, Germany
Random hexamers	Applied Biosystems, Life Technologies; Carlsbad, USA
Ready-to-use pNPP substrate for ELISA	MABTECH; Nacka Strand, Sweden
Restore Plus Western Blot Stripping Buffer	Pierce, Thermo Fisher Scientific; Schwerte, Germany
Sodium Bicarbonate (NaHCO ₃)	Sigma-Aldrich; St. Louis, USA
Sodium Carbonate (Na ₂ CO ₃)	Sigma-Aldrich; St. Louis, USA
Sodium Pyruvate	Life Technologies; Carlsbad, USA
SuperSignal West Dura Chemiluminescent Duration Substrate	Pierce, Thermo Fisher Scientific; Schwerte, Germany
SuperSignal West Femto Chemiluminescent Duration Substrate	Pierce, Thermo Fisher Scientific; Schwerte, Germany
TEMED	AppliChem; Darmstadt, Germany
Triton™ X-100	Sigma-Aldrich; Taufkirchen, Germany
Tween 20	AppliChem; Darmstadt, Germany
Tryptan Blue Solution (0.4%)	Sigma-Aldrich; Taufkirchen, Germany
UltraPure Dnase/Rnase-Free Distilled Water	Invitrogen, Life Technologies; Carlsbad, USA
Xylene	Sigma-Aldrich; Taufkirchen, Germany

3.4 Cell culture

3.4.1 Cell lines

To create a better overview in the results section, hybridoma cell lines will be referred to as H1, H2 or H3 according to the following table. All cell lines represent suspension cell lines, apart from A549 which is adherent.

Table 6: Cell lines

Cell line	Cell type	Origin	Distributor/Provider
A549	Lung adenocarcinoma	Human	ATCC; Manassas, USA
P3X63Ag8.653 (AG8)	Myeloma	Mouse	Kindly provided by Dr. Aloys Schepers, Monoclonal Antibody Core Facility, Helmholtz-Zentrum München, Germany
M6A8 (H2)	Hybridoma	Mouse	Kindly provided by Dr. Aloys Schepers
MEM-56 (H1)	Hybridoma	Mouse	Kindly provided by Dr. Aloys Schepers
MIS24C8 (H3)	Hybridoma	Mouse and rat	Kindly provided by Dr. Aloys Schepers
RAJI	Burkitt's lymphoma	Human	Kindly provided by Prof. Edgar Meinel, Institute of Clinical Neuroimmunology, Ludwig-Maximilians-Universität München, Germany

3.4.2 Cell culture media

Table 7: Cell culture media

Medium	Company
DMEM/F12 (1:1)	Gibco, Life Technologies; Carlsbad, USA
Opti-MEM I Reduced Serum Medium	Gibco, Life Technologies; Carlsbad, USA
Phosphate Buffered Saline (PBS), 1x	Gibco, Life Technologies; Carlsbad, USA
RPMI 1690, supplemented with L-Glutamine	Gibco, Life Technologies; Carlsbad, USA

3.5 Small interfering RNA (siRNA)

All small interfering RNAs (siRNAs) were purchased as predesigned products from Ambion, Life Technologies, Carlsbad, USA.

Table 8: Small interfering RNA (siRNA).

siRNA	Species	siRNA ID
scrambled <i>Silencer</i> ® Negative control No. 1	None	AM4611
<i>Silencer</i> ® Select FKBP11 siRNA	Human	s27898
<i>Silencer</i> ® Select FKBP11 siRNA	Mouse and rat	s82617
<i>Silencer</i> ® Select XBP1 siRNA	Human	5533

3.6 Kits

Table 9: Kits

Name	Manufacturer
GeneAmp PCR Kit	Applied Biosystems, Life Technologies; Carlsbad, USA
Human IgG ELISA development Kit	MABTECH; Nacka Strand, Sweden
Pierce BCA Protein Assay Kit	Biochrom; Berlin, Germany
Rneasy Mini Kit	QIAGEN; Hilden, Germany
Subcellular Protein Fractionation Kit for Cultured Cells	Thermo Fisher Scientific; Darmstadt, Germany

3.7 Cytokines, enzymes and inhibitors

Table 10: Cytokines, enzymes and inhibitors

Name	Manufacturer
0.25% Trypsin-EDTA solution	Sigma-Aldrich; Taufkirchen, Germany
Cyclosporin A (CsA)	Sigma Aldrich; St. Louis, USA
FK506 monohydrate (tacrolimus)	Sigma Aldrich; St. Louis, USA
IL-2	Roche Diagnostics; Mannheim, Germany

Table 10: Cytokines, enzymes and inhibitors (continued)

Name	Manufacturer
MuLV Reverse Transcriptase	Applied Biosystems, Life Technologies; Carlsbad, USA
R848 (Resiquimod)	InvivoGen; San Diego, USA
Ribonuclease A (Rnase) from bovine pancreas	Sigma Aldrich; St. Louis, USA
Rnase Inhibitor	Applied Biosystems, Life Technologies; Carlsbad, USA
Tunicamycin	Sigma Aldrich; St. Louis, USA
Trypsin from bovine pancreas	Sigma Aldrich; St. Louis, USA

3.8 Antibodies

3.8.1 Antibodies for Western Blot

Table 11: Primary antibodies for Western Blot

Target	Antibody	Dilution	Manufacturer
ACTB	HRP-conjugated anti-ACTB antibody	1:150000	Sigma Aldrich; St. Louis, USA
BiP	Rabbit monoclonal anti-BiP	1:1000	Cell Signaling; Boston, USA
Calreticulin	Rabbit polyclonal anti-Calreticulin antibody	1:1000	Cell Signaling; Boston, USA
FKBP5	Rabbit monoclonal anti-FKBP5	1:500	Cell Signaling; Boston, USA
FKBP11	Rabbit polyclonal anti-FKBP11	1:1000	Atlas; Stockholm, Sweden
GAPDH	HRP-conjugated anti-GAPDH antibody	1:1000	Cell Signaling; Boston, USA
IgA	Goat polyclonal anti human IgA	1:500	Sigma-Aldrich; St. Louis, USA
IgG	Rabbit monoclonal anti human IgG	1:1000	Abcam; Cambridge, United Kingdom
IgM	Goat polyclonal anti human IgM	1:500	Sigma Aldrich; St. Louis, USA
Lamin A/C	Rabbit polyclonal anti-Lamin A/C antibody	1:1000	Cell Signaling; Boston, USA
PDIA3	mouse monoclonal anti-Erp57 (PDIA3)	1:2000	Abcam; Cambridge, United Kingdom

Table 12: Secondary antibodies for Western Blot

Target	Antibody	Dilution	Manufacturer
Goat IgG	ECL HRP-conjugated anti-goat IgG	1:60000	GE Healthcare; Freiburg, Germany
Mouse IgG	ECL HRP-conjugated anti-mouse IgG	1:60000	GE Healthcare; Freiburg, Germany
Rabbit IgG	ECL HRP-conjugated anti-rabbit IgG	1:60000	GE Healthcare; Freiburg, Germany

3.8.2 Antibodies for immunofluorescence stainings

Table 13: Primary antibodies for immunofluorescence stainings

Target	Antibody	Dilution	Manufacturer
CD20	?	?	?
CD27	Mouse monoclonal anti-CD27	?	Abcam, Cambridge, United Kingdom
CD38	Mouse monoclonal anti-CD38	1:200	Santa Cruz, Dallas, USA
CD45	Mouse monoclonal anti-CD45	1:200	Sigma Aldrich, St. Louis, USA
CD138	Mouse monoclonal anti-CD138	1:200	Sigma Aldrich, St. Louis, USA
FBKP11	Rabbit polyclonal anti-FKBP11	1:100	Atlas, Stockholm, Sweden
IgA	Goat polyclonal anti human IgA	1:100	Sigma-Aldrich, St. Louis, USA
IgG	Mouse monoclonal anti human IgG	1:150	Abcam, Cambridge, United Kingdom
IgM	Goat polyclonal anti human IgM	1:100	Sigma Aldrich, St. Louis, USA

Table 14: Secondary antibodies for immunofluorescence stainings

Target	Antibody	Dilution	Manufacturer
Goat IgG	Alexa Fluor 488 Donkey anti-goat IgG (H+L)	1:250	ThermoFisher Scientific; Rockford, USA
Goat IgG	Alexa Fluor 568 Donkey anti-goat IgG (H+L)	1:250	ThermoFisher Scientific; Rockford, USA
Mouse IgG	Alexa Fluor 488 Donkey anti-mouse IgG (H+L)	1:250	ThermoFisher Scientific; Rockford, USA
Mouse IgG	Alexa Fluor 568 Donkey anti-mouse IgG (H+L)	1:250	ThermoFisher Scientific; Rockford, USA
Rabbit IgG	Alexa Fluor 488 Donkey anti-rabbit IgG (H+L)	1:250	ThermoFisher Scientific; Rockford, USA
Rabbit IgG	Alexa Fluor 568 Donkey anti-rabbit IgG (H+L)	1:250	ThermoFisher Scientific; Rockford, USA

3.8.3 Antibodies for ELISA

Antibody	Species	Dilution	Manufacturer/Provider
Anti-human IgG mAb MT78; ALP conjugated	Mouse	1:1000	MABTECH; Nacka Strand, Sweden
Anti-human IgG mAb MT145	Mouse	1:25	MABTECH; Nacka Strand, Sweden
Lyophilised human IgG standard	Human	Serial	MABTECH; Nacka Strand, Sweden
Anti-mouse IgG (H/L); HRP conjugated	Goat	1:1000	Biorad; Hercules, USA
Monoclonal anti-fibrillin-1, Nr. 78	Mouse	See 4.3	Kindly provided by Dr. Hans-Peter Bächinger, Department of Biochemistry and Molecular Biology, Oregon Health & Science University, Portland, USA

3.8.4 Antibodies for flow cytometry

All primary antibodies for flow cytometry were purchased from BioLegend, San Diego, USA and were used at a concentration of 5µl per 100µl of whole blood as recommended by the distributor. Appropriate isotype control antibodies were purchased from the same distributor and applied conforming to the concentrations of the primary antibodies.

Table 15: Antibodies for flow cytometry

Target	Fluorophore	Clone	Isotype
CD3	APC/Cy7	HIT3a	Mouse IgG2a, κ
CD20	APC/Cy7	2H7	Mouse IgG2b, κ
CD27	PE/Cy7	O323	Mouse IgG1, κ
CD38	APC	HB-7	Mouse IgG1, κ

3.9 Primers for qRT-PCR

All primers were synthesized by MWG Eurofins, Ebersberg, Germany.

Table 16: Primer sequences

Target	Species	Forward primer (5'-3')	Reverse primer (5'-3')
FKBP11	human	GCAATCATTCCTTCTCACT	AGTAGTTGGCTCGGATTAG
Fkbp11	mouse	ACTACACGGGCAGTTTGGTAG	GCTCCAGACCTGGAATCACC
MZB1	human	ACTGGCAGGACTACGG	AAGTAGTGCAAACATGTCCT
PRDM1	human	GGAACTTCTTGTGTGGTATT	TCTGTGTTTGTGTGAGATTC
XBP1	human	CTGAGTCCGCAGCAG	TCCAAGTTGTCCAGAATG
GAPDH	human	TGACCTCAACTACATGGTTTACATG	TTGATTTTGGAGGGATCTCG
Gapdh	mouse	TGTGTCCGTCGTGGATCTGA	CCTGCTTCACCACCTTCTTGA

3.10 Software

Table 17: Software

Software name	Company
Adobe Illustrator	Adobe Inc.; San José, USA
BD FACSDIVA™	BD Biosciences; Heidelberg, Germany
FlowJo Software	TreeStar Inc.; Ashland, USA
GraphPad Prism	GraphPad Software; La Jolla, USA
ImageJ	National Institutes of Health; Bethesda, USA
Image Lab Software	Biorad; Hercules, USA
LightCycler® 480 SW	Roche Diagnostics; Mannheim, Germany
Magelan Software	Tecan; Crailsheim, Germany
Microsoft Office	Microsoft; Redmond, USA
Tristar MicroWin 2000	Berthold Technologies; Bad Wildbach, Germany
ZEN 2010 – Digital Imaging for Lightmicroscopy Software	Zeiss; Oberkochen, Germany

4 Methodology

4.1 Human materials

4.1.1 Patient samples

Patient lung tissue samples and blood specimen were obtained from two independent cohorts from the CPC-M bioArchive (Munich, Germany) and from the UGMLC Giessen Biobank (Giessen, Germany). Human material from the CPC-M bioArchive was authorized by the local ethics committee of Ludwig-Maximilians University of Munich, Germany (333-10). Likewise, human material from the UGMLC Giessen Biobank was approved by the Ethics Committee of the Justus-Liebig-University School of Medicine, Giessen, Germany (No. 31/93, 84/93, 29/01, 10/06, 111/08, and 58/15). Written informed consent was obtained from each subject. The tissue microarray (Multi-normal human tissues, 96 samples, 35 organs/sites from three individuals) was purchased commercially from Abcam, Cambridge, United Kingdom (ab178228).

4.1.2 Gene expression data

Preliminary data on FKBP_s in normal histology control (n = 43) and IPF lung tissues (n = 99) were previously collected from the gene expression microarray data set generated on lung tissue samples obtained from the National Lung, Heart, and Blood Institute–funded Tissue Resource Consortium, as described before (Yang, Pedersen et al. 2014, Bauer, Tedrow et al. 2015). Gene expression microarray data (Agilent Technologies, Santa Clara, CA), along with the associated clinical data, can be viewed on the Lung Genomics Research Consortium website (<https://www.lung-genomics.org/research/>) as well as on accession number GSE47460 or the Lung Tissue Research Consortium website (<http://www.ltrcpublic.com>). Significance was calculated using t statistics, while multiple testing was controlled by the false discovery rate method at 5% (Herazo-Maya, Noth et al. 2013).

4.2 Cell culture experiments

4.2.1 Cell culture conditions

A549 cells were maintained in DMEM/F12 medium supplemented with 10% FBS and 100 U/mL penicillin/streptomycin. For experiments, passages p3-p5 were used at a

confluency of 70-80%. RAJI, AG8 and the hybridoma cell lines (H1, H2 and H3) were cultured in RPMI 1690 medium supplemented with L-Glutamine, 10% FBS, 10mM Sodium Pyruvate, Non-essential Amino Acid Solution (1x) and 100 U/mL penicillin/streptomycin. Cells were grown at a density ranging from 2×10^5 – 9×10^5 cells/ml and splitting was performed accordingly. Finally, peripheral blood mononuclear cells (PBMCs) were isolated from whole blood as shown below and cultured in the same manner as RAJI, AG8 and hybridoma cells. All cells were cultivated at 37°C in a direct heat CO₂ incubator containing 5% CO₂. All experiments were repeated at least three times to obtain independent biological replicates.

4.2.2 Isolation of peripheral blood mononuclear cells (PBMCs)

PBMCs were isolated from blood of healthy donors using density gradient centrifugation. For isolation, blood was drawn from healthy individuals and left in heparinized vials for a maximum of one hour at room temperature. Next, blood was mixed in equal parts with PBS and the mixture was carefully poured into a 50ml centrifugation tube containing 15ml of Lymphoprep™ density gradient medium. The vial was centrifuged for 20min at 1080 g at 20°C without brake, resulting in the PBMCs being gathered in a single layer. PBMCs were then transferred to prewarmed medium and washed once using prewarmed medium. For this purpose, cells were spun down at 250 g at +4°C. Afterwards, PBMCs were seeded in a cell culture dish at a concentration of 1×10^6 cells/ml.

4.2.3 Plasma cell differentiation of PBMCs

Following isolation, PBMCs were seeded in a cell culture dish at a concentration of 1×10^6 cells/ml and stimulated by 1000U/ml of recombinant IL-2 and 2.5µg/ml of the TLR 7+8 ligand R848 (resiquimod), which is an established procedure to initiate plasma cell differentiation (Pinna, Corti et al. 2009, Laurent, Hoffmann et al. 2015). As a control, the same volumes of diluents were added to the PBMCs. After 7 days of incubation at 37°C, supernatants were collected to determine IgG concentration. An appropriate number of cells was used to produce cytopins. The remaining cells were harvested for RNA and protein isolation.

4.2.4 Generation of cytopins

To generate cytopins, 100µl of cell suspension ($0.8 - 1.2 \times 10^6$ cells/ml) were transferred into a Cytotunnel™ and spun down to a microscope slide at 300 RPM using a Cytospin™

4 Cyto centrifuge. The cytopins were allowed to dry overnight and the cells were fixed by application of 3.7% paraformaldehyde (PFA) in DPBS for 5min.

4.2.5 MTT cytotoxicity assay

To evaluate cell viability upon tunicamycin treatment or knockdown of FKBP11, methylthiazolyldiphenyl-tetrazolium bromide (MTT) was dissolved in PBS and added to the cultivated cells at a final concentration of 0.5mg/ml and incubated at 37°C for 30 min. For adherent cells, the supernatant was aspirated and crystals were solubilized in 0.5ml isopropanol/0.1% Triton X-100 for 30 min on a shaker at room temperature. Optical density was then measured at 570nm using the Sunrise multiplate reader. To estimate the percentage of viable cells, the optical density of the specimen was divided over the optical density received from a control not having received any intervention. For suspension cells, the procedure was similar with the exception that the cells were pelleted at 300 g prior to aspiration of the supernatant.

4.2.6 Trypan Blue exclusion assay

To estimate the number of viable cells, cell suspensions were mixed with equal volumes of Trypan Blue solution (1:10 in PBS) and transferred to a Neubauer chamber. Next, viable cells in four squares were manually counted, excluding blue cells. The number of cells per ml was then calculated using the following formula:

$$\text{Cells/ml} = (\text{Number of Cells} \times 10000) / (\text{Number of squares} \times \text{dilution})$$

To determine the total number of cells, the calculated value was multiplied by the total volume of the cell suspension.

4.2.7 Tunicamycin treatment of A549 and RAJI cells

The artificial ER stress inducer tunicamycin was used to induce ER stress in A549 and RAJI cells. For tunicamycin treatment of A549 cells, see 4.2.8. For RAJI, cells were washed once in PBS and resuspended in starvation medium (RPMI 1640, 0.5% FBS) at a density of 3×10^5 – 5×10^5 cells/ml. Following 24 hours of starvation, cells were washed in PBS and resuspended in starvation medium containing different concentrations of tunicamycin (0.01mg/ml, 0.1µg/ml, 0.5µg/ml, 1µg/ml or 5µg/ml) or an equal volume of DMSO as a non-treated negative control. 24 hours later, cell viability was evaluated by an MTT cytotoxicity assay to rule out any relevant cell death due to tunicamycin

treatment. Expression of *FKBP11* was then assessed on both protein and transcript levels. To verify successful induction of ER stress, expression of *BiP* was visualized using Western Blot analysis.

4.2.8 SiRNA-mediated transfection of A549 cells

For experiments involving A549 cells, knockdown was achieved using reverse transfection. First, transfection mixtures containing Opti-MEMTM I Reduced Serum Medium, Lipofectamine RNAiMAX and relevant siRNA (*FKBP11* siRNA, *XBP1* siRNA) or negative control, scrambled siRNA (scr siRNA) were prepared and incubated for 20 minutes in 6-well plates. Next, A549 cells were detached using trypsin and resuspended in DMEM/F12 medium supplemented with 10% FBS. The resulting cell suspensions were transferred onto the prepared transfection mixtures. The final siRNA concentration was 10nM, and the cells were seeded at a density of 5×10^4 – 5.5×10^4 cells/cm². After an incubation time of 6–8 hours, A549 cells were starved overnight using starvation medium (DMEM/F12, 0.5% FBS) and treated with tunicamycin at different concentrations (0.01µg/ml, 0.1µg/ml, 1µg/ml) or equal volumes of DMSO as a negative control. After 24 hours, cell viability was assessed by Trypan blue exclusion assay and an MTT cytotoxicity assay. The remaining cells were used to isolate protein and RNA in order to perform Western Blot and qPCR analysis. Figure 7 summarizes the experimental setup.

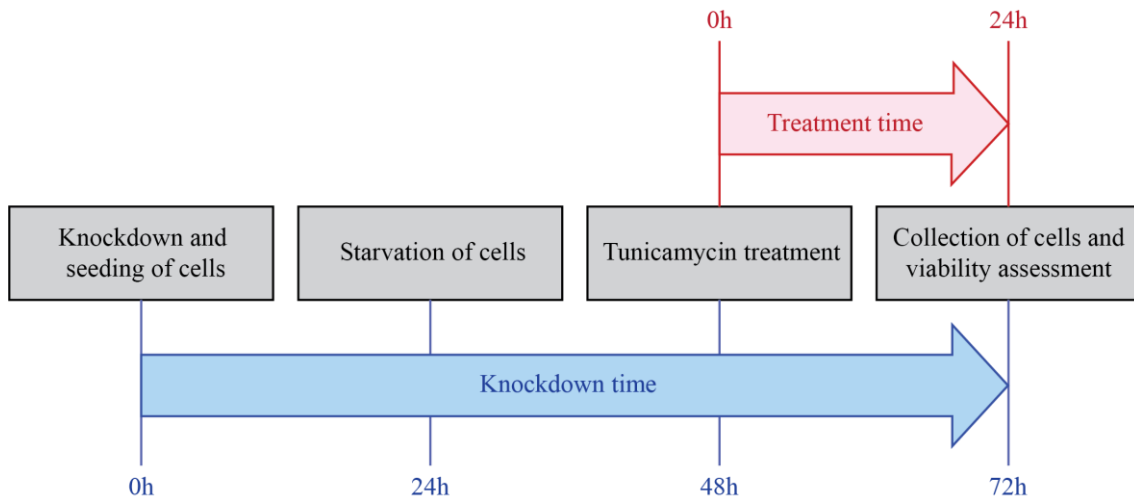


Figure 7: Experimental setup of siRNA-mediated knockdown with subsequent tunicamycin treatment.

Following knockdown and seeding of A549 cells for 24h, cells were starved for another 24h in starvation medium. Then, the tunicamycin treatment was initiated. After 24h of treatment, viability was assessed and the cells were harvested for further analysis.

4.2.9 siRNA-mediated transfection of the hybridoma cell line H3

For the hybridoma cell line H3, transfection was attained by electroporation as shown before (Steinbrunn, Chatterjee et al. 2014). H3 cells at a density ranging from 3×10^5 – 5×10^5 cells/ml were spun down at 300 g and resuspended in fresh RPMI 1640 medium without supplements at a concentration of 6×10^7 cells/ml. After addition of FKBP11 siRNA (targeting both mouse and rat) at a concentration of $3 \mu\text{M}$ or negative control, scrambled siRNA (scr siRNA) at the same concentration, 200 μl of the mixture were transferred to a 2mm electroporation cuvette. Electroporation was then carried out with a Gene Pulser by application of a single exponential decay pulse at a capacity setting of 960 μF and a voltage of 250V. Subsequently, cells were transferred to prewarmed full medium, and stored at 37°C. After 48 hours, cell viability was assessed by Trypan blue exclusion assay and an MTT cytotoxicity assay. Moreover, supernatants were stored to determine levels of antibodies and the cells were harvested in order to review knockdown efficiency on both protein and transcript levels.

4.3 Unfolding and refolding of immunoglobulin G

Antibody refolding was essentially performed as described earlier (Lilie, Lang et al. 1993, Lilie 1997). A monoclonal, mouse anti fibrillin-1 antibody (Reinhardt, Keene et al. 1996)

was denatured using a denaturation solution (3M Guanidine HCl, 0.1M Tris, 0.005M EDTA, pH 7.0) for 24h at an antibody concentration of 80 μ g/ml at 4°C. For initiation of refolding, the denatured antibody solution was diluted under manual shaking by 10 fold in either PBS only, PBS containing a PPIase or PBS containing a control protein (RNase 45 μ M) at 10°C, resulting in an antibody concentration of 8 μ g/ml. Recombinant PPIases used were either Cyclophilin B (5 μ M, positive control) or FKBP11 (45 μ M) (Ishikawa, Mizuno et al. 2017), both of which were kindly provided by Dr. Hans-Peter Bächinger (Department of Biochemistry and Molecular Biology, Oregon Health & Science University, Portland, USA). At given time points, aliquots of the refolding mixture were withdrawn and diluted under vigorous stirring by 12-fold in trypsinized milk (300U/ml Trypsin, 5% Milk, PBS) and kept on ice to stop further refolding. Final antibody concentrations were 0.66 μ g/ml. After completion of the final time point, the amount of correctly refolded antibody was determined by ELISA (see 4.4.1). The experimental setup is pictured in Figure 8.

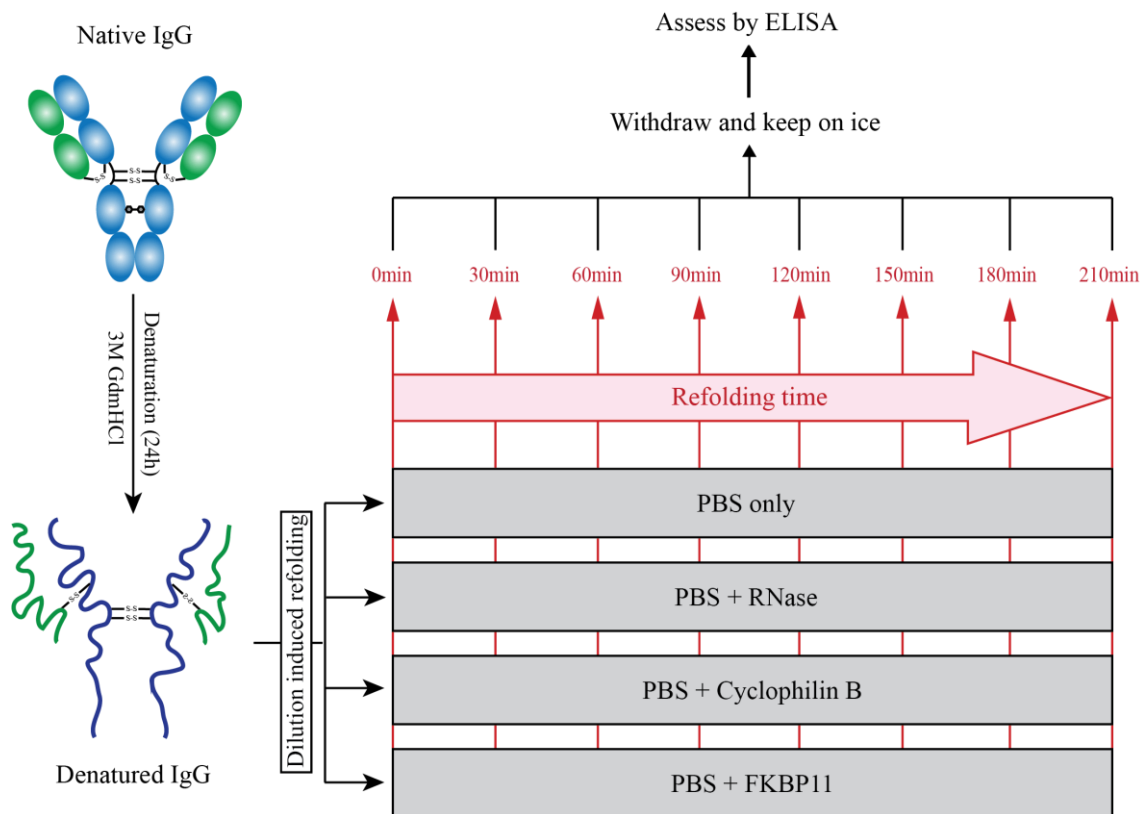


Figure 8: Experimental setup of denaturation and subsequent refolding of IgG.

Following denaturation with 3M GdnHCl, refolding was initiated by dilution (1:10) in either PBS, PBS containing RNase, or PBS containing a PPIase (CypB or FKBP11). At given time points, specimen were withdrawn, trypsinized and kept on ice to prevent further refolding. After collection of all specimen, an ELISA was performed to assess the yield of correctly refolded IgG in each withdrawn specimen.

For experiments involving inhibition of PPIase activity, FKBP11 was preincubated for 1 hour with either FK506 (180 μ M) or DMSO as a negative control at +10 $^{\circ}$ C. As further negative controls, PBS was preincubated with either FK506 (180 μ M) or DMSO. Subsequently, antibody refolding was performed as described above.

4.4 Immunological methods

4.4.1 Enzyme-linked immunosorbent assay (ELISA)

For determination of IgG concentrations in PBMC supernatants, a human IgG ELISA kit was utilized. A high binding ELISA plate was coated with MT145 antibody (in PBS) overnight. After washing once with PBS, blocking was performed for 1 hour with PBS-Tween (0.05% Tween 20). Subsequently, PBMC supernatants acquired after 7 days of IL2/R848 treatment were incubated for 1 hour followed by a washing step. The secondary

antibody MT78-ALP, conjugated with alkaline phosphatase, was applied for 1 hour (diluted in PBS), and, posterior to washing 5 times, ready-to-use pNPP substrate for ELISA was instilled as an appropriate substrate for 20 minutes. Finally, optical density was measured at 405nm using a Sunrise multiplate reader and antibody concentration was calculated by comparison with a standard curve received with the lyophilized human IgG standard.

To assess the rate of correctly refolded IgG, a high binding ELISA plate was coated with recombinantly expressed rf11 (Reinhardt, Keene et al. 1996), which was kindly provided by Dr. Hans-Peter Bächinger, diluted at a concentration of 5µg/ml in coating buffer (0.035M NaHCO₃, 0.015M Na₂CO₃, pH 9.6), overnight. After washing one time with TBS-Tween (0.025% Tween 20), the coated wells were blocked with 5% milk in PBS for one hour. Then, aliquots from the refolding experiment were incubated for one hour. The plate was washed once, followed by one hour of incubation with an HRP-linked anti-mouse antibody. After rinsing the plate 5 times, 3,3',5,5'-Tetramethylbenzidine (TMB) substrate was incubated for 20 minutes and the signal was read at 650nm using a Sunrise multiplate reader. In the graphs, values shown represent the optical density measured at 650nm minus blank values which were received by incubation with trypsinized milk without a primary antibody.

4.4.2 Flow cytometry

To assess the number of circulating plasma cells in blood of IPF patients in comparison with healthy donors, plasma cells from whole blood of IPF patients and healthy donors (all from the CPC-M bioArchive) were sorted using flow cytometry and identified as identified as CD20-/CD3-/CD27+/CD38+ cells (Figure 9). First, venous blood from IPF patients or healthy individuals was collected in EDTA-coated vacutainer tubes. For each staining, 100µl of blood were incubated with appropriate antibodies used to gate for plasma cells (Table 15) for 20 min at 4°C protected from light. In parallel, blood from the same specimen was stained with appropriate isotype controls. Next, lysis of erythrocytes was performed with a Coulter Q-Prep working station followed by data acquisition in a BD LSRII flow cytometer. FlowJo software was used for data analysis. Data was presented as ratios of CD3-/CD20-/CD27+/CD38+ cells to live cells. Negative thresholds for gating were set according to isotype-labelled controls.

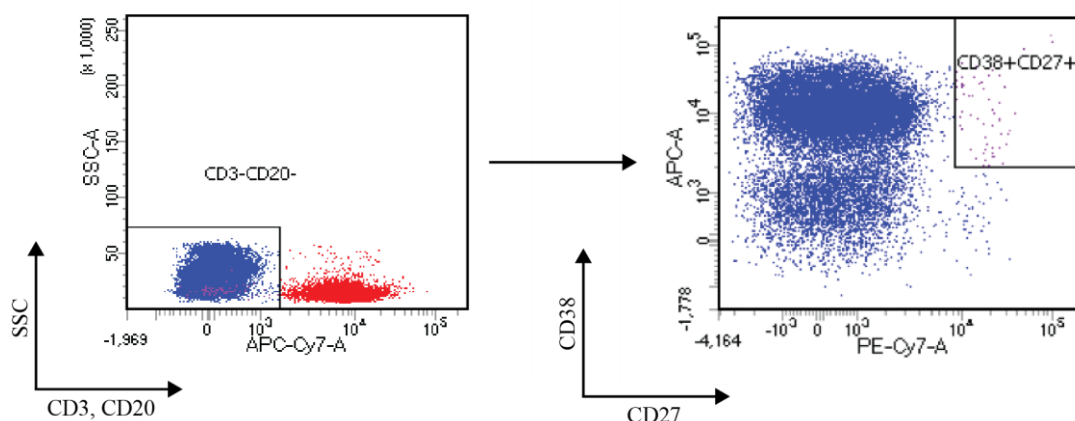


Figure 9: Gating strategy for the detection of circulating plasma cells.

Representative flow cytometry dot-plots of whole blood after red blood cell lysis. Cells were stained with a set of primary, monoclonal antibodies and gated for CD20-/CD3-/CD27+/CD38+ cells, which were characterized as circulating plasma cells. The gates were based on isotype-stained control samples. APC = Allophycocyanin, Cy7 = Cyanine 7, PE = Phycoerythrin, SSC = Side scattered.

4.4.3 Immunohistochemistry

4.4.3.1 Immunofluorescent stainings of tissue sections

For deparaffinization and rehydration, paraffin-embedded sections were placed at 60°C for at least 30min, followed by tissue deparaffinization and hydration using a Microm HMS 740 Robot-Stainer according to the protocol described in Table 18.

Table 18: Deparaffinization protocol

Description	Reagent	Cycles	Time
Deparaffinization step	Xylene	2x	5min
Hydration step	100% ethanol	2x	2min
	90% ethanol	1x	1min
	80% ethanol	1x	1min
	70% ethanol	1x	1min
	dH ₂ O	1x	30sec

After deparaffinization, slides were transferred into citrate buffer (1x, pH 6.0) and heated in a 2100 Antigen Retriever decloaking chamber for 30 seconds at 125°C, and 10 seconds at 90°C, in order to retrieve antigens. Subsequently, sections were allowed to cool down and placed into a blocking solution consisting of 5% BSA in Tris buffer (0.5M Tris, 1.5M

NaCl, pH 6.8) for 40 min to prevent nonspecific binding. Next, primary antibody solutions (Table 13) prepared in antibody diluent were applied to each tissue section for 1 hour and washed three times in Tris buffer (5 min for each washing step). Slides were then incubated with secondary antibodies conjugated to appropriate fluorophores (Table 14) and DAPI (1:1000) for 1 hour. Again, slides were rinsed three times in Tris buffer and covered with Fluorescence Mounting Medium. For examination of the stainings, the Axio Imager Microscope was used.

To quantify FKBP11+/CD38+ cells in IPF and donor sections, ten images sized 1.5mm² were randomly taken of each section. Then, FKBP11+/CD38+ cells were counted from each image, and the counted cells for all 10 images were added up. The person performing the cell counting was not informed about which sections belonged to IPF patients or control.

4.4.3.2 Immunofluorescence stainings of cytopins

All of the following steps were performed at room temperature. After generation and fixation of the cytopins (see 4.2.4), the cells were washed once with DPBS and permeabilized with 0.2% Triton X-100 in DPBS for 2 min to expose intracellular antigens. Next, cells were washed once in DPBS and blocking was performed for 1 hour using a blocking solution (5% BSA, 0.2% Tween, DPBS) to avoid unspecific binding. Primary antibodies prepared in blocking solution were then applied onto the cells for 1 hour, followed by washing three times in DPBS. Subsequently, secondary antibodies conjugated to appropriate fluorophores and DAPI, both diluted in blocking solution, were incubated for 1 hour. Finally, the cytopins were cleansed three times with DPBS and covered with Fluorescence Mounting Medium. The stainings were inspected using the Axio Imager Microscope or Confocal microscope LSM.

4.4.4 Protein analysis

4.4.4.1 Protein isolation

To isolate protein from liquid nitrogen-frozen tissue, samples were homogenized using a Mikro-Dismembrator and taken up in Radio-Immunoprecipitation Assay (RIPA) buffer (50mM Tris HCl pH 7.4, 150mM NaCl, 1% Triton X100, 0.5% sodium deoxycholate, 1mM EDTA, 0.1% SDS) containing a protease and a phosphatase inhibitor cocktail. The solution was then incubated for 30 min on ice, succeeded by short sonification and

centrifugation for 15 min at 13000 RPM at 4°C to clarify the lysates. Pellets were discarded and protein concentration was measured via Pierce BCA Protein Assay Kit following the manufacturer's instructions.

To receive protein from cultured cells, suspension cells were spun down at 300 g and pellets were incubated in RIPA buffer supplemented with a protease and a phosphatase inhibitor cocktail for at least 30 min on ice, followed by centrifugation at 15000 RPM at 4°C. The pellets were discarded and protein concentrations determined as explained above. For adherent cells, the procedure was similar, with the difference that cells were detached using cells scrapers and taken up in RIPA buffer supplemented with a protease and a phosphatase inhibitor cocktail

4.4.4.2 Subcellular fractionation of cultured cells

To generate protein fractions based on their subcellular localization, a subcellular fractionation was performed using a Subcellular Protein Fractionation Kit for Cultured Cells. For adherent cell lines, cells were detached by 0.25% Trypsin-EDTA solution, centrifuged 5 min at 500 g and washed by resuspending the cell pellet in ice-cold PBS. Suspension cell lines were directly centrifuged for 5min at 500 g and washed in the same manner. The resulting cell suspensions were transferred to a 1.5ml centrifuge tube and centrifuged for 3 min at 500 g. The supernatants were discarded and the subcellular fractionation carried out according to the manufacturer's instructions.

4.4.4.3 SDS-Page and Western Blot analysis

Following denaturation of protein samples by Laemmli buffer (65 mM Tris-HCl pH 6.8, 10% Glycerol, 2% SDS, 0.01% bromophenol blue, 100mM DTT) at 95°C for 5-10min, proteins were concentrated on a 4 % SDS-PAGE Stacking gel and subsequently separated by size on a 10% SDS-PAGE Separation gel at 150V per gel for 90 min. The composition of the gels is shown in detail in Table 19 and Table 20.

Table 19: Composition of 4% SDS-PAGE Stacking gel

Reagent	Volume
Millipore-H ₂ O	1.50ml
0.5 M Tris-HCl pH 6.8	630 μ l
10 % SDS	30 μ l
Acrylamide/Bisacrylamide	330 μ l
TEMED	2 μ l
10% APS	13 μ l

Table 20: Composition of 10% SDS-PAGE Separation gel

Reagent	Volume
Millipore-H ₂ O	3.61ml
1.5 M Tris-HCl pH 6.8	2.25ml
10 % SDS	90 μ l
Acrylamide/Bisacrylamide	3ml
TEMED	7.2 μ l
10% APS	45 μ l

After separation, immunoblotting of the protein to a methanol-activated polyvinylidene difluoride (PVDF) membrane was performed at 240mA per gel for 90 min. To prevent non-specific binding, the membrane was blocked with 5% milk in TBS-T (0.1% Tween 20, TBS). This was succeeded by overnight application of primary antibodies (Table 11) at 4°C. After washing the membrane in TBS-T for three times, the membrane was incubated with an appropriate secondary antibody (Table 12) for 1 hour at room temperature. Again, the membrane was washed three times, and proteins were visualized with the Gel imagine system ChemiDoc XRS+ after application of a suitable substrate (SuperSignal™ West Dura Extended Duration Substrate or SuperSignal™ West Femto Maximum Sensitivity Substrate). Detected bands were quantified using Image Lab software or ImageJ software and relative protein abundance was calculated by dividing the band intensity of the target protein over the loading control (ACTB) of the same sample.

4.5 Molecular biological methods

4.5.1 RNA expression analysis

4.5.1.1 RNA isolation

For isolation of RNA from cell cultures, the RNeasy Mini Kit (QIAGEN, Hilden, Germany) was used. For suspension cell cultures, cells were spun down at 300 g and the pellet was resuspended in the lysis buffer provided with the kit. Then, the instructions provided with the kit were followed. After isolation, total RNA was eluted in 35µl of DNase/RNase-free dH₂O and the concentration determined at a wavelength of 260nm using NanoDrop 1000.

For adherent cells, the procedure was similar with the difference that instead of centrifugation, the cells were detached using a cell scraper and diluted in lysis buffer.

4.5.1.2 cDNA synthesis by Reverse Transcription

Following isolation, 1µg of RNA was diluted in 20µl of DNase/RNase-free dH₂O and denatured using an Eppendorf Mastercycler according to the following settings: lid=45°C, 70°C for 10 min and 4°C for 5 min. After denaturation, reagents provided with the GeneAmp PCR kit were added as shown in Table 21, followed by reverse transcription using an Eppendorf Mastercycler (settings: lid=105°C, 20°C for 10 min, 42°C for 60 min and 99°C for 5 min). Finally, the resulting cDNA was diluted at a ratio of 1:4 with DNase/RNase-free dH₂O.

Table 21: Mastermix for cDNA synthesis

Reagent	Stock concentration	Final concentration (40µl)	Final volume (µl)
10x PCR Buffer II	10x	1x	4
MgCl ₂ solution	25mM	5mM	8
PCR Nucleotide Mix (dNTP)	10mM	1mM	4
Random Hexamers	50µM	2.5µM	2
RNase Inhibitor	20u/µl	1u/µl	2
MuLV Reverse Transcriptase	50u/µl	2.5u/µl	2
Denaturated RNA	-	-	18
Total volume of the master mix			40

4.5.1.3 Quantitative Real-Time Polymerase Chain Reaction (qRT-PCR)

To determine relative transcript abundance of a specific gene, quantitative real-time PCR (qRT-PCR) was performed using SYBR Green PCR master mix and primer mixtures (Table 16) with a LightCycler® 480II. The exact composition of reaction mixes is shown in Table 22. The protocol set for the qRT-PCR reaction is summarized below. Denaturation, annealing and elongation were repeated in 45 cycles. Results were indicated as “ $-\Delta C_p$ ” values ($-\Delta C_p = C_p^{\text{reference}} - C_p^{\text{target}}$). For standardization of relative mRNA expression, GAPDH was employed as an endogenous control.

Table 22: qPCR reaction mix

Reagent	Stock concentration	Final concentration	Final volume (μl)
DNase/RNase-free H ₂ O	-	-	1
SYBR Green PCR master mix	2x	1x	5
Forward/Reverse Primer Mix	10 μM each	0.5 μM each	2
cDNA	6.25ng/ μl	12.5ng/ μl	2
Total volume of reaction mix			10

Cycle step	Temperature	Duration	
Initial denaturation	95°C	5min	
Denaturarion	95°C	5sec	45 cycles
Annealing	59°C	5sec	
Elongation	72°C	20sec	
Melting curve	60-95°C	1min	
Cooling down	4°C	On hold	

4.5.2 SiRNA-mediated transfections

For siRNA-mediated transfections, see 4.2.8 and 4.2.9.

4.6 Statistical analysis

Statistical analysis was performed using GraphPad PRISM 5. Data are presented as mean and standard error of the mean (SEM). Each experiment was performed at least three times. Paired data were analyzed by a paired t-test if not indicated otherwise. For unpaired

data, a two-tailed Mann-Whitney was used if not indicated otherwise. A p-value < 0.05 was considered significant. More details on the statistical analysis and on the number of replicates can be found in the associated figure legends.

5 Results

5.1 FKBP11 is highly increased in IPF lung tissues

FKBP proteins fulfil versatile functions in different cell types and have been reported to be involved in various pathologies. In IPF, FKBP10 was previously shown to be increased in IPF lung tissues and to contribute towards the progression of the disease (Staab-Weijnitz, Fernandez et al. 2015, Knüppel, Heinzelmann et al. 2018).

To assess a potential impact of other FKBP proteins on IPF, the working team of Prof. Eickelberg has formerly analyzed differential expression of FKBP proteins within a microarray dataset consisting of 43 healthy control samples and 99 IPF samples (Bauer, Tedrow et al. 2015). With a false discovery rate of 5%, and a fold change cut off of 2.0, FKBP11 (fold change: +2.2) and FKBP5 (fold change: -3.4) were the most differentially expressed FKBP proteins (fold change: +2.2). Interestingly, FKBP11 was more upregulated than FKBP10 (fold change: +1.7), and thus the most upregulated FKBP protein (Figure 10, preliminary data).

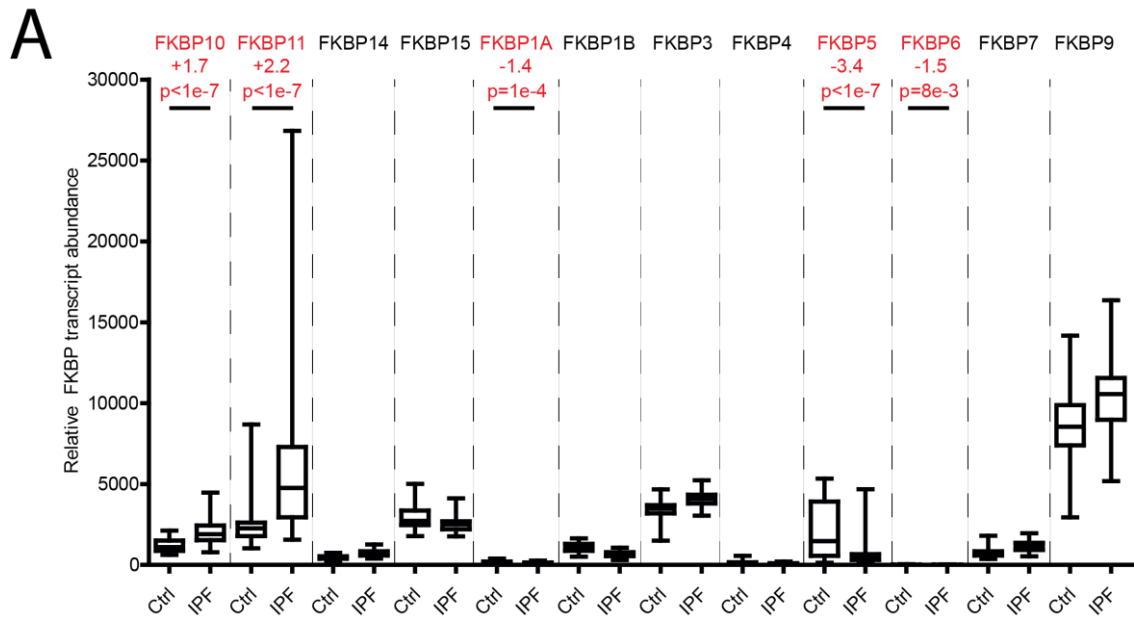


Figure 10: Differential expression of FKBP proteins in IPF lungs (preliminary data).

FKBP gene expression data was extracted from microarray data of normal histology controls ($n = 43$) and samples from IPF patients ($n = 99$) and presented in a Box- and whisker plot. With a false discovery rate of 5% and a fold change cut-off of 2.0, FKBP11 and FKBP5 were the most differentially expressed FKBP proteins, with FKBP11 being the most upregulated (fold change of +2.2). With a fold change of +1.7, FKBP10 expression was also significantly increased in agreement with previous reports (Staab-Weijnitz, Fernandez et al. 2015, Knüppel, Heinzlmann et al. 2018). Results are shown as mean of relative FKBP transcript abundance and error bars represent SEM. Significance was calculated using t statistics (p-values indicated in red), and multiple testing was controlled by the false discovery rate method at 5% (Herazo-Maya et al., 2013).

To verify these findings, protein expression of FKBP5 and FKBP11 was assessed in total lung tissue homogenates of two independent IPF cohorts. While protein levels of FKBP5 did not differ significantly from healthy control lungs (preliminary data, not shown), protein levels of FKBP11 were highly increased in IPF (Figure 11).

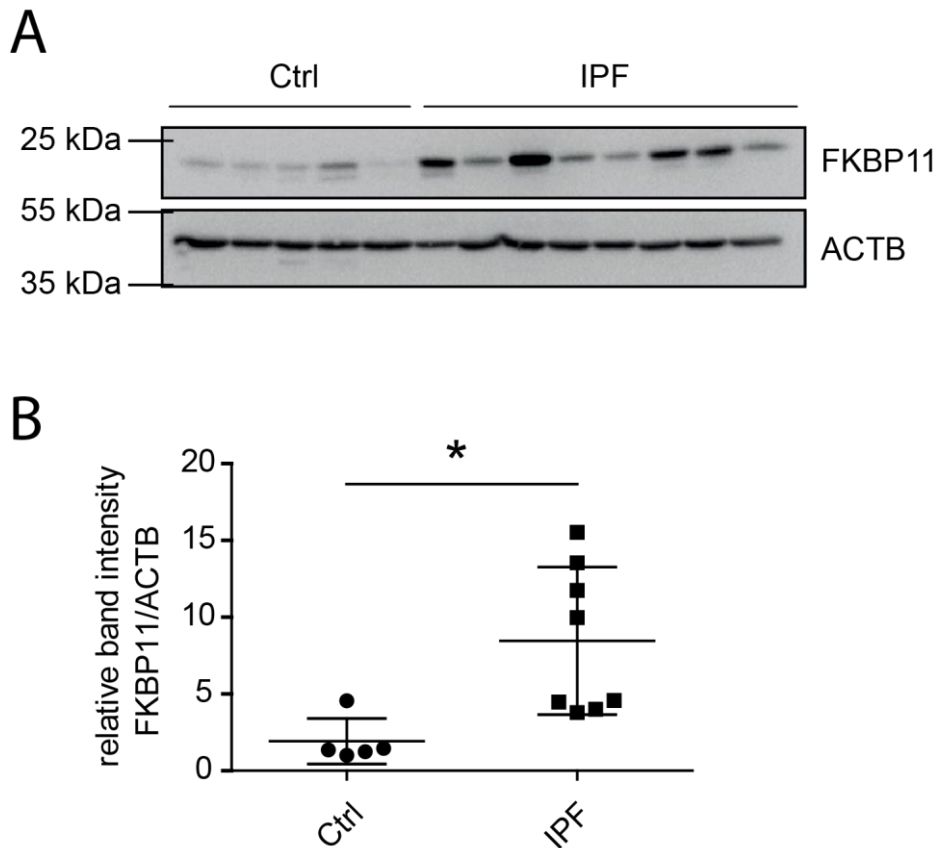


Figure 11: FKBP11 is upregulated in lung tissues of IPF patients.

Western Blot analysis of FKBP11 was performed from whole lung tissue homogenates from donor samples (ctrl) and patients with IPF. Samples were obtained from the UGMLC Giessen Biobank (donor: n=5, IPF: n=8). FKBP11 was significantly upregulated in IPF tissues as compared to donor tissues (ctrl). Results are shown as mean of Western Blot densitometry (relative units, normalized to ACTB) and error bars represent SEM. A two-tailed Mann-Whitney test was used for statistical analysis (* $p < 0.05$). ACTB = β -actin as loading control.

5.2 FKBP11 is identified in CD27⁺/CD38⁺/CD138⁺/CD3⁻/CD20⁻/CD45⁻ plasma cells in IPF lungs

In order to further characterize expression of *FKBP11* in IPF lungs, immunofluorescent stainings of IPF lung tissue sections were performed using different markers of the hematopoietic lineage.

5.2.1 FKBP11 is identified in CD27⁺/CD38⁺/CD138⁺/CD3⁻/CD20⁻/CD45⁻ plasma cells in IPF lungs.

In immunofluorescent stainings, FKBP11 was exclusively expressed by CD27⁺/CD38⁺/CD138⁺/CD3⁻/CD20⁻/CD45⁻ cells in IPF lungs (Figure 12A and B).

This set of markers is typical of plasma cells (Tellier and Nutt 2017). In contrast, FKBP11 was not identified in CD20+ and CD45+ cells (Figure 12B), being typical of naïve B cells (Pagel, Hedin et al. 2003), and neither in CD3+ cells (Figure 12B), marking T cells (Clevers, Alarcon et al. 1988). Moreover, FKBP11 was also found to be expressed in CD38+ plasma cells in lymphatic tissues of the body, such as spleen, tonsils, small intestine and thymus, by using immunofluorescence of a tissue microarray (Figure 12C). This indicates that FKBP11 expression is likely to be a general feature of plasma cells.

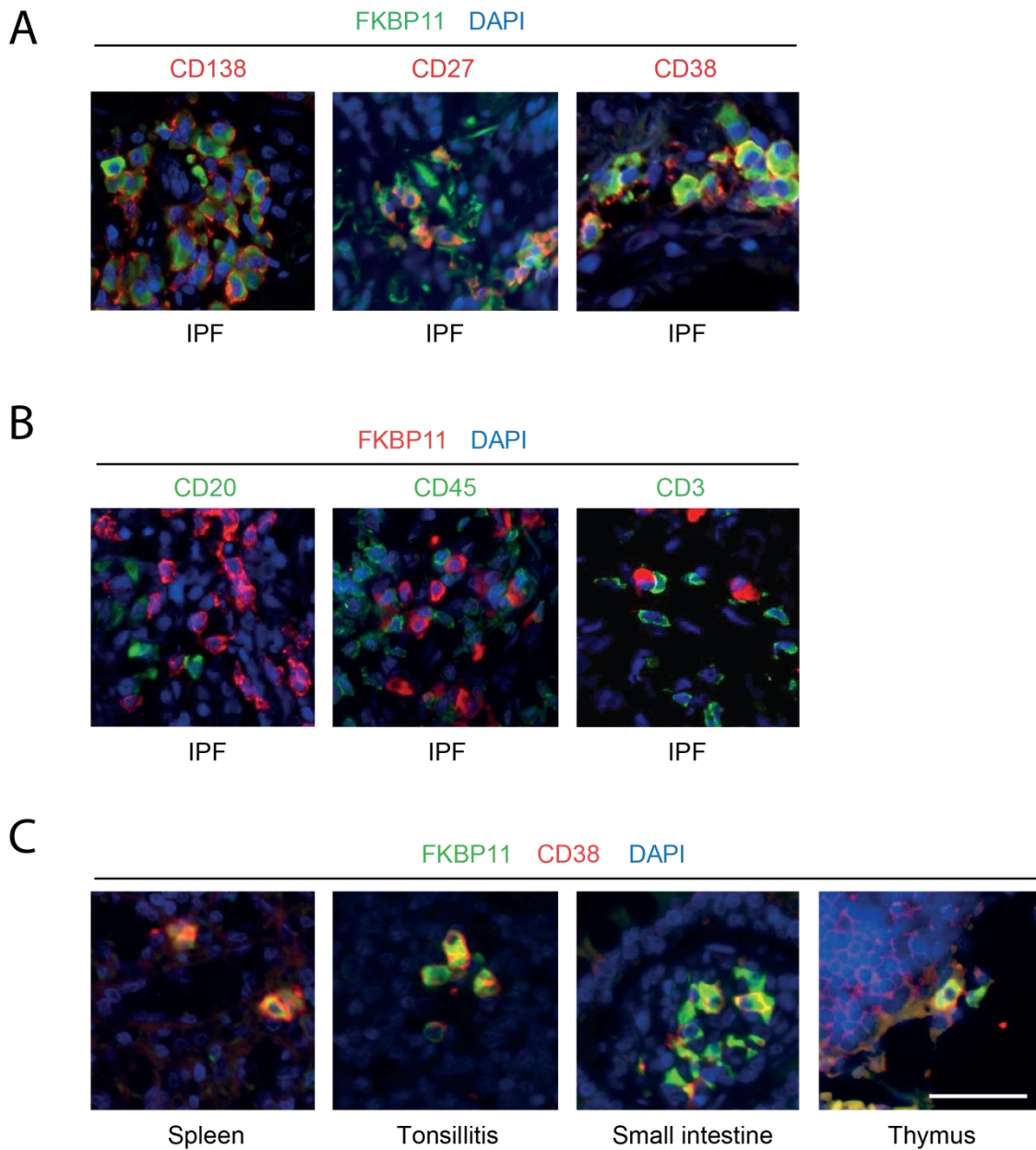


Figure 12: FKBP11 is identified in CD27⁺/CD38⁺/CD138⁺/CD3⁻/CD20⁻/CD45⁻ plasma cells.

Immunofluorescent stainings with different markers of the hematopoietic lineage in IPF lung tissue sections obtained from the CPC-M bioArchive (A and B) and a commercially acquired tissue microarray (C) were carried out. In tissue sections from IPF patients, FKBP11 was identified in CD27⁺/CD38⁺/CD138⁺/CD3⁻/CD20⁻/CD45⁻ cells (A and B). Using a tissue microarray, FKBP11⁺/CD38⁺ cells were found in other lymphatic tissues of the body (C), namely spleen, tonsils, small intestine and thymus. For each staining, one representative image is shown. Each tissue on the microarray contained tissues from three individual, healthy donors (n=3). Scale bar: 200 μ m.

5.2.2 IPF lungs show an elevated number of plasma cells as compared to donor lungs

In consistency with the increase of FKBP11 in lung tissue homogenates of IPF patients shown in Figure 11, the number of plasma cells in immunofluorescent stainings of IPF tissue sections was drastically increased as compared to control sections (Figure 13A and B). This suggests the cause of the elevated FKBP11 levels to be an elevated number of plasma cells. In contrast, using FACS analysis on peripheral blood, no significant increase in circulating plasma cells was detected (Figure 13C). Plasma cells were gated as CD3⁻/CD20⁻/CD27⁺/CD38⁺ cells and displayed in proportion to all living cells (for further details and gating strategy see 4.4.2 and Figure 9). This suggests that plasma cells in IPF lungs differentiate from naïve B cells within the lungs.

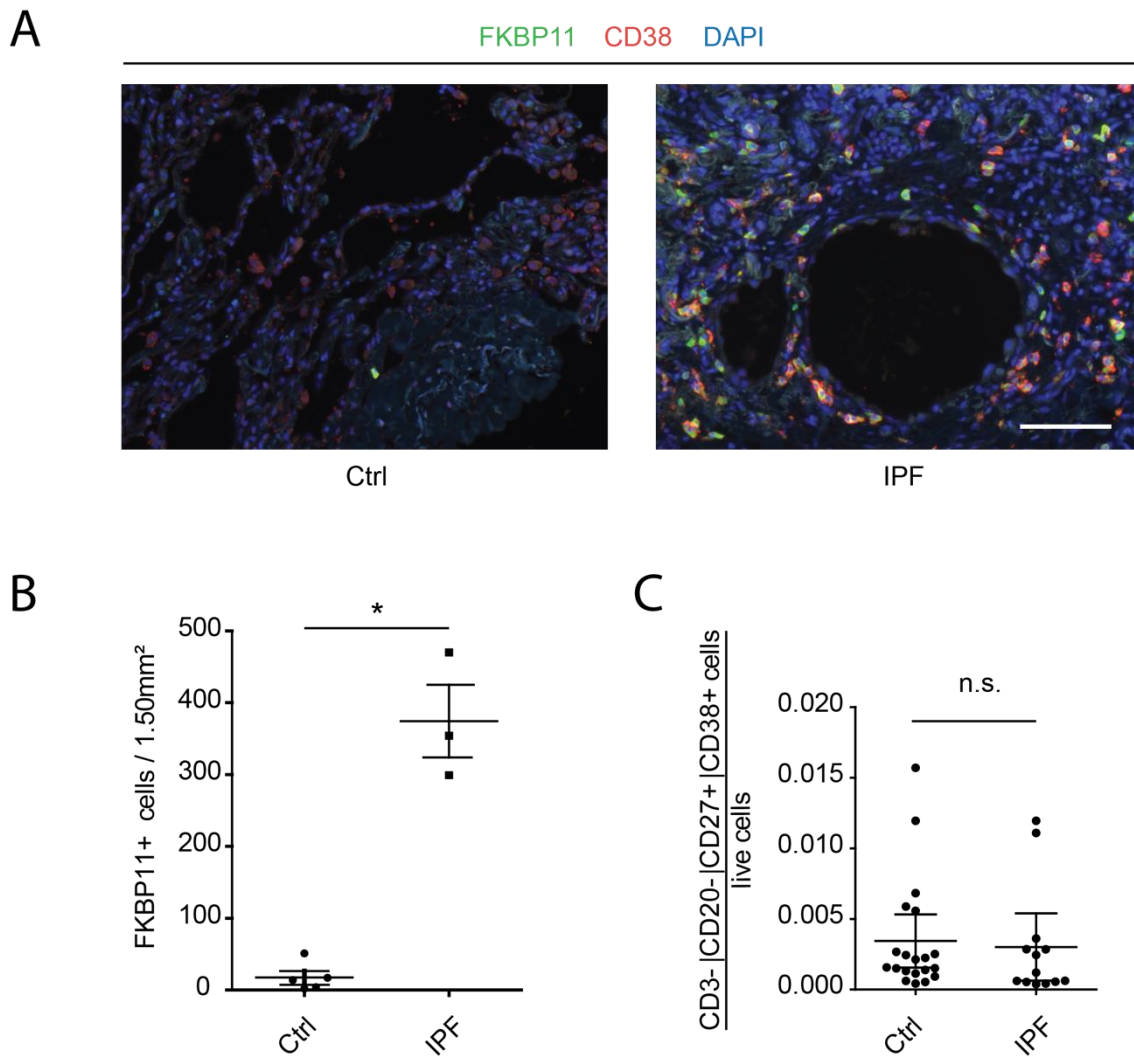


Figure 13: Plasma cells are highly elevated in IPF lungs.

FKBP11+/CD38+ cells were counted in immunofluorescent stainings of control (ctrl, n=5) and IPF (n=3) lung tissue sections from the CPC-M bioArchive. For each section, 10 random images of 1.5mm² were taken and cells counted in each image were added (B). Representative images are shown in (A). To determine the numbers of circulating plasma cells, blood from healthy controls (n=20) and IPF patients (n=13) from the CPC-M bioArchive was sorted for CD3-/CD20-/CD27+/CD38+ cells using flow cytometry (C). In IPF tissue sections, FKBP11+/CD38+ cells were highly elevated as compared to control (B). In peripheral blood, the number of circulating plasma cells was unchanged (C). Results are shown as mean of FKBP11+ cells counts or ratios of CD3-/CD20-/CD27+/CD38+ cells to live cells and error bars represent SEM. For statistical analysis, a two-tailed Mann-Whitney test was used (*p<0.05). Scale bar: 50µm.

5.2.3 FKBP11 is expressed by CD38- secretory cells

Utilizing the same tissue microarray as in 5.2.1, expression of *FKBP11* was analyzed in several different body tissues. Besides plasma cells (CD38+), secretory cells from the pancreas and stomach (both CD38-) showed expression of FKBP11 (Figure 14A). This

is consistent with previous findings suggesting a role of FKBP11 in secretory tissues (Rulten, Kinloch et al. 2006).

Contrarily, other tissues from the tissue microarray, for instance, lung and muscle tissue, did not show expression of either FKBP11 or CD38 (Figure 14B).

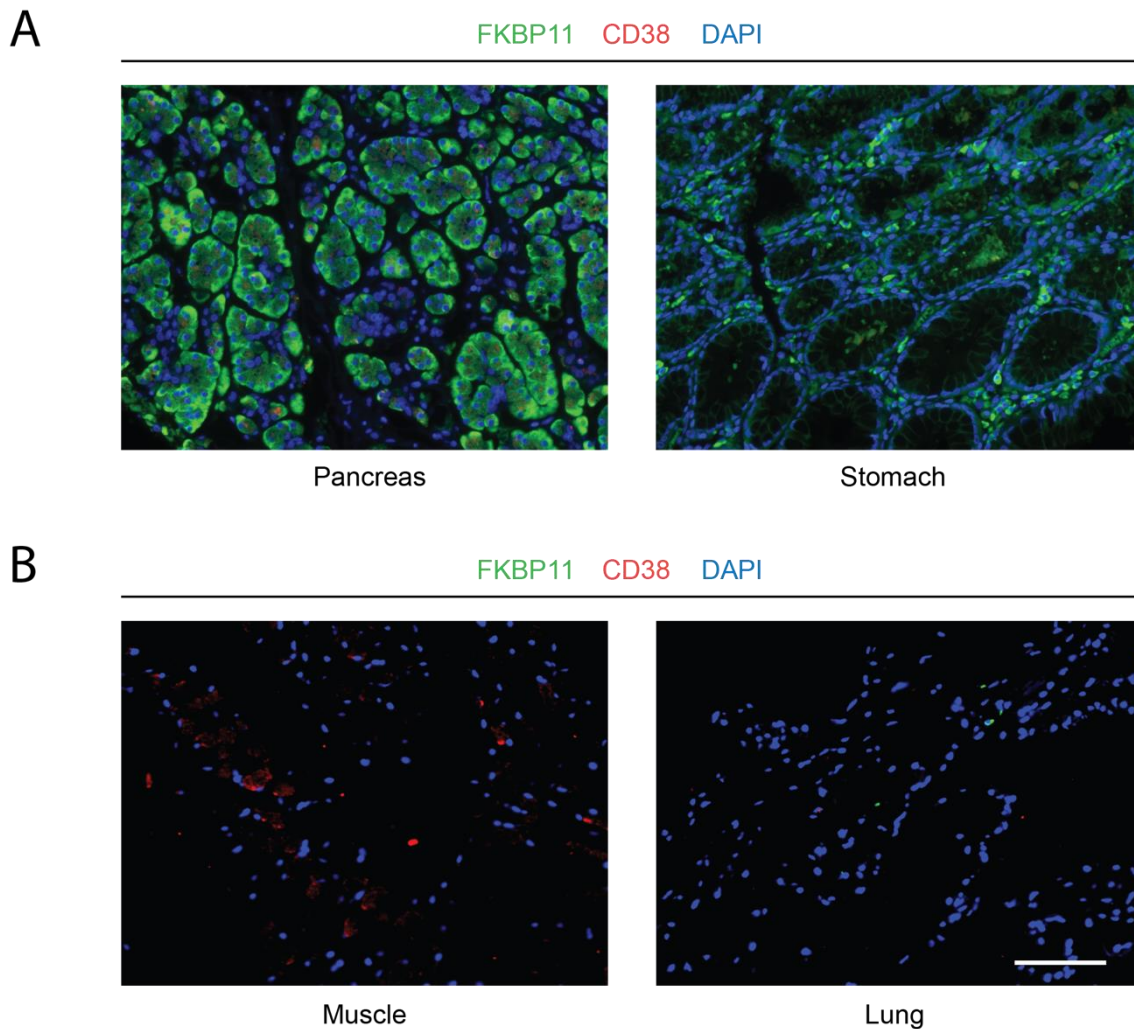


Figure 14: FKBP11 is expressed by CD38- secretory cells in the pancreas and stomach.

A human tissue microarray was stained for FKBP11 and CD38 (also used in Figure 12C). FKBP11+/CD38+ cells are shown in Figure 12C. Pancreas and stomach showed non-plasma (CD38-), FKBP11+ cells (A). The remaining tissues on the tissue microarray, for instance, muscle and lung, did not show expression of FKBP11 (B). Each tissue on the microarray contained tissues from three individual, healthy donors (n=3), and one representative image is shown. Scale bar: 50 μ m.

5.3 In vitro plasma cell differentiation leads to an upregulation of FKBP11.

Given the specific expression of FKBP11 in plasma cells (Figure 12A and C), but not in naïve B cells (Figure 12B), it was hypothesized that FKBP11 is upregulated within the

process of B cell to plasma cell differentiation. To evaluate this, PBMCs from healthy donors were isolated and treated with a combination of IL2 and R848 (resiquimod) for 7 days. This treatment has previously been shown to result in selective activation of memory B cells into antibody producing plasma cells (Pinna, Corti et al. 2009, Laurent, Hoffmann et al. 2015).

5.3.1 IL2/R848 treatment induces plasma cell differentiation

Isolation of PBMCs and subsequent 7-day treatment with a combination of IL2 and R848 lead to an elevated concentration of IgG within cell culture supernatants as compared to vehicle control (Figure 15A). Moreover, cytopins stained for IgG following 7-day treatment showed an elevated number of IgG+ cells (Figure 15B), suggesting that plasma cell differentiation occurred. This was verified by determination of two established markers of B cell activation, namely PRDM-1 (Shaffer, Lin et al. 2002) and MZB1 (Schiller, Mayr et al. 2017). Both markers were significantly increased (Figure 15C). Finally, upregulation of BiP (also HSPA5, GRP78) affirmed promotion of the UPR as an important part of plasma cell differentiation (Figure 16B).

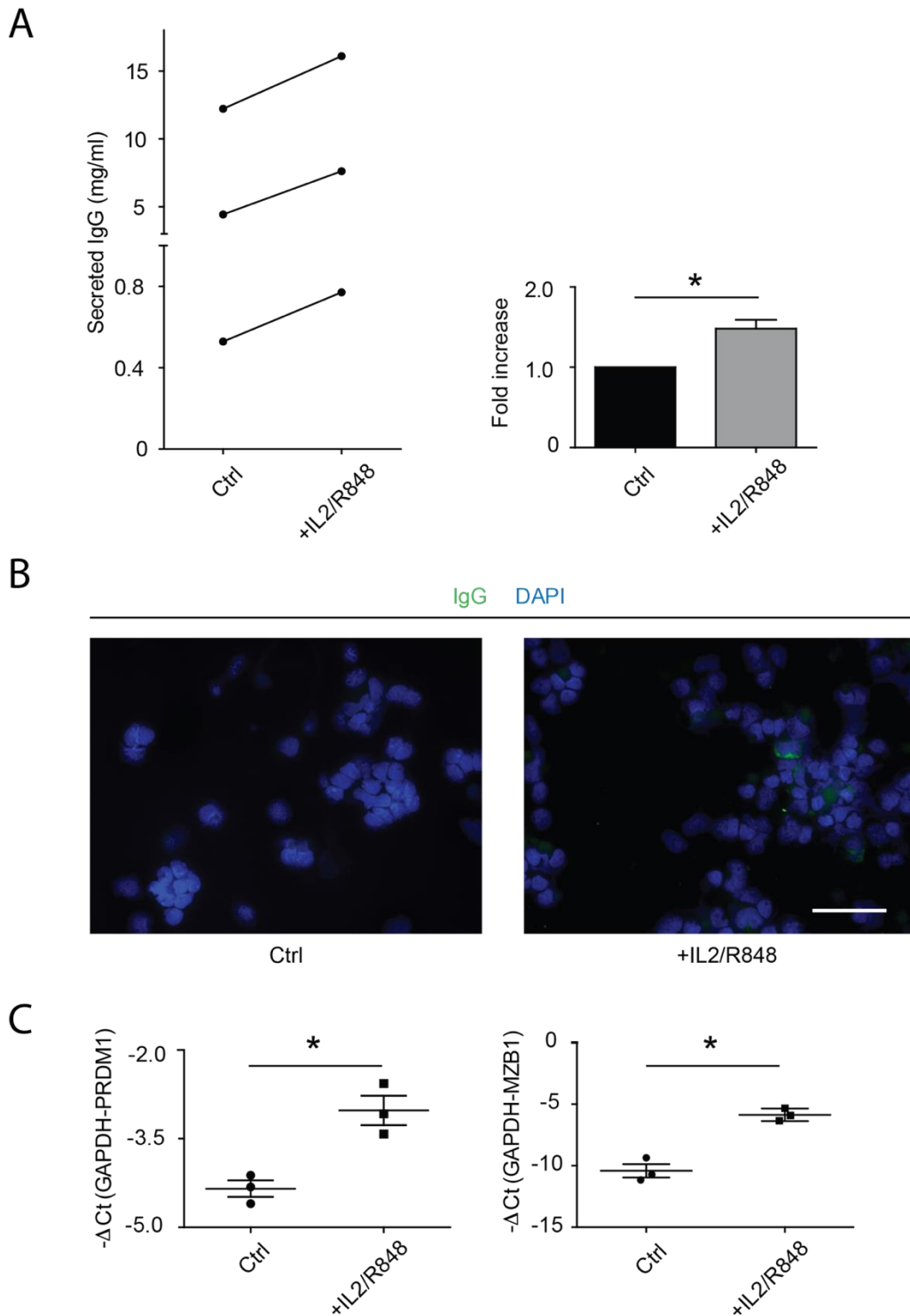


Figure 15: IL2/R848 treatment induces plasma cell differentiation.

PBMCs were isolated from blood of three individual, healthy donors ($n=3$) and treated with a combination of IL2 and R848 or vehicle control (ctrl). Following IL2/R848 treatment, IgG levels in the supernatants were elevated in comparison to control in absolute and relative numbers (A), and cytopins showed IgG positive PBMCs (B). At the same time, transcript levels of the plasma cell differentiation markers MZB1 and PRDM1 were increased (C). Results are shown as mean of relative IgG production or transcript levels (normalized to GAPDH) and error bars represent SEM. A paired t-test was used for statistical analysis ($*p<0.05$). Scale bar: 200 μm .

5.3.2 Plasma cell differentiation induces FKBP11

Determination of FKBP11 in PBMCs treated with IL2/R848 showed a significant elevation of FKBP11 on both transcript (Figure 16A) and protein levels (Figure 16B), indicating that FKBP11 is upregulated within the process of B cell to plasma cell differentiation.

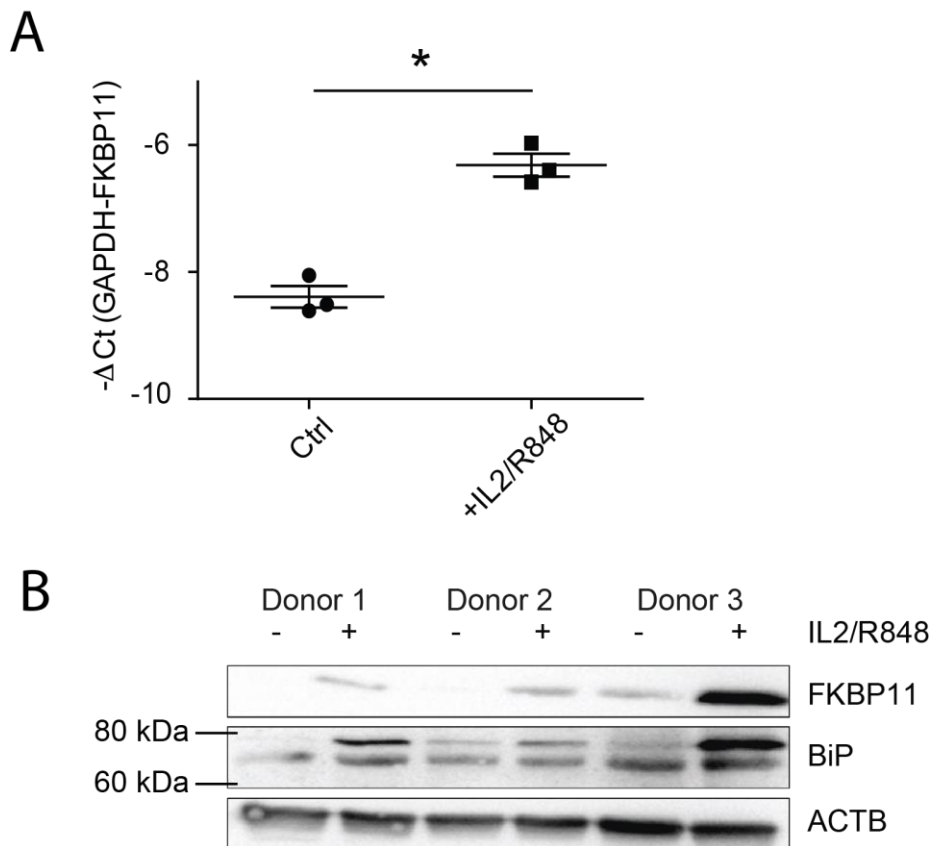


Figure 16: Plasma cell differentiation induces FKBP11.

Following IL2/R848 treatment of PBMCs (Figure 15), transcript and protein levels of FKBP11 were determined. Following treatment, FKBP11 was elevated in comparison to control (ctrl) on both transcript (A) and protein (B) levels. Upregulation of BiP indicated induction of the UPR as a part of plasma cell differentiation (B). The experiment was performed using PBMCs from three individual, healthy donors (n=3). Results are shown as mean of transcript levels (normalized to GAPDH) and error bars represent SEM. A paired t-test was used for statistical analysis (*p<0.05). ACTB = β -actin as loading control.

5.4 FKBP11 is upregulated upon ER stress in an XBP1-dependent manner

For plasma cell differentiation, B cells require to upregulate the unfolded protein response (UPR) in preparation for high rates of antibody production (Tellier and Nutt 2018). The UPR, again, is induced by accumulation of unfolded proteins resulting in ER stress.

Moreover, FKBP11 has been characterized as an ER-resident peptidyl prolyl isomerase (PPIase) (Ishikawa, Mizuno et al. 2017).

Based on these considerations, regulation of FKBP11 upon ER stress was analyzed by induction of ER stress using tunicamycin, an artificial inducer of ER stress (Bassik and Kampmann 2011). Subsequently, subcellular fractionation was performed to detect subcellular localization of FKBP11 in tunicamycin treated cells. The experiments were performed in two different cell lines, namely A549 (derived from lung adenocarcinoma) and RAJI (derived from Burkitt's lymphoma).

5.4.1 FKBP11 is upregulated upon ER stress

24h-treatment of A549 and RAJI cells with tunicamycin lead to an induction of ER stress as indicated by upregulation of BiP (Figure 17). At the same time, tunicamycin treatment lead to upregulation of FKBP11 in a dose dependent manner in both cell lines (Figure 17), suggesting regulation of FKBP11 by ER stress.

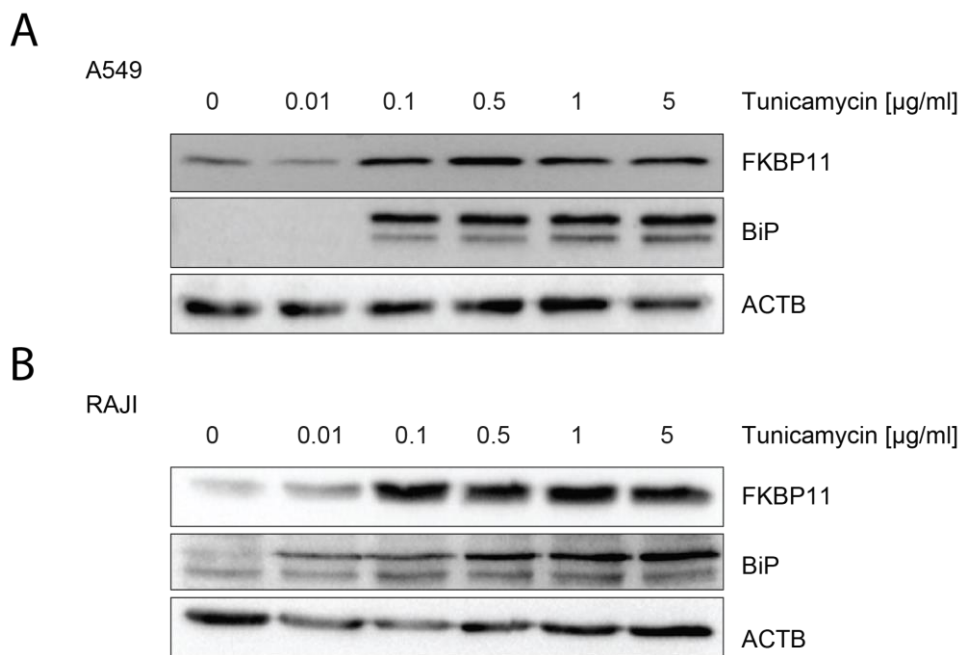


Figure 17: FKBP11 is upregulated upon ER stress.

A549 (from lung adenocarcinoma) and RAJI cells (from Burkitt's lymphoma) were treated with increasing concentrations of tunicamycin to induce ER stress. Upon tunicamycin treatment, FKBP11 was elevated in both A549 (A) and RAJI (B) cells in a dose dependent manner in comparison to vehicle control. Upregulation of BiP confirmed induction of the UPR (A and B). The experiment was performed three times under the same conditions (n=3), and one representative Western Blot was shown for each cell line. ACTB = β -actin as loading control.

5.4.2 FKBP11 localizes to the ER

Given that a concentration of 0.1 μ g/ml tunicamycin was sufficient for induction of ER stress (Figure 17), this concentration was used for the subsequent experiments.

Subcellular fractionation of tunicamycin treated cells displayed predominance of FKBP11 in the microsomal fraction in both A549 and RAJI cells (Figure 18). This pattern was also observed for Protein disulfide-isomerase 3 (PDIA3), a known ER resident protein (Bottomley, Batten et al. 2001). In consistency with previous findings indicating ER residency of FKBP11 (Ishikawa, Mizuno et al. 2017), these results confirm ER residency of FKBP11.

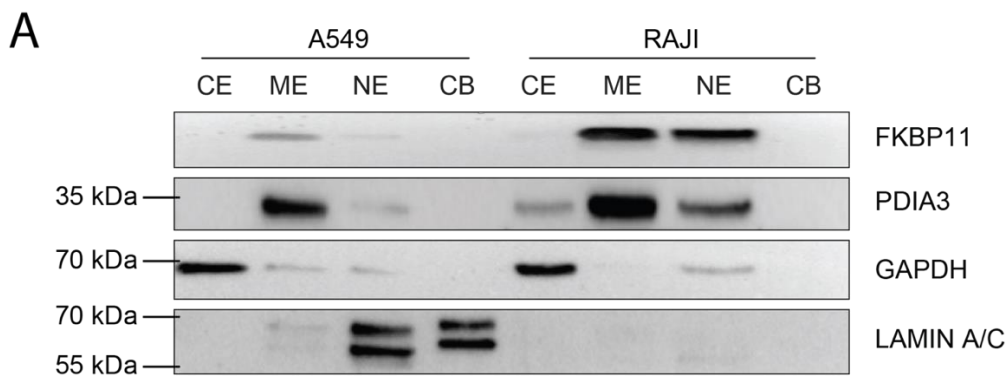


Figure 18: FKBP11 localizes to the ER.

Following tunicamycin treatment (0.1 μ g/ml) of A549 and RAJI cells (Figure 8), subcellular fractionation was performed. Subcellular fractionation showed a similar enrichment pattern for FKBP11 as for the ER-resident Protein disulfide-isomerase 3 (PDIA3), with main localization in the microsomal (ME) and the nuclear extract (NE), but no detection in the cytosolic extract (CE) and in the chromatin-bound extract (CB).

5.4.3 XBP1 mediates upregulation of FKBP11 in ER stress

ER stress is mediated by different pathways inducing distinct transcription factors, including XBP1, ATF4 and ATF6 (Hetz 2012). XBP1, in particular, has been ascribed as an essential factor in plasma cell differentiation and as an important transcription factor of protein folding catalysts within plasma cells (Iwakoshi, Lee et al. 2003). Therefore, siRNA silencing experiments were conducted in order to clarify if FKBP11 is regulated depending on XBP1.

In fact, A549 cells with prior silencing of XBP1 using siRNA showed nearly no upregulation of FKBP11 upon ER stress induced by tunicamycin, as compared to scr

(scrambled) siRNA control (Figure 19B and C). The effective silencing was affirmed on transcript levels (Figure 19A). Taken together, these findings suggest a regulation of FKBP11 by ER stress in an XBP1 dependent manner.

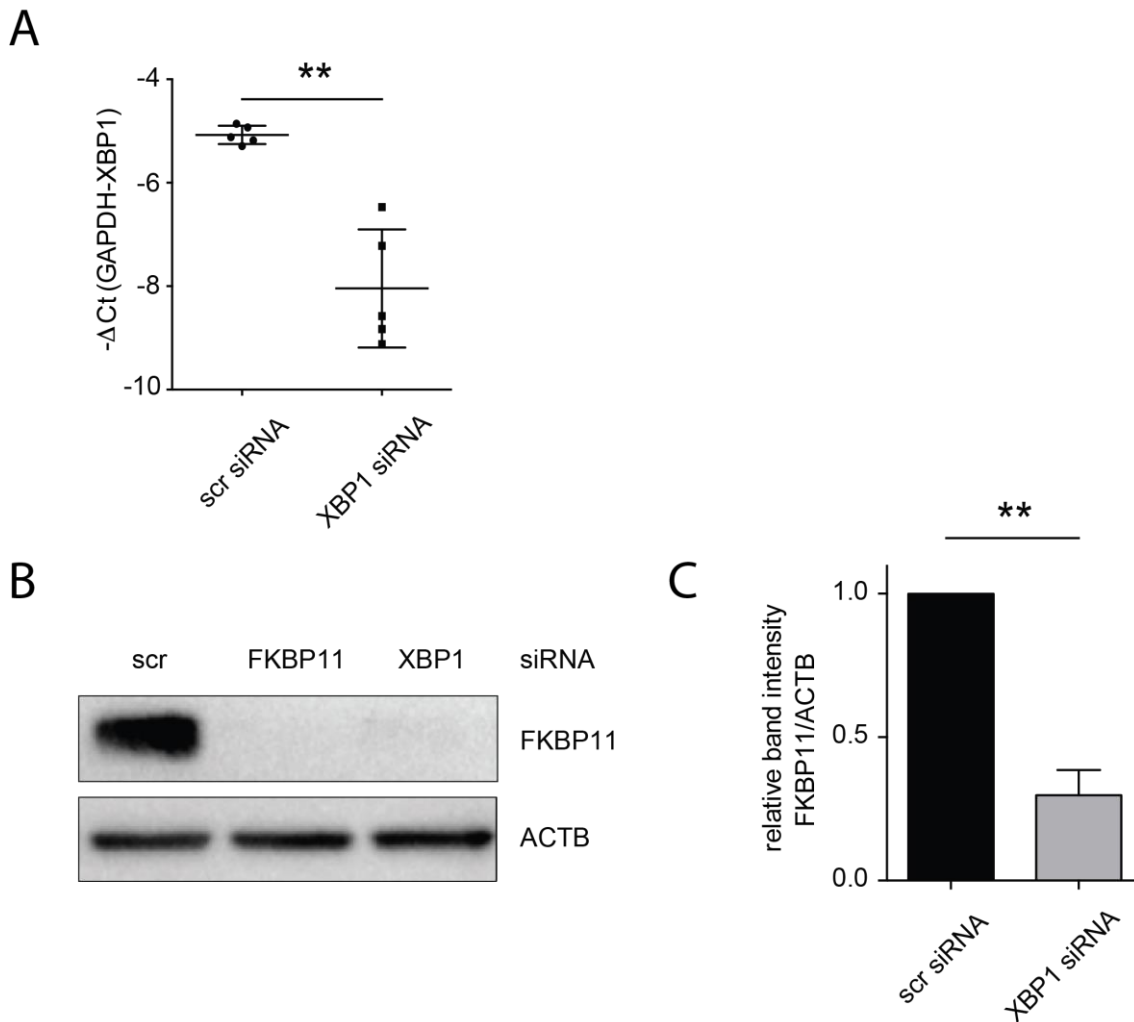


Figure 19: XBP1 mediates upregulation of FKBP11 in ER stress.

A549 cells were transfected using lipofectamine with XBP1 siRNA for XBP1 knockdown or scrambled (scr) siRNA for control and subsequently treated with tunicamycin (0.1μg/ml) for ER stress induction. Transfection with XBP1 siRNA led to knockdown of XBP1 as assessed by qPCR (A, normalized to GAPDH). Following tunicamycin treatment, cells with knockdown of XBP1 did not upregulate FKBP11, as compared to control (scr) showing a clear upregulation of FKBP11 (B,C). The experiment was performed five times under the same conditions (n=5), and one representative Western Blot is shown. Results are shown as mean of transcription levels (normalized to GAPDH) or Western Blot densitometry (relative units, normalized to ACTB) and error bars represent SEM. A paired t-test was used for statistical analysis (*p<0.05, **p<0.01). ACTB = β-actin as loading control.

5.4.4 FKBP11 protects from ER stress induced cell death

To assess the importance of FKBP11 within the unfolded protein response, the effect of siRNA silencing of FKBP11 under the conditions of ER stress was assessed. Upon treatment with tunicamycin, A549 cells with prior siRNA silencing of FKBP11 showed a higher susceptibility towards ER stress mediated cell death as compared to scr siRNA control (Figure 20A). This argues for a protective role of FKBP11 under conditions of ER stress.

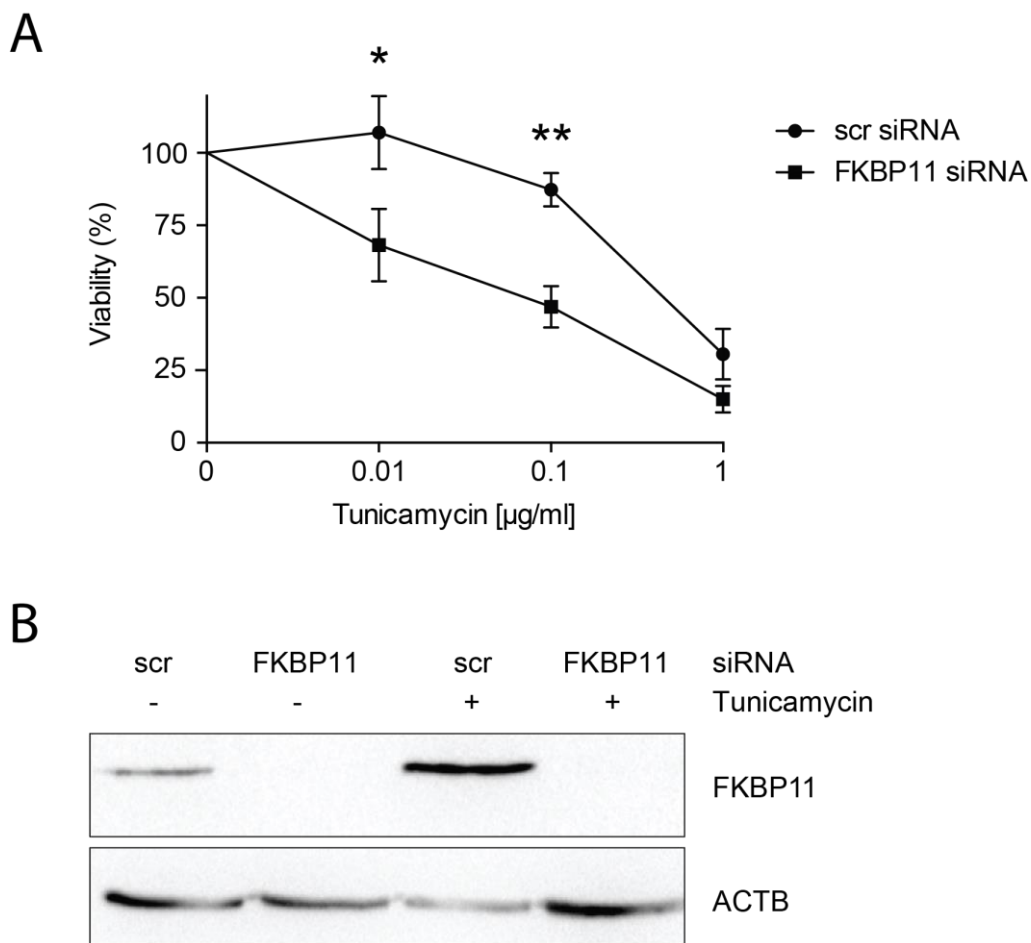


Figure 20: FKBP11 protects from ER stress induced cell death.

A549 cells were transfected using lipofectamine with FKBP11 siRNA for FKBP11 knockdown or scrambled (scr) siRNA for control and subsequently treated with increasing concentrations of tunicamycin for ER stress induction. Transfection with FKBP11 siRNA led to knockdown of FKBP11 as assessed by Western Blot (B, tunicamycin concentration used: 0.1µg/ml). Following tunicamycin treatment, cells with prior knockdown of FKBP11 (FKBP11 siRNA) showed a decreased viability as compared to control (scr siRNA) in trypan blue exclusion (A). The experiment was performed three times under the same conditions (n=3), and one representative Western Blot is shown. Results are shown as mean of percentage of viable cells and error bars represent SEM. A paired t-test was used for statistical analysis (*p<0.05 **, p<0.01). ACTB = β -actin as loading control.

5.5 FKBP11 is a capable antibody folding catalyst

After assessing expression and regulation of FKBP11, the function of FKBP11 was finally to be analyzed. As FKBP11 was specifically expressed by plasma cells (Figure 12 and Figure 13), and upregulated within the process of B cell to plasma cell differentiation (Figure 16), it was hypothesized that FKBP11 is directly involved in the process of antibody production within plasma cells.

5.5.1 FKBP11 is highly expressed in antibody producing hybridoma cell lines

Hybridoma cell lines are used for the production of large amounts of monoclonal antibodies. A hybrid cell line is formed after fusion of antibody producing splenocytes from immunized mice or rats and an immortalized B cell line, a myeloma. As a consequence, the hybridoma combines the capability of antibody production from the antibody producing splenocytes, as well as the longevity and reproductivity from the myeloma (Nelson, Reynolds et al. 2000).

Protein extracts from three antibody producing rat hybridomas (H1-H3) showed high expression of FKBP11 as compared to control (Figure 21A). The mouse myeloma cell line P3X63-Ag8.653 (AG8), which was utilized for fusion of the hybridomas, was used as a control. As expected, AG8, as a non-antibody producing cell line, did not show expression of IgG within the protein extracts as compared to the hybridomas (Figure 21A).

Moreover, subcellular fractionation of H3 displayed an equivalent enrichment pattern as Calreticulin (Figure 21B), another marker of the ER (Michalak, Groenendyk et al. 2009). Using confocal microscopy of H3, colocalization of FKBP11 and Concanavalin A, a marker of the ER (Herman and Shannon 1984), was illustrated (Figure 21C), confirming ER residency of FKBP11 in antibody producing cells.

Taken together, these results support a role of FKBP11 in antibody producing cells.

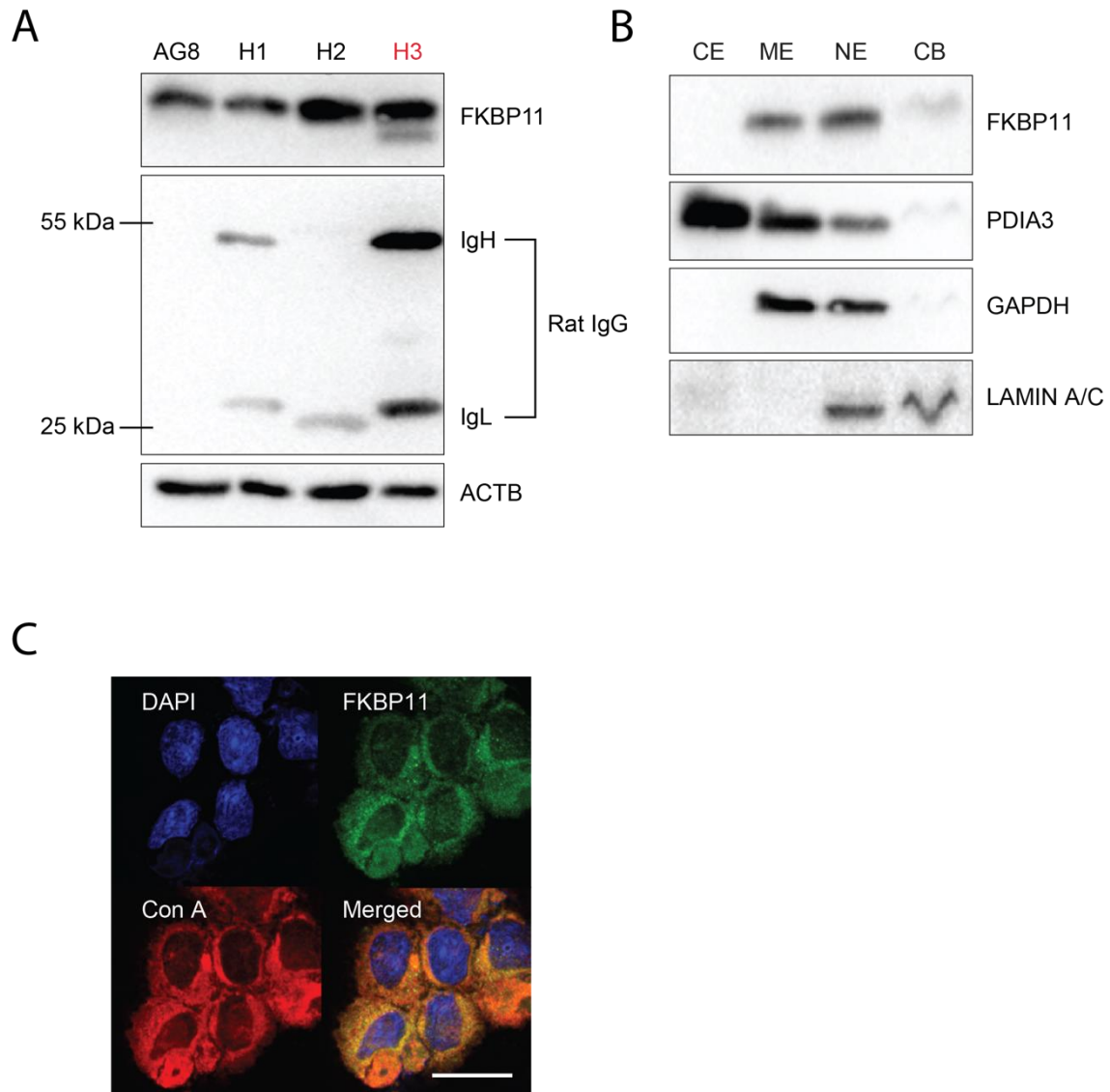


Figure 21: FKBP11 is highly expressed in antibody producing hybridoma cell lines.

Expression of FKBP11 was assessed in antibody producing rat/mouse hybridoma cell lines (H1-H3) using Western Blot analysis (A), and subcellular localization of FKBP11 was determined using subcellular fractionation (B) and confocal microscopy of a cytospin of H3 (C). Protein extracts from three different rat/mouse hybridoma cell lines showed elevated levels of FKBP11 and IgG, as compared to the control mouse myeloma cell line P3X63-Ag8.653(AG8) used for fusion of the hybridomas (A). Subcellular fractionation showed a similar enrichment pattern for FKBP11 as for the ER-resident protein calreticulin (CALR), with main localization in the microsomal (ME) and the nuclear extract (NE), but no detection in the cytosolic (CE) and chromatin-bound (CB) extract (B). Confocal microscopy of a cytospin of H3 displayed colocalization of FKBP11 with Concanavalin A (ConA), a known ER marker (C). ACTB = β -actin as loading control. Scale bar: 20 μ m.

5.5.2 Silencing of FKBP11 results in depressed antibody production

Given the high levels of FKBP11 and IgG in protein extracts (Figure 21A), H3 was chosen for loss of function experiments to further characterize the function of FKBP11. Silencing of FKBP11 was performed using electroporation and subsequent delivery of FKBP11-specific siRNA, resulting in an average knockdown efficiency of 67% (Figure 22A and B).

After 24h, supernatants were immunoblotted and stained for rat IgG, showing significantly less IgG heavy chains (IgH) in supernatants of cells with prior silencing of FKBP11 as compared to scr siRNA control (Figure 22A and C). This further supports a function of FKBP11 in antibody production.

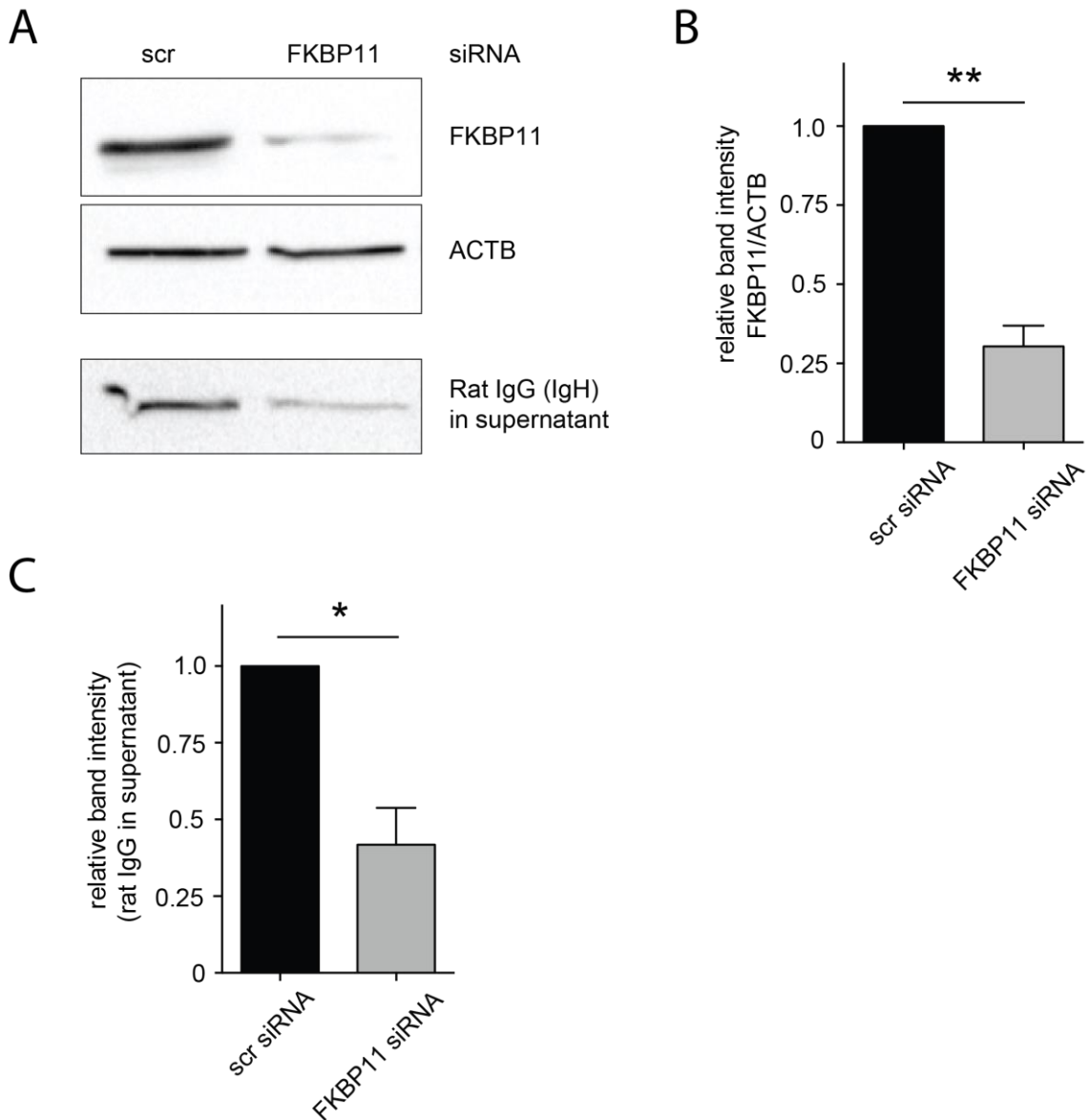


Figure 22: Knockdown of FKBP11 results in depressed antibody production.

The hybridoma cell line H3 (Figure 21) was electroporated and subsequently transfected with FKBP11 siRNA for FKBP11 knockdown or scrambled siRNA (scr) for control. Transfection with FKBP11 siRNA led to knockdown of FKBP11 as assessed by Western Blot (A, B), with an average knockdown efficiency of $67 \pm 16\%$. Knockdown of FKBP11 resulted in less secreted antibodies, as assessed by Western blot analysis of IgG heavy chains (IgH) in the cell culture supernatants (A, C). The experiment was performed four times under the same conditions ($n=4$), and one representative Western Blot is shown. Results are shown as mean of Western Blot densitometry (relative units, normalized to ACTB) and error bars represent SEM. A paired t-test was used for statistical analysis (* $p<0.05$ **, $p<0.01$). ACTB = β -actin as loading control.

5.5.3 FKBP11 is capable of antibody folding *in vitro*

To finally address the hypothesis of FKBP11 functioning as an antibody foldase, an *in vitro* antibody refolding assay was used. In this assay, IgG was fully denatured using

guanidine hydrochloride (GdnHCl). Following denaturation, refolding kinetics in absence and presence of the purified, recombinant FKBP domain of FKBP11 (amino acids Gly28-Ala146, as described in (Ishikawa, Mizuno et al. 2017)) were monitored by an IgG ELISA. The readouts of the ELISA indicated the amount of correctly refolded IgG only, for the reason that antigen-antibody binding is strictly dependent on the native three-dimensional structure of the IgG (Lilie, Lang et al. 1993, Lilie 1997). As negative controls, a vehicle control (PBS) and another protein (RNase) were used. As a positive control, CypB, a commonly known antibody folding PPIase (Feige, Hendershot et al. 2010), was used.

Addition of the purified, recombinant FKBP domain of FKBP11 to the refolding of denatured IgG resulted in an increase of both the rate of refolding and the total yield of correctly refolded IgG as compared to negative controls (Figure 23A). Compared to CypB, however, considerably higher concentrations of FKBP11 (45 μ M of FKBP11 in comparison to 5 μ M of CypB) were required to demonstrate similar effects on refolding activity (Figure 23A).

Prior incubation of the purified, recombinant FKBP domain of FKBP11 with tacrolimus (FK506) inhibited the effects of FKBP11 on antibody folding as compared to prior incubation with vehicle control (DMSO) (Figure 23B). Tacrolimus is a known inhibitor of many FKBP proteins, due to its ability to bind the PPIase activity-bearing FKBP domain (Kay 1996).

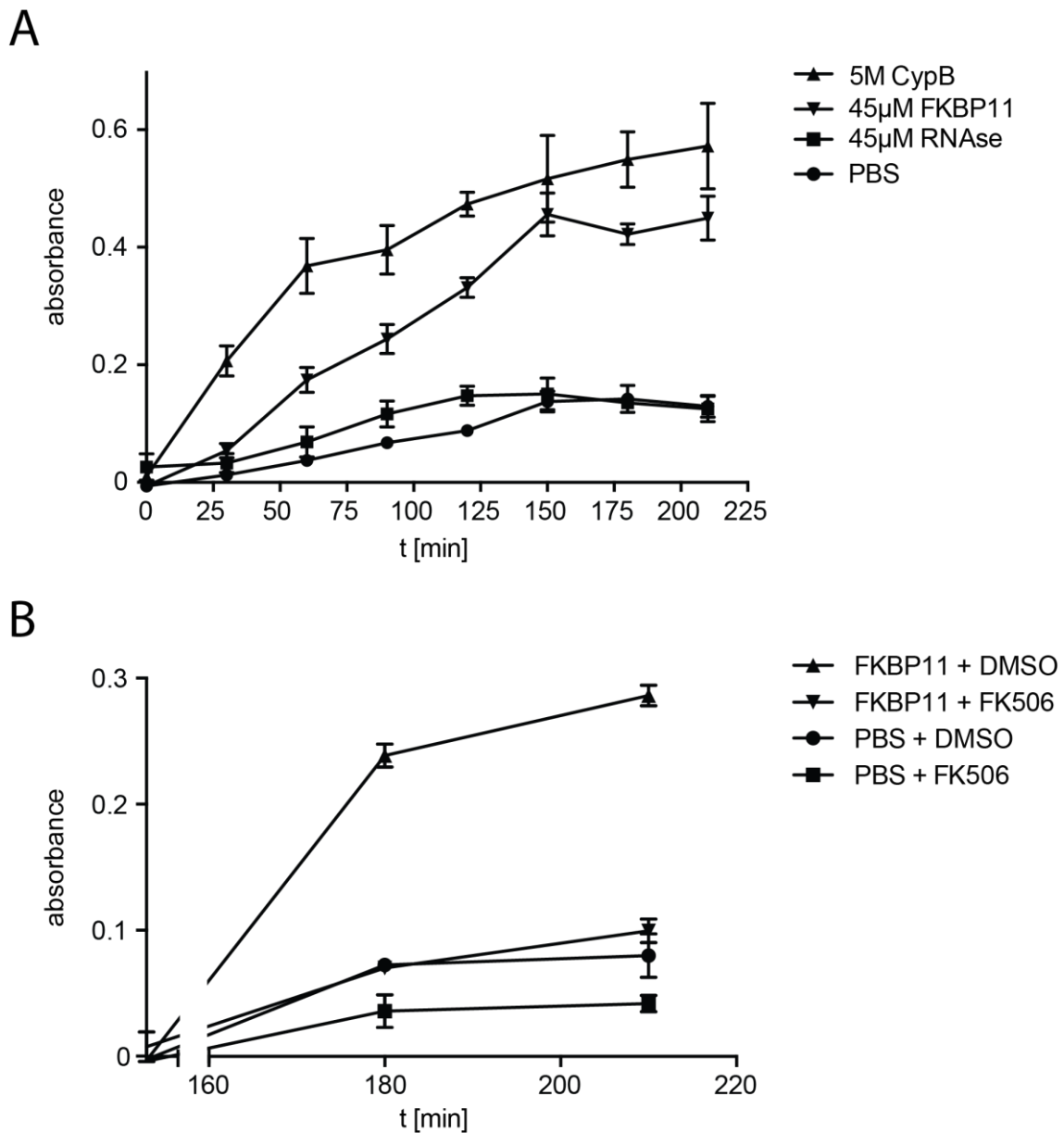


Figure 23: FKBP11 is capable of antibody folding *in vitro*.

Whole IgG was denatured using guanidine hydrochloride (GdnHCl). After denaturation, refolding was initiated by dilution with either pure PBS (vehicle control), 45µM of RNase (negative control, diluted in PBS), 5µM of recombinant Cyclophilin B (CypB, positive control, diluted in PBS) or 45µM of the recombinant FKBP domain of FKBP11 (diluted in PBS). For the refolding experiments, the purified FKBP domain of FKBP11 (amino acids G28 - A146) without the N-terminal signal peptide and the C-terminal transmembrane region was used. Dilution with FKBP11 resulted in an increase of both refolding speed and total yield of refolded IgG as compared to negative controls (PBS, Rnase) (A). In contrast with the positive control (CypB), higher concentrations of FKBP11 were required to demonstrate a similar effect on refolding (45µM of FKBP11 by contrast with 5µM of CypB) (B). The effects of FKBP11 were inhibited by prior incubation with tacrolimus (FK506) (C). The experiment was performed three times under the same conditions (n=3). Results are shown as mean of absorbance minus blank values, and error bars represent SEM.

5.6 Antibody yields are elevated in IPF

Given increased levels of FKBP11 in IPF lung tissues (Figure 11), and the function of FKBP11 in antibody folding (Figure 23), it was assumed that antibody levels in IPF lung tissues are increased. To assess this, immunoblots of IPF lung tissues were stained for the antibody isotypes IgG, IgA and IgM. Moreover, immunofluorescent stainings were performed to evaluate colocalization of FKBP11 with the antibody isotypes IgG, IgA and IgM.

IPF lung tissue samples from MLTs showed increased levels of the antibody isotypes IgG (consistent with data shown before in (Schiller, Mayr et al. 2017)), IgA and IgM as compared to donor samples (Figure 24A).

Interestingly, in immunofluorescence stainings of IPF tissue sections, FKBP11 did only colocalize with plasma cells expressing antibody isotypes IgG and IgA, but not with IgM (Figure 24B).

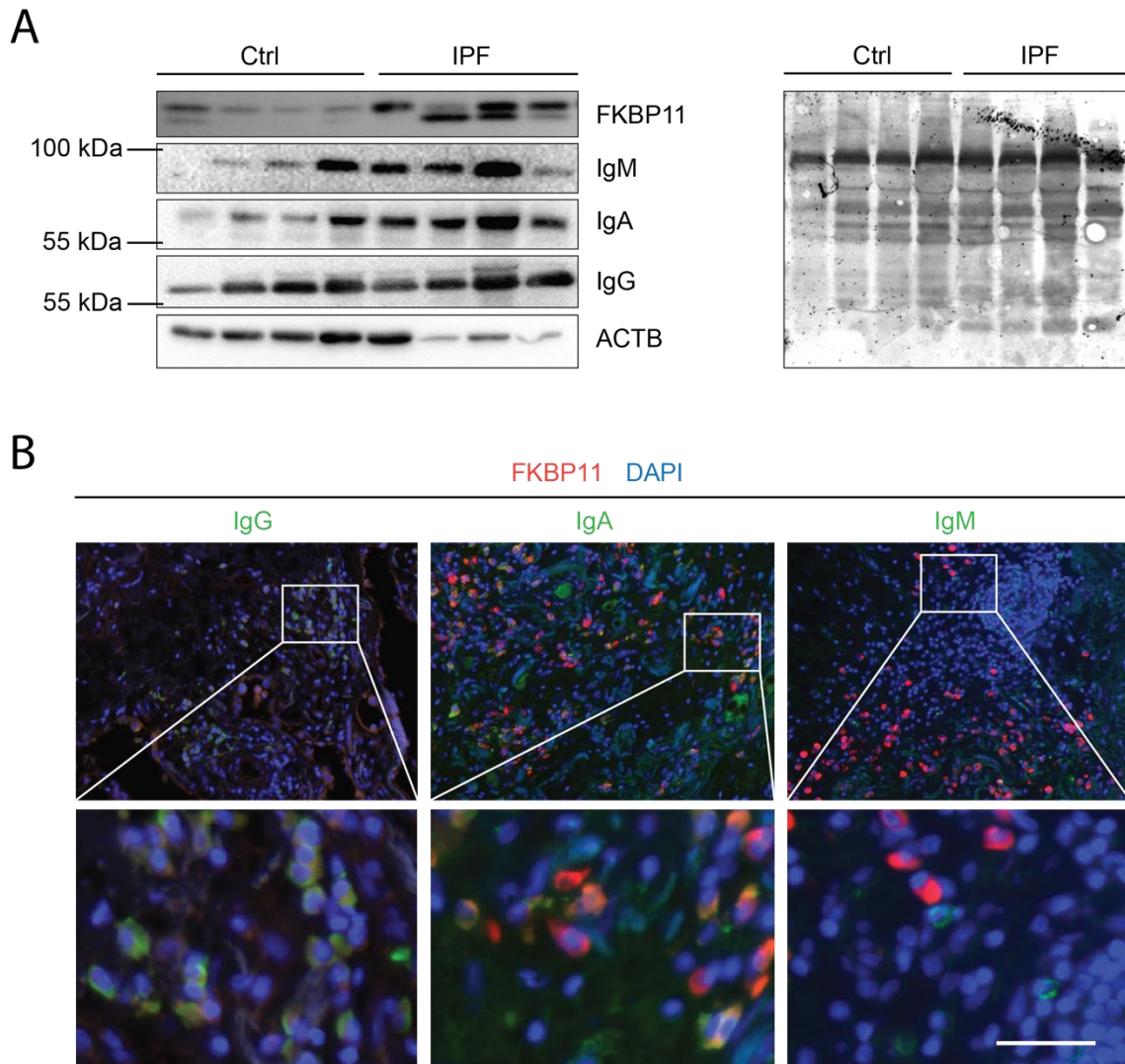


Figure 24: Antibody yields are increased in IPF lung tissues.

Western Blot analysis of FKBP11 and antibody isotypes IgG, IgA and IgM was performed from whole tissue homogenates obtained by the CPC-M bioArchive from donor samples (n=4) and IPF patients (n=4). An amido black staining was used as loading control (A). In addition, immunofluorescent stainings of IPF tissue sections obtained by the CPC-M bioArchive were stained for antibody isotypes IgG, IgA or IgM and FKBP11. For each antibody isotype, three IPF tissue sections (n=3) were stained, and one representative image was shown for each isotype (B). In IPF, protein levels of FKBP11 and the antibody isotypes IgG, IgA and IgM were increased as compared to control (ctrl) (A). In immunofluorescence, FKBP11 colocalized mainly with IgG+ and IgA+ cells, but not with IgM+ cells (B). ACTB = β -actin as loading control. Scale bar: 50 μ m.

In summary, these results support a potential impact of antibodies and thereby autoimmunity on IPF disease.

6 Discussion

6.1 Overview

A profound knowledge of the process of antibody folding as well as plasma cell differentiation may not only pave the way for the development of antibody-based therapeutic compounds, but could also provide novel targets in treatment of autoimmune diseases and idiopathic pulmonary fibrosis (IPF), a fatal disease with autoimmune features. On the contrary, the process of antibody folding in the endoplasmatic reticulum (ER) along with antibody folding catalysts is still uncompletely defined. In this study, the immunophilin FKBP11 was found to be a novel, plasma cell-specific antibody folding catalyst. FKBP11 was highly increased in IPF and specifically expressed by tissue resident plasma cells in both IPF lungs and lymphoid organs. B cell to plasma cell differentiation, as well as induction of ER stress, upregulated FKBP11 in an XBP1-dependent manner, while silencing of FKBP11 in a human lung carcinoma cell line resulted in a high susceptibility towards ER stress induced cell death. Finally, FKBP11 catalyzed antibody folding in vitro. In accordance, silencing of FKBP11 in an antibody secreting hybridoma cell line lead to a decline in secreted antibodies.

6.2 FKBP11 is a plasma cell specific protein and increased in IPF

IPF is an interstitial lung disease (ILD) defined by chronic, progressive scarring of the lungs, ultimately leading to death within few years (Fernandez and Eickelberg 2012). The pathogenesis of IPF is uncompletely understood, and autoimmune processes are becoming increasingly evident to be involved (Xue, Kass et al. 2013, Hoyne, Elliott et al. 2017, Schiller, Mayr et al. 2017). In the current study, protein levels of FKBP11 were highly increased in IPF as compared to healthy donor lungs (Figure 11), which is supported by data from a preceding proteomics study with FKBP11 being among the significantly upregulated proteins (Schiller, Mayr et al. 2017). Another FKBP protein, FKBP10, has been upregulated in the same proteomics study, which is consistent with previous publications identifying FKBP10 as profibrotic mediator in IPF and a novel drug target in IPF treatment (Staab-Weijnitz, Fernandez et al. 2015, Knüppel, Heinzelmann et al. 2018). Taken together, these results support a role of FKBP proteins within IPF disease.

Immunofluorescence revealed that FKBP11 was specifically expressed by CD45-/CD20-/CD38+/CD27+/CD138+ plasma cells in IPF (Figure 12 and Figure 13). Importantly, CD20+ B cells did not show expression of FKBP11 (Figure 12B), suggesting FKBP11 to be an exclusive feature of plasma cells, which they obtain after completing differentiation from naïve B cells. This was confirmed by an *in vitro* B cell to plasma cell differentiation assay (adapted from (Pinna, Corti et al. 2009)), showing that FKBP11 is upregulated within the process of B cell to plasma cell differentiation (Figure 16). In addition, CD38+ plasma cells in primary and secondary lymphoid organs, including thymus, tonsils, spleen, and small intestine, showed colocalization with FKBP11 (Figure 12C), speaking in favor of FKBP11 to be a protein which is expressed by plasma cells in general. In agreement, overexpression of FKBP11 using a transgenic lentiviral mouse model has been shown to favor plasma cell differentiation upon lipopolysaccharide (LPS) treatment. The same mice showed higher serum levels of basal IgG3, speaking for a higher proportion of plasma cells (Xue, Kass et al. 2013). Moreover, *FKBP11* expression in peripheral B cells sorted from systemic lupus erythematosus (SLE) patients has been found to be associated with elevated numbers of peripheral plasma blasts (Garaud, Schickel et al. 2011). Overall, these results argue for a crucial function of FKBP11 in plasma cell biology.

In accordance with increased protein levels of FKBP11 in IPF, the number of FKBP11+/CD38+ plasma cells in immunofluorescent stainings of IPF was drastically elevated in comparison to healthy donor lungs (Figure 13A and B). This is supported by a previous publication showing elevated numbers of MZB1+/CD38+ plasma cells in IPF (Schiller, Mayr et al. 2017). Given specific expression of *FKBP11* in CD3-/CD20-/CD38+/CD27+ plasma cells in IPF lung tissue (Figure 12), this cell population was gated in peripheral blood of IPF patients and healthy controls and analyzed using FACS analysis. In contrast to IPF lung tissue, the proportion of circulating plasma cells over all viable cells in IPF patients was very small (0.3%) and did not significantly differ from healthy controls (Figure 13C). This result suggests that the majority of plasma cells in IPF lungs differentiates from resident B cells, rather than migrating from peripheral organs. Opposed to this, a preceding study has found the proportion of plasmablasts (CD2+/CD38+) over all gated B cells from peripheral blood of IPF patients (CD19+/CD20-/CD3-/IgD-) to be increased in IPF (Xue, Kass et al. 2013). However, this result is barely comparable with the findings of the present study, as the present study did not gate for CD19, because it has been stated that a high proportion of plasma cells loses

expression of *CD19* (Table 1, (Caraux, Klein et al. 2010)). Further, the present study did not standardize with regard to B cells, but to all viable cells gated.

As outlined above, autoimmune features, including autoantibodies, are increasingly recognized to play a role in the pathogenesis of IPF (Kahloon, Xue et al. 2012, Xue, Kass et al. 2013, Donahoe, Valentine et al. 2015, Schiller, Mayr et al. 2017). As increased levels of IgG, IgA and IgM (Figure 24A), as well as strong expression of *FKBP11* along with high numbers of FKBP11+ plasma cells in IPF lungs (Figure 11 and Figure 13) were observed, a role of autoimmunity in IPF is supported. Interestingly, treatment with tacrolimus (FK506), which in our study significantly inhibited FKBP11-mediated antibody folding *in vitro* (Figure 23B), has been associated with improved medial survival durations, and lower rates of re-acute exacerbations in patients with acute exacerbations of IPF (Horita, Akahane et al. 2011). In addition, tacrolimus has been shown to inhibit collagen synthesis *in vitro*, and to attenuate lung fibrosis in the bleomycin (BLM) induced lung fibrosis model (Nagano, Iyonaga et al. 2006). However, application of tacrolimus in the acute injury phase of the BLM model has been seen to result in deterioration of the lung injury (Nagano, Iyonaga et al. 2006). Tacrolimus only binds FKBP11 with low affinity *in vitro* (Rulten, Kinloch et al. 2006), and has been ascribed to bind FKBP1A with the highest affinity (Kang, Hong et al. 2008), making it questionable whether tacrolimus can have an impact on IPF that is particularly mediated via inhibition of FKBP11. As a consequence, it still remains elusive whether the observations on FKBP11 in IPF found in the present study represent epiphenomena occurring as a part of unspecific inflammation processes, or actual disease-promoting autoimmune mechanisms. A targeted therapy aiming at plasma cells in particular, e.g. in the form of anti-CD 38 antibodies as they are currently in clinical trials for multiple myeloma (van de Donk, Janmaat et al. 2016), could provide new insights on this.

6.3 Plasma cell differentiation and the unfolded protein response upregulate FKBP11

To prepare for biosynthesis and secretion of enormous amounts of antibodies, plasma cells need to massively expand their rough ER along with upregulation of ER-resident chaperones and folding catalysts. This is achieved within the process of B cell to plasma cell differentiation by activation of the unfolded protein response (UPR), a reaction that is usually triggered by ER stress caused by accumulation of misfolded proteins. More precisely, two master regulators of B cell to plasma cell differentiation have been

identified to mediate the UPR: PRDM-1 and XBP1, while XBP1 is a downstream effector of PRDM-1 (Iwakoshi, Lee et al. 2003, Nutt, Hodgkin et al. 2015, Grootjans, Kaser et al. 2016, Minnich, Tagoh et al. 2016).

Here, FKBP11 was induced upon B cell to plasma cell differentiation (Figure 15 and Figure 16). In consistency with a role of FBKP11 in protein folding, FKBP11 was upregulated upon induction of ER stress via tunicamycin in two distinct cell lines (Figure 17), namely A549 (derived from human lung adenocarcinoma) and RAJI (derived from human B cells). In both cell lines, FKBP11 was ER-resident, as assessed by subcellular fractionation (Figure 18). Furthermore, knockdown of XBP1 with subsequent induction of ER stress repressed upregulation of FKBP11 (Figure 19), indicating that upregulation of FKBP11 is mediated by XBP1. This is in agreement with previous findings, showing ER stress dependent upregulation of FKBP11 (Jeong, Jang et al. 2017, Wang, Cui et al. 2018) and pointing towards FKBP11 being a transcriptional target of XBP1 (Shaffer, Shapiro-Shelef et al. 2004, Wang, Deng et al. 2019).

Of note, induction of ER stress via tunicamycin in A549 cells with prior knockdown of FKBP11 was associated with a decline in cell viability upon tunicamycin treatment (Figure 20), illustrating an increased susceptibility towards ER stress induced cell death. This is in agreement with a previous study, showing that overexpression of FKBP11 in inflamed intestinal epithelial cells, displaying features of ER stress, attenuates expression of pro-apoptotic markers along with a decrease in apoptosis (Wang, Cui et al. 2018). Whether this decline in cell viability is a consequence of an accumulation of misfolded proteins in the ER due to an impaired folding machinery, or the consequence of a loss of a pro-survival factor, remains elusive. However, given the function of FKBP11 in antibody folding (see 6.4), the former is more likely. Overall, these results indicate that plasma cells upregulate FKBP11 in an XBP1-dependent manner as a part of the UPR and support an important function of FKBP11 within the ER in the process of UPR in general.

6.4 FKBP11 acts as a competent antibody folding catalyst

Antibody function strictly relies on a functional, three-dimensional structure. This is assured by a sufficiently functioning folding machinery in the ER, consisting of several chaperones and folding catalysts including heat shock proteins (Hsp), peptidyl-prolyl *cis-trans* isomerases (PPIases), glycan-binding proteins and oxidoreductases (Feige, Hendershot et al. 2010, Feige and Buchner 2014). Importantly, the process of peptidyl-

prolyl *cis-trans* isomerization, an intrinsically slow reaction catalyzed by PPIases, determines the rates of many protein folding procedures and is involved in regulatory events in folded proteins (Göthel and Marahiel 1999). Likewise, antibody domains are rich in prolines, making up 5-10% of their primary sequence. The proline residues have been suggested to protect antibody domains from cleavage by extracellular proteases, and to reduce aggregation tendency (Feige and Buchner 2014). Thus, PPIases are universally acknowledged to play an important role within antibody folding. Still, the knowledge on PPIases involved in antibody folding is rather superficial, and a role of PPIases within human plasma cells is poorly characterized. So far, only two distinct PPIases have been proposed to be involved in the process of antibody folding, namely Cyclophilin B (CypB) (Meunier, Usherwood et al. 2002, Feige, Groscurth et al. 2009, Jansen, Määttä et al. 2012, Lee, Choi et al. 2012) and FKBP1A (FKBP12) (Lilie, Lang et al. 1993). In the present study, FKBP11 was identified as a novel antibody folding PPIase within human plasma cells (Figure 12 and Figure 23).

With FKBP1A, the first association of immunophilins of the FKBP family with antibody folding has been made. Using an *in vitro* refolding assay similar to the refolding assay used in the present study, denatured IgG fab fragment has been refolded either under addition of recombinant FKBP1A or a vehicle control. Addition of recombinant FKBP1A has accelerated the refolding process, and has resulted in an increased yield of refolded antibodies in total (Lilie, Lang et al. 1993). However, given that FKBP1A is a protein specifically expressed in the cytosol (Tong and Jiang 2015), it is unlikely to fold antibodies *in vivo*, as this process takes place in the ER (Hendershot and Sitia 2004, Feige, Hendershot et al. 2010, Feige and Buchner 2014).

CypB is universally accepted as an ER-resident antibody folding PPIase (Feige, Hendershot et al. 2010). This concept has been established upon the following key findings: First, recombinant CypB has been shown to catalyze antibody folding *in vitro* within the same assay as used for FKBP1A (Lilie, Lang et al. 1993). This result was confirmed by our refolding assay, in which CypB served as a positive control (Figure 23). Second, using a crosslinking approach, CypB has been found to be a part of a large ER-localized multiprotein complex that is associated with unassembled and incompletely folded Ig heavy chains (Meunier, Usherwood et al. 2002). Moreover, (Lee, Choi et al. 2012) have reported that inhibition of the PPIase domain of CypB by its natural binding partner, cyclosporin A (CsA), impairs antibody folding on a posttranslational stage in a

murine, antibody secreting hybridoma cell line, as well as in primary B cells. More recently, a novel complex between CypB and the protein disulfide isomerase (PDI) ERp72 (PDIA4) has been identified within the ER by ER-specific pulldown and a yeast-two hybrid system. Taking advantage of a CH1-CL assembly assay (first described in (Feige, Groscurth et al. 2009)), which can monitor disulfide bond formation between the constant parts of the IgG heavy and light chain, CypB has been observed to augment PDI activity of ERp72 (Jansen, Määttä et al. 2012).

Despite all this evidence for a function of CypB in antibody folding, the relative contribution of CypB remains elusive. So far, no study has addressed specific expression of *CypB* in plasma cells. On the contrary, *CypB* is known to be expressed ubiquitously in almost all tissues (Ryffel, Woerly et al. 1991), arguing for a far more general role of CypB in protein folding. Moreover, upregulation of CypB within the process of B cell to plasma cell differentiation, which would underline the importance of CypB for antibody folding in plasma cells, has not been observed.

In the present study, in contrast, human FKBP11 was characterized as a novel, plasma cell specific PPIase with strong *in vitro* and *in vivo* evidence. Using an *in vitro* refolding assay, we demonstrated that the purified FKBP domain of human FKBP11 accelerated the rate of IgG refolding and increased the yield of totally refolded IgG (Figure 23A). Inhibition of the PPIase activity with tacrolimus, on the other hand, repressed these effects (Figure 23B), which confirms that the PPIase domain of FKBP11 is capable of antibody folding *in vitro*. Consistently, FKBP11 colocalized with at least two major antibody isotypes, namely IgG and IgA, in lung tissue from IPF patients (Figure 24B). Knockdown of FKBP11 in an antibody secreting hybridoma cell line, innately showing high levels of FKBP11 (Figure 21A), led to a decline in IgG levels in the cell culture supernatant (Figure 22), additionally highlighting the importance of FKBP11 for antibody folding in plasma cells. In the same cell line, ER-residency was confirmed by confocal microscopy, illustrating colocalization of FKBP11 with Concanavalin A (Figure 21C), a known ER-resident protein, and by subcellular fractionation, indicating a similar enrichment pattern as the ER resident protein calreticulin (Figure 21B). Furthermore, *FKBP11* was exclusively expressed by plasma cells (Figure 12A and C), whereas naïve B cells did not display relevant expression (Figure 12B). This was additionally confirmed by a human test system illustrating that plasma cell differentiation induced by a combination of IL-2 and R848 was accompanied by upregulation of FKBP11 (Figure 15 and Figure 16).

Finally, FKBP11 was identified as a transcriptional target of XBP1 (Figure 19), which is known to induce the UPR along with plasma cell differentiation (Iwakoshi, Lee et al. 2003).

With this, FKBP11 might be a potential drug target for autoimmune diseases and IPF. Tacrolimus inhibited the effects of FKBP11 on antibody folding (Figure 23B). Moreover, tacrolimus has been reported to inhibit plasma cell proliferation and differentiation, which might have been mediated by an effect on FKBP11 (De Bruyne, Bogaert et al. 2015). In an independent study, however, this finding was not supported (Traitanon, Mathew et al. 2015). Also, the concentrations used for inhibition of FKBP11 by tacrolimus were high (180 μ M), and unlikely to be achieved at this concentration in the plasma of patients due to toxic side effects of tacrolimus. This is in agreement with preceding studies, reporting FKBP11 to bind tacrolimus only weakly *in vitro* (Rulten, Kinloch et al. 2006). As a consequence, FKBP11 is unlikely to be used pharmaceutically as a target of tacrolimus. Therefore, new strategies need to be developed to target FKBP11 more specifically, which could then provide more perspectives in the form of novel targeted therapies.

Besides its potential as a novel drug target, FKBP11 could be a possible tool to improve recombinant antibody production in cultivated mammalian cells. The majority of therapeutic proteins, including antibodies, are produced in cultivated mammalian cells with titers reaching more than 10g/L (Wurm 2004, Kim, Kim et al. 2012). Still, due to an increasing biopharmaceutical market, productivity needs to be enhanced. Importantly, the limiting factor in enhancing productivity is considered to be posttranslational modifications, such as protein folding, assembly and secretion of the protein (Kim, Kim et al. 2012). A previous study has shown that overexpression of CHOP, a UPR related protein, increases antibody production in chinese hamster ovary (CHO) cells (Nishimiya, Mano et al. 2013). Moreover, overexpression of XBP1 has led to enhanced secretory capacity of CHO cells (Tigges and Fussenegger 2006). Similarly, overexpression of FKBP11 could result in increased productivity of antibody producing cells, given its function in antibody folding.

6.5 Conclusions and outlook

In conclusion, FKBP11 was identified as a novel, plasma cell specific antibody folding catalyst, that is highly increased in IPF. It was upregulated as a transcriptional target of XBP1 within B cell to plasma cell differentiation as a part of the UPR and its knockdown

resulted in reduced antibody folding capacity as well as increased susceptibility towards ER stress induced cell death. Figure 25 gives an overview on the regulation and function of FKBP11.

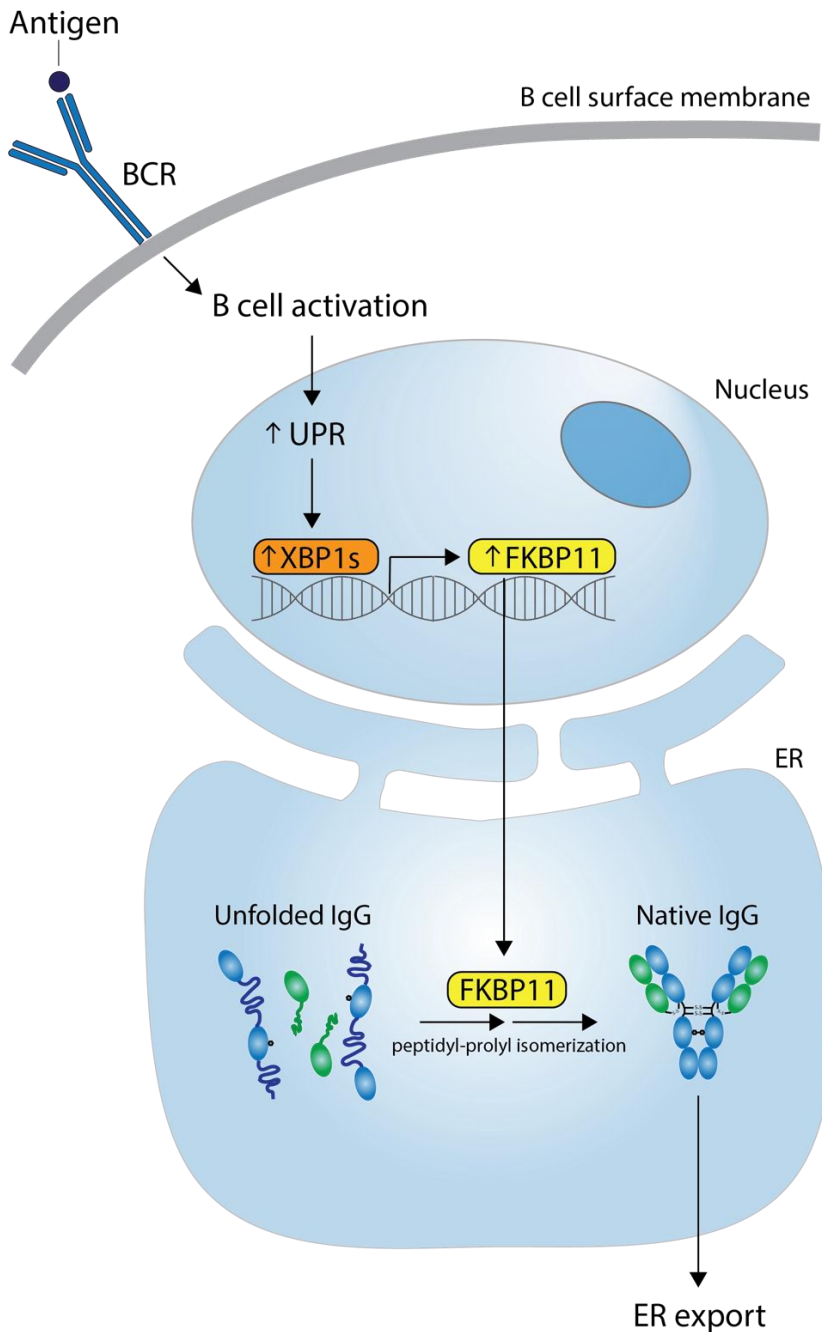


Figure 25: Regulation and function of FKBP11.

Binding of an antigen to its respective B cell receptor (BCR) on the cell surface of a B cell results in B cell activation and plasma cell differentiation. As a result of B cell activation, the unfolded protein response (UPR) is induced, leading to increased levels of spliced XBP1 (sXBP1). sXBP1, in turn, serves as a transcription factor and thereby induces expression of FKBP11. Once translocated into the endoplasmic reticulum (ER), FKBP11 contributes to antibody folding in the ER by its peptidyl-prolyl *cis-trans* isomerase activity.

These results aid a better understanding of B cell and plasma cell biology, as well as the process of antibody folding. By this, novel strategies are implied to enable a greater manipulation of the humoral immune system both to improve immunity and to thwart autoimmune pathologies. Furthermore, it can be helpful to overcome current limitations in the production of monoclonal antibodies. Still, further investigations are necessary to see if FKBP11 in particular will be useful as a drug target in this context or can even be utilized as a recombinantly produced compound.

Finally, these findings highlight the importance of FKBP proteins in human diseases. While this study supports a role of FKBP11 in IPF and autoimmune diseases, other FKBP proteins have been proposed to be implicated in numerous pathologies, including cancer, cardiac diseases and neurodegenerative disorders. As a consequence, it is becoming increasingly evident, that a systematic and detailed analysis of tacrolimus and its analogues as inhibitors of not only FKBP1A, but also other FKBP proteins, will provide new therapeutic options for various pathologies.

7 References

Alexander, T., R. Sarfert, J. Klotsche, A. A. Köhl, A. Rubbert-Roth, H.-M. Lorenz, J. Rech, B. F. Hoyer, Q. Cheng, A. Waka, A. Taddeo, M. Wiesener, G. Schett, G.-R. Burmester, A. Radbruch, F. Hiepe and R. E. Voll (2015). "The proteasome inhibitor bortezomib depletes plasma cells and ameliorates clinical manifestations of refractory systemic lupus erythematosus." Annals of the Rheumatic Diseases **74**(7): 1474.

Amaravadhi, H. and Y. Ho Sup (2016). "Immunophilins: Structures, Mechanisms and Ligands." Current Molecular Pharmacology **9**(1): 37-47.

Bassik, M. C. and M. Kampmann (2011). "Knocking out the door to tunicamycin entry." Proceedings of the National Academy of Sciences **108**(29): 11731.

Bauer, Y., J. Tedrow, S. d. Bernard, M. Birker-Robaczewska, K. F. Gibson, B. J. Guardela, P. Hess, A. Klenk, K. O. Lindell, S. Poirey, B. Renault, M. Rey, E. Weber, O. Nayler and N. Kaminski (2015). "A Novel Genomic Signature with Translational Significance for Human Idiopathic Pulmonary Fibrosis." American Journal of Respiratory Cell and Molecular Biology **52**(2): 217-231.

Bauer, Y., J. Tedrow, S. de Bernard, M. Birker-Robaczewska, K. F. Gibson, B. J. Guardela, P. Hess, A. Klenk, K. O. Lindell, S. Poirey, B. Renault, M. Rey, E. Weber, O. Nayler and N. Kaminski (2015). "A novel genomic signature with translational significance for human idiopathic pulmonary fibrosis." American journal of respiratory cell and molecular biology **52**(2): 217-231.

Bellan, M., F. Patrucco, F. Barone-Adesi, F. Gavelli, L. M. Castello, A. Nerviani, L. Andreoli, L. Cavagna, M. Pirisi and P. P. Sainaghi (2020). "Targeting CD20 in the treatment of interstitial lung diseases related to connective tissue diseases: A systematic review." Autoimmunity Reviews **19**(2): 102453.

Bonner, J. M. and G. L. Boulianne (2017). "Diverse structures, functions and uses of FK506 binding proteins." Cellular Signalling **38**: 97-105.

Bottomley, M. J., M. R. Batten, R. A. Lumb and N. J. Bulleid (2001). "Quality control in the endoplasmic reticulum: PDI mediates the ER retention of unassembled procollagen C-propeptides." Current Biology **11**(14): 1114-1118.

Butler, M. W. and M. P. Keane (2019). The Role of Immunity and Inflammation in IPF Pathogenesis. Idiopathic Pulmonary Fibrosis: A Comprehensive Clinical Guide. K. C. Meyer and S. D. Nathan. Cham, Springer International Publishing: 97-131.

Caraux, A., B. Klein, B. Paiva, C. Bret, A. Schmitz, G. M. Fuhler, N. A. Bos, H. E. Johnsen, A. Orfao, M. Perez-Andres and N. Myeloma Stem Cell (2010). "Circulating human B and plasma cells. Age-associated changes in counts and detailed characterization of circulating normal CD138- and CD138+ plasma cells." Haematologica **95**(6): 1016-1020.

Chaplin, D. D. (2010). "Overview of the immune response." The Journal of allergy and clinical immunology **125**(2 Suppl 2): S3-S23.

- Chizzolini, C. (2008). "T cells, B cells, and polarized immune response in the pathogenesis of fibrosis and systemic sclerosis." Current Opinion in Rheumatology **20**(6): 707-712.
- Chung, J. B., M. Silverman and J. G. Monroe (2003). "Transitional B cells: step by step towards immune competence." Trends in Immunology **24**(6): 342-348.
- Clevers, H., B. Alarcon, T. Wileman and C. Terhorst (1988). "The T Cell Receptor/CD3 Complex: A Dynamic Protein Ensemble." Annual Review of Immunology **6**(1): 629-662.
- Cyster, J. G. and C. D. C. Allen (2019). "B Cell Responses: Cell Interaction Dynamics and Decisions." Cell **177**(3): 524-540.
- Davidson, A. and B. Diamond (2001). "Autoimmune Diseases." New England Journal of Medicine **345**(5): 340-350.
- De Bruyne, R., D. Bogaert, N. De Ruyck, B. N. Lambrecht, M. Van Winckel, P. Gevaert and M. Dullaers (2015). "Calcineurin inhibitors dampen humoral immunity by acting directly on naive B cells." Clinical and experimental immunology **180**(3): 542-550.
- Donahoe, M., V. G. Valentine, N. Chien, K. F. Gibson, J. S. Raval, M. Saul, J. Xue, Y. Zhang and S. R. Duncan (2015). "Autoantibody-Targeted Treatments for Acute Exacerbations of Idiopathic Pulmonary Fibrosis." PLOS ONE **10**(6): e0127771.
- Feige, M. J. and J. Buchner (2014). "Principles and engineering of antibody folding and assembly." Biochimica et Biophysica Acta (BBA) - Proteins and Proteomics **1844**(11): 2024-2031.
- Feige, M. J., S. Groscurth, M. Marcinowski, Y. Shimizu, H. Kessler, L. M. Hendershot and J. Buchner (2009). "An unfolded CH1 domain controls the assembly and secretion of IgG antibodies." Molecular cell **34**(5): 569-579.
- Feige, M. J., L. M. Hendershot and J. Buchner (2010). "How antibodies fold." Trends in biochemical sciences **35**(4): 189-198.
- Fernandez, I. E. and O. Eickelberg (2012). "New cellular and molecular mechanisms of lung injury and fibrosis in idiopathic pulmonary fibrosis." The Lancet **380**(9842): 680-688.
- Fingerlin, T. E., W. Zhang, I. V. Yang, H. C. Ainsworth, P. H. Russell, R. Z. Blumhagen, M. I. Schwarz, K. K. Brown, M. P. Steele, J. E. Loyd, G. P. Cosgrove, D. A. Lynch, S. Groshong, H. R. Collard, P. J. Wolters, W. Z. Bradford, K. Kossen, S. D. Seiwert, R. M. du Bois, C. K. Garcia, M. S. Devine, G. Gudmundsson, H. J. Isaksson, N. Kaminski, Y. Zhang, K. F. Gibson, L. H. Lancaster, T. M. Maher, P. L. Molyneaux, A. U. Wells, M. F. Moffatt, M. Selman, A. Pardo, D. S. Kim, J. D. Crapo, B. J. Make, E. A. Regan, D. S. Walek, J. J. Daniel, Y. Kamatani, D. Zelenika, E. Murphy, K. Smith, D. McKean, B. S. Pedersen, J. Talbert, J. Powers, C. R. Markin, K. B. Beckman, M. Lathrop, B. Freed, C. D. Langefeld and D. A. Schwartz (2016). "Genome-wide imputation study identifies novel HLA locus for pulmonary fibrosis and potential role for auto-immunity in fibrotic idiopathic interstitial pneumonia." BMC Genetics **17**(1): 74.
- Forthal, D. N. (2014). "Functions of Antibodies." Microbiology spectrum **2**(4): 1-17.

- François, A., A. Gombault, B. Villeret, G. Alsaleh, M. Fanny, P. Gasse, S. M. Adam, B. Crestani, J. Sibilia, P. Schneider, S. Bahram, V. Quesniaux, B. Ryffel, D. Wachsmann, J.-E. Gottenberg and I. Couillin (2015). "B cell activating factor is central to bleomycin- and IL-17-mediated experimental pulmonary fibrosis." Journal of Autoimmunity **56**: 1-11.
- Garaud, J.-C., J.-N. Schickel, G. Blaison, A.-M. Knapp, D. Dembele, J. Ruer-Laventie, A.-S. Korganow, T. Martin, P. Soulas-Sprauel and J.-L. Pasquali (2011). "B Cell Signature during Inactive Systemic Lupus Is Heterogeneous: Toward a Biological Dissection of Lupus." PLoS ONE **6**(8): e23900.
- Göthel, S. F. and M. A. Marahiel (1999). "Peptidyl-prolyl cis-trans isomerases, a superfamily of ubiquitous folding catalysts." Cellular and Molecular Life Sciences CMLS **55**(3): 423-436.
- Gottenberg, J. E., L. Guillevin, O. Lambotte, B. Combe, Y. Allanore, A. Cantagrel, C. Larroche, M. Soubrier, L. Bouillet, M. Dougados, O. Fain, D. Farge, X. Kyndt, O. Lortholary, C. Masson, B. Moura, P. Remy, T. Thomas, D. Wendling, J. M. Anaya, J. Sibilia and X. Mariette (2005). "Tolerance and short term efficacy of rituximab in 43 patients with systemic autoimmune diseases." Annals of the Rheumatic Diseases **64**(6): 913.
- Grimaldi, C. M., R. Hicks and B. Diamond (2005). "B Cell Selection and Susceptibility to Autoimmunity." The Journal of Immunology **174**(4): 1775.
- Grootjans, J., A. Kaser, R. J. Kaufman and R. S. Blumberg (2016). "The unfolded protein response in immunity and inflammation." Nature Reviews Immunology **16**(8): 469-484.
- Hendershot, L. M. and R. Sitia (2004). CHAPTER 17 - Immunoglobulin Assembly and Secretion. Molecular Biology of B Cells. T. Honjo, F. W. Alt and M. S. Neuberger. Burlington, Academic Press: 261-273.
- Herazo-Maya, J. D., I. Noth, S. R. Duncan, S. Kim, S.-F. Ma, G. C. Tseng, E. Feingold, B. M. Juan-Guardela, T. J. Richards, Y. Lussier, Y. Huang, R. Vij, K. O. Lindell, J. Xue, K. F. Gibson, S. D. Shapiro, J. G. N. Garcia and N. Kaminski (2013). "Peripheral blood mononuclear cell gene expression profiles predict poor outcome in idiopathic pulmonary fibrosis." Science translational medicine **5**(205): 205ra136-205ra136.
- Herman, E. M. and L. M. Shannon (1984). "Immunocytochemical localization of concanavalin A in developing jack-bean cotyledons." Planta **161**(2): 97-104.
- Hetz, C. (2012). "The unfolded protein response: controlling cell fate decisions under ER stress and beyond." Nat Rev Mol Cell Biol **13**(2): 89-102.
- Hetz, C. and F. R. Papa (2018). "The Unfolded Protein Response and Cell Fate Control." Molecular Cell **69**(2): 169-181.
- Hoebe, K., E. Janssen and B. Beutler (2004). "The interface between innate and adaptive immunity." Nature Immunology **5**(10): 971-974.
- Hofmann, K., A.-K. Clauder and R. A. Manz (2018). "Targeting B Cells and Plasma Cells in Autoimmune Diseases." Frontiers in immunology **9**: 835-835.

- Horita, N., M. Akahane, Y. Okada, Y. Kobayashi, T. Arai, I. Amano, T. Takezawa, M. To and Y. To (2011). "Tacrolimus and Steroid Treatment for Acute Exacerbation of Idiopathic Pulmonary Fibrosis." Internal Medicine **50**(3): 189-195.
- Hoyne, G. F., H. Elliott, S. E. Mutsaers and C. M. Prele (2017). "Idiopathic pulmonary fibrosis and a role for autoimmunity." Immunol Cell Biol **95**(7): 577-583.
- Ishikawa, Y., K. Mizuno and H. P. Bächinger (2017). "Ziploc-ing the Structure 2.0: endoplasmic reticulum resident peptidyl prolyl isomerases show different activities toward hydroxyproline." Journal of Biological Chemistry **292**(22): 9273-9282.
- Iwakoshi, N. N., A.-H. Lee and L. H. Glimcher (2003). "The X-box binding protein-1 transcription factor is required for plasma cell differentiation and the unfolded protein response." Immunological Reviews **194**(1): 29-38.
- Iwakoshi, N. N., A.-H. Lee, P. Vallabhajosyula, K. L. Otipoby, K. Rajewsky and L. H. Glimcher (2003). "Plasma cell differentiation and the unfolded protein response intersect at the transcription factor XBP-1." Nature Immunology **4**(4): 321-329.
- Jansen, G., P. Määttänen, A. Y. Denisov, L. Scarffe, B. Schade, H. Balghi, K. Dejgaard, L. Y. Chen, W. J. Muller, K. Gehring and D. Y. Thomas (2012). "An interaction map of endoplasmic reticulum chaperones and foldases." Molecular & cellular proteomics : MCP **11**(9): 710-723.
- Janssens, S., B. Pulendran and B. N. Lambrecht (2014). "Emerging functions of the unfolded protein response in immunity." Nature immunology **15**(10): 910-919.
- Jeong, M., E. Jang, S. S. Choi, C. Ji, K. Lee and J. Youn (2017). "The Function of FK506-Binding Protein 13 in Protein Quality Control Protects Plasma Cells from Endoplasmic Reticulum Stress-Associated Apoptosis." Frontiers in Immunology **8**: 222.
- Kahloon, R. A., J. Xue, A. Bhargava, E. Csizmadia, L. Otterbein, D. J. Kass, J. Bon, M. Soejima, M. C. Levesque, K. O. Lindell, K. F. Gibson, N. Kaminski, G. Banga, C. V. Oddis, J. M. Pilewski, F. C. Sciurba, M. Donahoe, Y. Zhang and S. R. Duncan (2012). "Patients with Idiopathic Pulmonary Fibrosis with Antibodies to Heat Shock Protein 70 Have Poor Prognoses." American Journal of Respiratory and Critical Care Medicine **187**(7): 768-775.
- Kang, C. B., Y. Hong, S. Dhe-Paganon and H. S. Yoon (2008). "FKBP Family Proteins: Immunophilins with Versatile Biological Functions." Neurosignals **16**(4): 318-325.
- Kay, J. E. (1996). "Structure-function relationships in the FK506-binding protein (FKBP) family of peptidylprolyl cis-trans isomerases." Biochemical Journal **314**(Pt 2): 361-385.
- Kim, J. Y., Y.-G. Kim and G. M. Lee (2012). "CHO cells in biotechnology for production of recombinant proteins: current state and further potential." Applied Microbiology and Biotechnology **93**(3): 917-930.
- King, T. E., A. Pardo and M. Seldman (2011). "Idiopathic pulmonary fibrosis." The Lancet **378**(9807): 1949-1961.

- Knüppel, L., K. Heinzelmann, M. Lindner, R. Hatz, J. Behr, O. Eickelberg and C. A. Staab-Weijnitz (2018). "FK506-binding protein 10 (FKBP10) regulates lung fibroblast migration via collagen VI synthesis." Respiratory Research **19**(1): 67.
- Knüppel, L., K. Heinzelmann, M. Lindner, R. Hatz, J. Behr, O. Eickelberg and C. A. Staab-Weijnitz (2018). "FK506-binding protein 10 (FKBP10) regulates lung fibroblast migration via collagen VI synthesis." Respiratory research **19**(1): 67-67.
- Komura, K., K. Yanaba, M. Horikawa, F. Ogawa, M. Fujimoto, T. F. Tedder and S. Sato (2008). "CD19 regulates the development of bleomycin-induced pulmonary fibrosis in a mouse model." Arthritis & Rheumatism **58**(11): 3574-3584.
- Lanzavecchia, A. (2018). "Dissecting human antibody responses: useful, basic and surprising findings." EMBO Molecular Medicine **10**(3): e8879.
- Laurent, S. A., F. S. Hoffmann, P.-H. Kuhn, Q. Cheng, Y. Chu, M. Schmidt-Supprian, S. M. Hauck, E. Schuh, M. Krumbholz, H. Rübsamen, J. Wanngren, M. Khademi, T. Olsson, T. Alexander, F. Hiepe, H.-W. Pfister, F. Weber, D. Jenne, H. Wekerle, R. Hohlfeld, S. F. Lichtenthaler and E. Meinel (2015). " γ -secretase directly sheds the survival receptor BCMA from plasma cells." **6**: 7333.
- LeBien, T. W. and T. F. Tedder (2008). "B lymphocytes: how they develop and function." Blood **112**(5): 1570-1580.
- Lee, J., T. G. Choi, J. Ha and S. S. Kim (2012). "Cyclosporine A suppresses immunoglobulin G biosynthesis via inhibition of cyclophilin B in murine hybridomas and B cells." International Immunopharmacology **12**(1): 42-49.
- Lilie, H. (1997). "Folding of the Fab fragment within the intact antibody." FEBS Letters **417**(2): 239-242.
- Lilie, H., K. Lang, R. Rudolph and J. Buchner (1993). "Prolyl isomerases catalyze antibody folding in vitro." Protein Science : A Publication of the Protein Society **2**(9): 1490-1496.
- Lin, I. Y., C. H. Yen, Y. J. Liao, S. E. Lin, H. P. Ma, Y. J. Chan and Y. M. Chen (2013). "Identification of FKBP11 as a biomarker for hepatocellular carcinoma." Anticancer Res **33**(6): 2763-2769.
- Liu, C. Y. and R. J. Kaufman (2003). "The unfolded protein response." Journal of Cell Science **116**(10): 1861.
- Lu, H., Y. Yang, E. M. Allister, N. Wijesekara and M. B. Wheeler (2008). "The Identification of Potential Factors Associated with the Development of Type 2 Diabetes." Molecular & Cellular Proteomics **7**(8): 1434.
- Ma, Y., Y. Shimizu, M. J. Mann, Y. Jin and L. M. Hendershot (2010). "Plasma cell differentiation initiates a limited ER stress response by specifically suppressing the PERK-dependent branch of the unfolded protein response." Cell Stress and Chaperones **15**(3): 281-293.
- Marrack, P. and J. Kappler (1994). "Subversion of the immune system by pathogens." Cell **76**(2): 323-332.

- Matsushita, T., T. Kobayashi, K. Mizumaki, M. Kano, T. Sawada, M. Tennichi, A. Okamura, Y. Hamaguchi, Y. Iwakura, M. Hasegawa, M. Fujimoto and K. Takehara (2018). "BAFF inhibition attenuates fibrosis in scleroderma by modulating the regulatory and effector B cell balance." Science advances **4**(7): eaas9944-eaas9944.
- Mayberry, J. P., S. L. Primack and N. L. Müller (2000). "Thoracic Manifestations of Systemic Autoimmune Diseases: Radiographic and High-Resolution CT Findings." RadioGraphics **20**(6): 1623-1635.
- Mehta, H., P.-O. Goulet, V. Nguyen, G. Pérez, M. Koenig, J.-L. Senécal and M. Sarfati (2016). "Topoisomerase I peptide-loaded dendritic cells induce autoantibody response as well as skin and lung fibrosis." Autoimmunity **49**(8): 503-513.
- Mei, H. E., S. Schmidt and T. Dörner (2012). "Rationale of anti-CD19 immunotherapy: an option to target autoreactive plasma cells in autoimmunity." Arthritis Research & Therapy **14**(5): S1.
- Meunier, L., Y.-K. Usherwood, K. T. Chung and L. M. Hendershot (2002). "A subset of chaperones and folding enzymes form multiprotein complexes in endoplasmic reticulum to bind nascent proteins." Molecular biology of the cell **13**(12): 4456-4469.
- Michalak, M., J. Groenendyk, E. Szabo, Leslie I. Gold and M. Opas (2009). "Calreticulin, a multi-process calcium-buffering chaperone of the endoplasmic reticulum." Biochemical Journal **417**(3): 651-666.
- Minnich, M., H. Tagoh, P. Bönelt, E. Axelsson, M. Fischer, B. Cebolla, A. Tarakhovsky, S. L. Nutt, M. Jaritz and M. Busslinger (2016). "Multifunctional role of the transcription factor Blimp-1 in coordinating plasma cell differentiation." Nature Immunology **17**: 331-343.
- Nagano, J., K. Iyonaga, K. Kawamura, A. Yamashita, H. Ichiyasu, T. Okamoto, M. Suga, Y. Sasaki and H. Kohrogi (2006). "Use of tacrolimus, a potent antifibrotic agent, in bleomycin-induced lung fibrosis." European Respiratory Journal **27**(3): 460-469.
- Nalysnyk, L., J. Cid-Ruzafa, P. Rotella and D. Esser (2012). "Incidence and prevalence of idiopathic pulmonary fibrosis: review of the literature." European Respiratory Review **21**(126): 355-361.
- Nandakumar, K. S., B. P. Johansson, L. Björck and R. Holmdahl (2007). "Blocking of experimental arthritis by cleavage of IgG antibodies in vivo." Arthritis & Rheumatism **56**(10): 3253-3260.
- Nelson, P. N., G. M. Reynolds, E. E. Waldron, E. Ward, K. Giannopoulos and P. G. Murray (2000). "Monoclonal antibodies." Molecular pathology : MP **53**(3): 111-117.
- Nguyen, D. C., C. J. Joyner, I. Sanz and F. E.-H. Lee (2019). "Factors Affecting Early Antibody Secreting Cell Maturation Into Long-Lived Plasma Cells." Frontiers in Immunology **10**: 2138.
- Nishimiya, D., T. Mano, K. Miyadai, H. Yoshida and T. Takahashi (2013). "Overexpression of CHOP alone and in combination with chaperones is effective in improving antibody production in mammalian cells." Applied Microbiology and Biotechnology **97**(6): 2531-2539.

- Nutt, S. L., P. D. Hodgkin, D. M. Tarlinton and L. M. Corcoran (2015). "The generation of antibody-secreting plasma cells." Nature Reviews Immunology **15**: 160-171.
- Pagel, J. M., N. Hedin, K. Subbiah, D. Meyer, R. Mallet, D. Axworthy, L. J. Theodore, D. S. Wilbur, D. C. Matthews and O. W. Press (2003). "Comparison of anti-CD20 and anti-CD45 antibodies for conventional and pretargeted radioimmunotherapy of B-cell lymphomas." Blood **101**(6): 2340-2348.
- Pinna, D., D. Corti, D. Jarrossay, F. Sallusto and A. Lanzavecchia (2009). "Clonal dissection of the human memory B cell repertoire following infection and vaccination." Eur J Immunol **39**(5).
- Qi, L., B. Tsai and P. Arvan (2017). "New Insights into the Physiological Role of Endoplasmic Reticulum-Associated Degradation." Trends in cell biology **27**(6): 430-440.
- Raghu, G., K. J. Anstrom, T. J. King, J. A. Lasky and F. J. T. I. P. F. C. R. Martinez (2012). "Prednisone, Azathioprine, and N-Acetylcysteine for Pulmonary Fibrosis." New England Journal of Medicine **366**(21): 1968-1977.
- Raghu, G., B. Rochweg, Y. Zhang, C. A. C. Garcia, A. Azuma, J. Behr, J. L. Brozek, H. R. Collard, W. Cunningham, S. Homma, T. Johkoh, F. J. Martinez, J. Myers, S. L. Protzko, L. Richeldi, D. Rind, M. Selman, A. Theodore, A. U. Wells, H. Hoogsteden and H. J. Schünemann (2015). "An Official ATS/ERS/JRS/ALAT Clinical Practice Guideline: Treatment of Idiopathic Pulmonary Fibrosis. An Update of the 2011 Clinical Practice Guideline." American Journal of Respiratory and Critical Care Medicine **192**(2): e3-e19.
- Reinhardt, D. P., D. R. Keene, G. M. Corson, E. Pöschl, H. P. Bächinger, J. E. Gambee and L. Y. Sakai (1996). "Fibrillin-1: Organization in Microfibrils and Structural Properties." Journal of Molecular Biology **258**(1): 104-116.
- Rolink, A. G., E. ten Boekel, T. Yamagami, R. Ceredig, J. Andersson and F. Melchers (1999). "B cell development in the mouse from early progenitors to mature B cells." Immunology Letters **68**(1): 89-93.
- Ruer-Laventie, J., L. Simoni, J. N. Schickel, A. Soley, M. Duval, A. M. Knapp, L. Marcellin, D. Lamon, A. S. Korganow, T. Martin, J. L. Pasquali and P. Soulas-Sprauel (2015). "Overexpression of Fkbp11, a feature of lupus B cells, leads to B cell tolerance breakdown and initiates plasma cell differentiation." Immun Inflamm Dis **3**(3): 265-279.
- Rulten, S. L., R. A. Kinloch, H. Tateossian, C. Robinson, L. Gettins and J. E. Kay (2006). "The human FK506-binding proteins: characterization of human FKBP19." Mammalian Genome **17**(4): 322-331.
- Ryffel, B., G. Woerly, B. Greiner, B. Haendler, M. J. Mihatsch and B. M. Foxwell (1991). "Distribution of the cyclosporine binding protein cyclophilin in human tissues." Immunology **72**(3): 399-404.
- Samy, E., S. Wax, B. Huard, H. Hess and P. Schneider (2017). "Targeting BAFF and APRIL in systemic lupus erythematosus and other antibody-associated diseases." International Reviews of Immunology **36**(1): 3-19.

Schiller, H. B., C. H. Mayr, G. Leuschner, M. Strunz, C. Staab-Weijnitz, S. Preisendörfer, B. Eckes, P. Moinzadeh, T. Krieg, D. A. Schwartz, R. A. Hatz, J. Behr, M. Mann and O. Eickelberg (2017). "Deep Proteome Profiling Reveals Common Prevalence of MZB1-positive Plasma B Cells in Human Lung and Skin Fibrosis." *American Journal of Respiratory and Critical Care Medicine* **196**(10):1298-1310.

Schroeder, H. W., Jr. and L. Cavacini (2010). "Structure and function of immunoglobulins." *The Journal of allergy and clinical immunology* **125**(2 Suppl 2): S41-S52.

Sgalla, G., B. Iovene, M. Calvello, M. Ori, F. Varone and L. Richeldi (2018). "Idiopathic pulmonary fibrosis: pathogenesis and management." *Respiratory Research* **19**(1): 32.

Shaffer, A. L., K.-I. Lin, T. C. Kuo, X. Yu, E. M. Hurt, A. Rosenwald, J. M. Giltane, L. Yang, H. Zhao, K. Calame and L. M. Staudt (2002). "Blimp-1 Orchestrates Plasma Cell Differentiation by Extinguishing the Mature B Cell Gene Expression Program." *Immunity* **17**(1): 51-62.

Shaffer, A. L., M. Shapiro-Shelef, N. N. Iwakoshi, A.-H. Lee, S.-B. Qian, H. Zhao, X. Yu, L. Yang, B. K. Tan, A. Rosenwald, E. M. Hurt, E. Petroulakis, N. Sonenberg, J. W. Yewdell, K. Calame, L. H. Glimcher and L. M. Staudt (2004). "XBPI, Downstream of Blimp-1, Expands the Secretory Apparatus and Other Organelles, and Increases Protein Synthesis in Plasma Cell Differentiation." *Immunity* **21**(1): 81-93.

Shum, A. K., M. Alimohammadi, C. L. Tan, M. H. Cheng, T. C. Metzger, C. S. Law, W. Lwin, J. Perheentupa, H. Bour-Jordan, J. C. Carel, E. S. Husebye, F. De Luca, C. Janson, R. Sargur, N. Dubois, M. Kajosaari, P. J. Wolters, H. A. Chapman, O. Kämpe and M. S. Anderson (2013). "BPIFB1 is a lung-specific autoantigen associated with interstitial lung disease." *Science translational medicine* **5**(206): 206ra139-206ra139.

Spagnolo, P., A. Tzouveleakis and F. Bonella (2018). "The Management of Patients With Idiopathic Pulmonary Fibrosis." *Frontiers in medicine* **5**: 148-148.

Staab-Weijnitz, C. A., I. E. Fernandez, L. Knüppel, J. Maul, K. Heinzelmann, B. M. Juan-Guardela, E. Hennen, G. Preissler, H. Winter, C. Neurohr, R. Hatz, M. Lindner, J. Behr, N. Kaminski and O. Eickelberg (2015). "FK506-Binding Protein 10, a Potential Novel Drug Target for Idiopathic Pulmonary Fibrosis." *American Journal of Respiratory and Critical Care Medicine* **192**(4): 455-467.

Staab-Weijnitz, C. A., I. E. Fernandez, L. Knüppel, J. Maul, K. Heinzelmann, B. M. Juan-Guardela, E. Hennen, G. Preissler, H. Winter, C. Neurohr, R. Hatz, M. Lindner, J. Behr, N. Kaminski and O. Eickelberg (2015). "FK506-Binding Protein 10, a Potential Novel Drug Target for Idiopathic Pulmonary Fibrosis." *Am J Respir Crit Care Med* **192**(4): 455-467.

Steinbrunn, T., M. Chatterjee, R. C. Bargou and T. Stühmer (2014). "Efficient transient transfection of human multiple myeloma cells by electroporation--an appraisal." *PloS one* **9**(6): e97443-e97443.

Steinfeld, S. D. and P. Youinou (2006). "Epratuzumab (humanised anti-CD22 antibody) in autoimmune diseases." *Expert Opinion on Biological Therapy* **6**(9): 943-949.

Tellier, J. and S. L. Nutt (2017). "Standing out from the crowd: How to identify plasma cells." European Journal of Immunology **47**(8): 1276-1279.

Tellier, J. and S. L. Nutt (2018). "Plasma cells: The programming of an antibody-secreting machine." European Journal of Immunology **49**(1): 30-37.

Tello, D., S. Spinelli, H. Souchon, F. A. Saul, M. M. Riottot, R. A. Mariuzza, M. B. Lascombe, A. Houdusse, J. L. Eiselé, T. Fischmann, V. Chitarra, G. Boulot, T. N. Bhat, G. A. Bentley, P. M. Alzari and R. J. Poljak (1990). "Three-dimensional structure and antigen binding specificity of antibodies." Biochimie **72**(8): 507-512.

Tigges, M. and M. Fussenegger (2006). "Xbp1-based engineering of secretory capacity enhances the productivity of Chinese hamster ovary cells." Metabolic Engineering **8**(3): 264-272.

Todd, D. J., L. J. McHeyzer-Williams, C. Kowal, A.-H. Lee, B. T. Volpe, B. Diamond, M. G. McHeyzer-Williams and L. H. Glimcher (2009). "XBP1 governs late events in plasma cell differentiation and is not required for antigen-specific memory B cell development." Journal of Experimental Medicine **206**(10): 2151-2159.

Tong, M. and Y. Jiang (2015). "FK506-Binding Proteins and Their Diverse Functions." Current molecular pharmacology **9**(1): 48-65.

Traitanon, O., J. M. Mathew, G. La Monica, L. Xu, V. Mas and L. Gallon (2015). "Differential Effects of Tacrolimus versus Sirolimus on the Proliferation, Activation and Differentiation of Human B Cells." PLOS ONE **10**(6): e0129658.

van de Donk, N. W. C. J., M. L. Janmaat, T. Mutis, J. J. Lammerts van Bueren, T. Ahmadi, A. K. Sasser, H. M. Lokhorst and P. W. H. I. Parren (2016). "Monoclonal antibodies targeting CD38 in hematological malignancies and beyond." Immunological Reviews **270**(1): 95-112.

Vittal, R., E. A. Mickler, A. J. Fisher, C. Zhang, K. Rothhaar, H. Gu, K. M. Brown, A. Emtiazdjoo, J. M. Lott, S. B. Frye, G. N. Smith, G. E. Sandusky, O. W. Cummings and D. S. Wilkes (2013). "Type V Collagen Induced Tolerance Suppresses Collagen Deposition, TGF- β and Associated Transcripts in Pulmonary Fibrosis." PLOS ONE **8**(10): e76451.

Wang, X., X. Cui, C. Zhu, M. Li, J. Zhao, Z. Shen, X. Shan, L. Wang, H. Wu, Y. Shen, Y. Ni, D. Zhang and G. Zhou (2018). "FKBP11 protects intestinal epithelial cells against inflammation-induced apoptosis via the JNK-caspase pathway in Crohn's disease." Molecular medicine reports **18**(5): 4428-4438.

Wang, X., Y. Deng, G. Zhang, C. Li, G. Ding, I. May Herman, H. Tran Diem, X. Luo, D.-S. Jiang, L. Li Dan, X. Wei, L. Xu, A. Ferdous, G. Gillette Thomas, E. Scherer Philipp, X. Jiang and V. Wang Zhao (2019). "Spliced X-box Binding Protein 1 Stimulates Adaptive Growth Through Activation of mTOR." Circulation **140**(7): 566-579.

Wurm, F. M. (2004). "Production of recombinant protein therapeutics in cultivated mammalian cells." Nature Biotechnology **22**(11): 1393-1398.

Xue, J., B. R. Gochuico, A. S. Alawad, C. A. Feghali-Bostwick, I. Noth, S. D. Nathan, G. D. Rosen, I. O. Rosas, S. Dacic, I. Ocak, C. R. Fuhrman, K. T. Cuenco, M. A. Smith,

S. S. Jacobs, A. Zeevi, P. A. Morel, J. M. Pilewski, V. G. Valentine, K. F. Gibson, N. Kaminski, F. C. Scirba, Y. Zhang and S. R. Duncan (2011). "The HLA class II Allele DRB1*1501 is over-represented in patients with idiopathic pulmonary fibrosis." *PloS one* **6**(2): e14715-e14715.

Xue, J., D. J. Kass, J. Bon, L. Vuga, J. Tan, E. Csizmadia, L. Otterbein, M. Soejima, M. C. Levesque, K. F. Gibson, N. Kaminski, J. M. Pilewski, M. Donahoe, F. C. Scirba and S. R. Duncan (2013). "Plasma B-Lymphocyte Stimulator (BLyS) and B-cell Differentiation in Idiopathic Pulmonary Fibrosis Patients*." *Journal of immunology (Baltimore, Md. : 1950)* **191**(5): 2089-2095.

Yang, I. V., B. S. Pedersen, E. Rabinovich, C. E. Hennessy, E. J. Davidson, E. Murphy, B. J. Guardela, J. R. Tedrow, Y. Zhang, M. K. Singh, M. Correll, M. I. Schwarz, M. Geraci, F. C. Scirba, J. Quackenbush, A. Spira, N. Kaminski and D. A. Schwartz (2014). "Relationship of DNA methylation and gene expression in idiopathic pulmonary fibrosis." *American journal of respiratory and critical care medicine* **190**(11): 1263-1272.

Yoshizaki, A., Y. Iwata, K. Komura, F. Ogawa, T. Hara, E. Muroi, M. Takenaka, K. Shimizu, M. Hasegawa, M. Fujimoto, T. F. Tedder and S. Sato (2008). "CD19 regulates skin and lung fibrosis via Toll-like receptor signaling in a model of bleomycin-induced scleroderma." *The American journal of pathology* **172**(6): 1650-1663.

8 List of tables

Table 1: Overview of characteristics of naïve B cells and ASCs (plasmablasts and plasma cells).	5
Table 2: Overview on the nomenclature of FKBP proteins.	14
Table 3: Instruments	22
Table 4: Technical equipment	24
Table 5: Chemicals and reagents	25
Table 6: Cell lines.....	28
Table 7: Cell culture media	28
Table 8: Small interfering RNA (siRNA).	29
Table 9: Kits	29
Table 10: Cytokines, enzymes and inhibitors.....	29
Table 11: Primary antibodies for Western Blot.....	30
Table 12: Secondary antibodies for Western Blot.....	31
Table 13: Primary antibodies for immunofluorescence stainings	31
Table 14: Secondary antibodies for immunofluorescence stainings	32
Table 15: Antibodies for flow cytometry	33
Table 16: Primer sequences.....	33
Table 17: Software.....	34
Table 18: Deparaffinization protocol	43
Table 19: Composition of 4% SDS-PAGE Stacking gel.....	46
Table 20: Composition of 10% SDS-PAGE Separation gel.....	46

Table 21: Mastermix for cDNA synthesis 47

Table 22: qPCR reaction mix 48

9 List of figures

Figure 1: Induction of the UPR as part of plasma cell differentiation.	7
Figure 2: Structure of an IgG molecule (antibody).	8
Figure 3: An overview on antibody folding in the ER.	10
Figure 4: Peptidyl-prolyl <i>cis-trans</i> isomerization reaction.	13
Figure 5: Domain structure of exemplary FKBP proteins.	14
Figure 6: IPF pathogenesis.	17
Figure 7: Experimental setup of siRNA-mediated knockdown with subsequent tunicamycin treatment.	39
Figure 8: Experimental setup of denaturation and subsequent refolding of IgG.	41
Figure 9: Gating strategy for the detection of circulating plasma cells.	43
Figure 10: Differential expression of FKBP proteins in IPF lungs (preliminary data). .	51
Figure 11: FKBP11 is upregulated in lung tissues of IPF patients.	52
Figure 12: FKBP11 is identified in CD27+/CD38+/CD138+/CD3-/CD20-/CD45- plasma cells.	54
Figure 13: Plasma cells are highly elevated in IPF lungs.	56
Figure 14: FKBP11 is expressed by CD38- secretory cells in the pancreas and stomach.	57
Figure 15: IL2/R848 treatment induces plasma cell differentiation.	59
Figure 16: Plasma cell differentiation induces FKBP11.	60
Figure 17: FKBP11 is upregulated upon ER stress.	61
Figure 18: FKBP11 localizes to the ER.	62
Figure 19: XBP1 mediates upregulation of FKBP11 in ER stress.	63

Figure 20: FKBP11 protects from ER stress induced cell death.	64
Figure 21: FKBP11 is highly expressed in antibody producing hybridoma cell lines... ..	66
Figure 22: Knockdown of FKBP11 results in depressed antibody production.	68
Figure 23: FKBP11 is capable of antibody folding <i>in vitro</i>	70
Figure 24: Antibody yields are increased in IPF lung tissues.	72
Figure 25: Regulation and function of FKBP11.....	80

10 Acknowledgements

First and foremost, I would like to sincerely thank my doctoral supervisor PD Dr. Claudia Staab-Weijnitz for giving me the chance to work on an exciting project in her research group. Not only was she an excellent supervisor, but also a great teacher and team leader. She gave me constant support and was always open for new ideas.

I would also like to thank Prof. Dr. Oliver Eickelberg for the trust in me and the opportunity to join his former institute and working group. By offering the scholarship of the CPC research school, he made it possible for me to start a structured doctorate and fully focus on it.

Special gratitude goes to the CPC-M bioArchive and its partners at the Asklepios Biobank Gauting, the Klinikum der Universität München and the Ludwig-Maximilians-Universität München, as well as UGMLC Biobank Giessen, for the provision of human biomaterial.

Moreover, I would like to express my deep appreciation to all former and current members of the former Eickelberg group for a good cooperation and a nice working atmosphere. I would particularly like to thank Elisabeth Hennen for teaching me how to work in a laboratory and how to carry out basic scientific methods, Dr. Larissa Knüppel for sharing tips and protocols regarding cell culture experiments, Daniela Dietel for showing me how to stain human tissue sections, Michael Gerckens for the support in confocal microscopy and interesting and challenging talks, and Dr. Isis Fernandez along with Flavia Greiffo for advising me how to perform FACS analysis of whole blood samples. I would also like to point out the help from Thomas Meul from the research group of Prof. Dr. Silke Meiners, who showed me how to use the electroporation system

I am very grateful to Dr. Hans-Peter Bächinger, who gave me the chance to spend a lab exchange in his working group at the Shriners' Hospital for Children in Portland, Oregon. Together with Dr. Yoshihiro Ishikawa, he provided great supervision and helped me to achieve some of the most important results of my thesis.

In addition, I would like to thank all members and organizers of the CPC research school, especially Prof. Dr. Dr. Melanie Königshoff, Dr. Doreen Franke, Dr. Darcy Wagner and again my supervisor Claudia. They set up a wonderful selection of courses, which helped me to get settled in the world of science. Also, I am very grateful for a travel grant funded

by the CPC research school which made my lab exchange in Portland possible. Part of the CPC research school was also a Thesis Committee: I highly appreciate the help of Prof. Dr. Edgar Meinel and Dr. Aloys Schepers. Not only did they support me with valuable ideas for my project, but they also provided me with cell lines for my experiments.

Finally, special thanks goes to my parents, Thomas and Hana Preisendörfer, who supported me throughout the course of my studies, my grandmother Anneliese Preisendörfer and my girlfriend Johanna Pribbernow.

11 Publications

11.1 Original works

Preisendörfer S, Ishikawa Y, Knüppel L, Winklmeier S, Fernandez IE, Binzenhöfer L, Juan-Guardela BM, Hennen E, Ruppert M, Guenther A, Kneidinger N, Frankenberger M, Hatz R, Behr J, Schepers A, Hilgendorff A, Kaminski N, Meinl E, Bächinger HP, Eickelberg O, Staab-Weijnitz C

“FK506-binding protein 11, a novel antibody folding catalyst in plasma cells.”

In preparation for resubmission.

Schiller HB, Mayr CH, Leuschner G, Strunz M, Staab-Weijnitz C, Preisendörfer S, Eckes B, Moinzadeh P, Krieg T, Schwartz DA, Hatz RA, Behr J, Mann M, Eickelberg O

“Deep Proteome Profiling Reveals Common Prevalence of MZB1-Positive Plasma B Cells in Human Lung and Skin Fibrosis.”

Am J Respir Crit Care Med. 2017, 196(10):1298-1310.

11.2 Poster presentations

- | | |
|-----------|--|
| Sept 2020 | 30th International Virtual Congress of the European Respiratory Society: <i>“FK506-binding protein 11, a plasma cell specific antibody folding catalyst, is increased in pulmonary fibrosis.”</i> |
| Mar 2018 | 59. Congress of the German Society of Pneumology and Respiratory Medicine e.V., Dresden, Germany: <i>“FK506-binding protein 11, a plasma cell specific antibody folding catalyst, is increased in pulmonary fibrosis.”</i> |
| Jun 2017 | 1. Munich Medical Science Conference, München, Germany: <i>“FK506-binding protein 11, a plasma cell specific protein folding catalyst, is increased in pulmonary fibrosis.”</i> |
| Jan 2017 | Science Meeting of the “German Center for lung research”, Munich, Germany: <i>“FK506-binding protein 11, a plasma cell specific protein folding catalyst, is increased in pulmonary fibrosis.”</i> |

12 Curriculum vitae

Personal details

Name: Stefan Preisendörfer
Date of birth: March 9, 1995, in Aschaffenburg, Germany
Nationality: German

Education

Oct 2013 – Dec 2020 **Ludwigs-Maximilians-Universität München, Medical Faculty**
3. State examination (November 13, 2020): *-very good-*
2. State examination (October 10, 2019): *-good-*
1. State examination (September 8, 2015): *-very good-*
Elective, clinical part (Cardiology): *-very good-*
Elective, preclinical part (Medical English): *-very good-*

Aug 2018 – Jan 2019 **Aarhus Universitet, Medical Faculty, Denmark**
Gynecology & Obstetrics, Pediatrics

Sept 2005 – Jun 2013 **Benediktinergymnasium Ettal, High School**
Abitur: *-very good-* (1.40)

Medical doctorate

Sept 2016 – Dec 2020 **Comprehensive Pneumology Center, München**
Supervisor: PD Dr. Claudia-Staab Weijnitz
Project title: “FK506-binding protein 11, a novel antibody folding catalyst in plasma cells”

Sept 2017 – Oct 2017 **Oregon Health and Science Campus, Portland, USA**
Laboratory exchange to establish *in vitro* antibody folding assay
Supervisor: Dr. Hans-Peter Bächinger

Clinical Experience

Jul 2020 – Oct 2020 **Klinikum Rechts der Isar, München**
Practical Year, Surgery

May 2020 – Jun 2020	Klinikum der Universität München, Innenstadt Practical Year, Internal medicine
Mar 2020 – Apr 2020	Princess Alexandra Hospital, Brisbane, Australia Practical Year, Internal medicine
Nov 2019 – Feb 2020	Klinikum Bogenhausen, München Practical Year, Anesthesia and intensive care medicine
Mar 2019	Royal Infirmary Hospital, Hull, Great Britain Medical elective, Radiology
Aug 2018	Deutsches Herzzentrum, München Medical elective, Cardiology
Mar 2018	Doctor's practice from Dr. Oliver Abbushi, Deisenhofen Medical elective, General medicine
Mar 2016	UniversitätsSpital Zürich Medical elective, Thoracic surgery
Mar 2015	Model Hospital, Kathmandu, Nepal Medical elective, General surgery

Scholarships and awards

2019-2020	<i>MeCuM StEP</i> , excellence program from the LMU München
2015-2020	Talent program from the <i>Konrad-Adenauer-Stiftung e.V</i>
2013-2020	Online scholarship for excellent performance at Abitur, from <i>efellows.net</i>
2017	Travel grant from the <i>Comprehensive Pneumology Center</i>
2016-2017	Scholarship for a structured doctorate from the <i>Comprehensive Pneumology Center</i>